

University of Montana

ScholarWorks at University of Montana

Graduate Student Theses, Dissertations, &
Professional Papers

Graduate School

2022

USING BONE BIOLOGY TO ENHANCE FORENSIC AND PALEOANTHROPOLOGICAL DNA ANALYSIS

Keith M. Biddle

Follow this and additional works at: <https://scholarworks.umt.edu/etd>

Let us know how access to this document benefits you.

Recommended Citation

Biddle, Keith M., "USING BONE BIOLOGY TO ENHANCE FORENSIC AND PALEOANTHROPOLOGICAL DNA ANALYSIS" (2022). *Graduate Student Theses, Dissertations, & Professional Papers*. 12036.
<https://scholarworks.umt.edu/etd/12036>

This Dissertation is brought to you for free and open access by the Graduate School at ScholarWorks at University of Montana. It has been accepted for inclusion in Graduate Student Theses, Dissertations, & Professional Papers by an authorized administrator of ScholarWorks at University of Montana. For more information, please contact scholarworks@mso.umt.edu.

USING BONE BIOLOGY TO ENHANCE FORENSIC AND
PALEOANTHROPOLOGICAL DNA ANALYSIS

By

Keith M. Biddle

Master of Arts, University of Montana, Missoula, USA, 2019

Dissertation

presented in partial fulfillment of the requirements
for the degree of

Doctor of Philosophy
in Molecular Anthropology

The University of Montana
Missoula, MT

17 December 2022

Approved by:

Scott Whittenburg,
Graduate School Dean

Meradeth Snow, PhD., Chair
Department of Anthropology

Anna Prentiss, PhD.,
Department of Anthropology

Randall Skelton, PhD.,
Department of Anthropology

Joe Pasternak, PhD.,
Montana State Crime Laboratory

Chris Palmer, PhD.,
Department of Chemistry

© COPYRIGHT

by

Keith M. Biddle

2022

All Rights Reserved

ABSTRACT

Biddle, Keith, PhD December 2022

Anthropology

Using Bone Biology to Enhance Forensic and Paleoanthropological DNA Analysis

Committee:

Chairperson: Meradeth Snow, PhD

Anna Prentiss, PhD

Randall Skelton, PhD

Joseph Pasternak, PhD

Chris Palmer, PhD

We know that the optimal site for DNA extraction from human skeletal remains lies primarily in the petrous portion of the crania, and secondarily in the dental pulp, but we do not know why. As for the optimal location in the post-crania, targeted extraction sites are based on experience or inference, not empirical data. So, where to sample for DNA when only post-cranial elements are available? There are many instances where the petrous and/or teeth are not present or cannot be sampled. The three main goals of the project are 1- develop our foundational knowledge of the underlying cellular and biochemical reasons behind differential DNA preservation, 2- develop a minimally destructive sampling method, and 3- to construct a guide for forensic and biological anthropologists to determine which post-cranial elements to use for optimal DNA extraction. Pinpointing the ideal sites for the DNA extraction process will be advantageous when limited elements are available. Over 200 sites will be sampled from across a skeleton (obtained through the Montana State Crime Lab) and quantified for the number of starting molecules of both nuclear and mitochondrial DNA. Additionally, the 21 CODIS markers will be tested to see which sampling locations and bone types afford more complete STR profiles. Uniquely, this project will: 1) utilize knowledge of the cellular components and biochemical processes specific to the growth and maintenance of bones to target specific sites on skeletal elements for optimal DNA extraction, 2) incorporate knowledge of cell types to investigate the specific type of bone (cortical or trabecular) that is best for sampling at that site, 3) design and construct a visual “heat map” of the human post-cranial skeleton for use in both forensic DNA and ancient DNA (aDNA) laboratories.

Table of Contents

Abstract

Introduction

Bone Biology & Biochemistry

Forensic DNA Analysis Using Human Bone Tissue

Molecular Taphonomy

Methods

 Sample Selection

 Sample Preparation

 Sample Collection

 ATR/FTIR

 DNA Extraction & Purification

 DNA Quantitation

 Amplification & STR Analysis

Results

Conclusions and Discussion

Works Cited

Appendices

Introduction

This project is an experiment in molecular anthropological data collection and analysis from a human post cranial skeleton. The ultimate goal is to develop a targeted, minimally destructive skeletal sampling method to aid forensic and biological anthropologists, as well as DNA analysts in the decision of where to obtain bone tissue samples for optimal DNA extraction. This will be important when dental and cranial elements are not available in order to guide researchers toward the optimal sampling site(s) on any given skeletal element from which to attempt extraction. Uniquely, this project will: 1) utilize knowledge of the cellular components and processes as well as the biochemical properties specific to the growth and maintenance of human bones in order to target specific sites on specific skeletal elements for optimal DNA extraction, 2) incorporate knowledge of cell types to investigate the specific type of bone (cortical or trabecular) best for sampling at that site, 3) design and construct a visual “heat map” of the human post-cranial skeleton for use in both forensic DNA and ancient DNA (aDNA) laboratories.

Unlike previous studies, this project begins from a targeted cellular and microstructure-based approach. Utilizing knowledge of the cell and tissue types, ontogeny, and chemical properties of bone, this project seeks a new explanation for differential DNA preservation in intra-and inter-elemental extraction sites. The project includes traditional chemical DNA extraction, amplification, and quantitation methods, as well as Attenuated Total Reflectance Fourier Transform Infrared spectroscopy (ATR-FTIR) to aid in the development of a precisely targeted, minimally destructive, approach to DNA extraction from human or hominin bone. Finally, the results will be used to create a sampling method that is more accurate, significantly less destructive, and thus

more cost and time efficient than methods used previously. The method can be used by forensic practitioners as well as biological anthropologists involved with genetic and genomic research of ancient humans and hominins. By starting from a cellular and biochemical launching point, this project seeks to bridge the knowledge gap between forensic anthropology, forensic DNA analysis, and biomedical understanding of human skeletal biology and to make that knowledge accessible and applicable to those professionals on the front lines of the real-world problem of identifying unknown human skeletal remains.

Historically, forensic anthropological studies investigating optimal DNA extraction sites have focused solely on the osteological element, assuming that external taphonomic factors are behind the relative qualities and quantities of genetic material obtained (1–8). In studies such as these, failure of an element to yield adequate DNA for a full STR profile was blamed on environmental variables such as time since death, soil type or pH levels, or exposure to water or sunlight, rather than the potential lack of appropriate cellular contribution at the extraction site. Some studies discuss the potential primacy of cellular contribution to the surviving genetic material and lament the lack of current documentation as to how different cell types contribute their endogenous DNA to the hydroxyapatite or dental tissue under investigation (1,2,9,10).

For example, in 2015, Higgins, et al. reported differential results between nuclear and mitochondrial DNA (mtDNA) in extractions from different dental tissues. Dentine yielded consistently higher amounts of mtDNA, whereas cementum was better for nuclear DNA. This very possibly could be due to different cellular populations operative during life and the authors state as much, adding that individual age is known to play a

role in both tissue consistency and cellular populations. Similarly, in 2019, Antinick and Foran reported greatest success in DNA extraction results with samples taken from the epiphyseal regions of long bones with somewhat less success in the metaphyseal regions, and least success in the diaphyseal sites. They, too, reported intra-element differences in DNA type success rates, further suggesting that mere osteocyte populations are not necessarily responsible for the genetic contribution. In one of the few documented attempts to reconcile DNA and bone cell type in 2017, Andronowski, et al. were unsuccessful in correlating osteocyte population to nuclear DNA yield. To date, no studies have been found that address the potential DNA contribution from either osteoblasts (including bone-lining cells) and/or osteoclasts.

Indeed the technology behind today's genetic analyses has advanced sufficiently that many post-mortem influences, which in the past seemed insurmountable, can be much more easily navigated with better sampling methods. Problems that are frequently encountered in DNA analysis such as chemical inhibitors that are extracted with the bone tissue and low DNA copy number can often be somewhat counteracted with enhanced chemistry at the extraction/purification phase and with the use of better primers at the amplification phase. Of course, some samples will be so degraded, either biochemically or at the molecular level, that nothing can be salvaged. But by starting from a more educated vantage point and utilizing technology that can identify the untenable samples prior to catastrophic tissue destruction, it is possible to optimize sampling such that taphonomic and diagenetic factors are more easily circumnavigated

This study provides a rare opportunity to investigate the role of the different osteological cell types: osteoblasts (including their differentiation into bone lining cells),

multinucleated osteoclasts in the process of bone matrix resorption at the time of death, and fully encapsulated osteocytes, as a potential reason for differential DNA preservation and extraction quantity and quality in modern forensic cases (1,10–23). The use of ATR-FTIR will help gauge which types of chemicals remain in each sample prior to traditional chemical extraction methods (24–30). This will give a strong indication of how much DNA remains in the sample by the presence or absence of the bond between the hydroxyapatite and the DNA molecules. Comparing different bone tissue types, the ATR-FTIR test will help pinpoint the cells that are responsible for observed differences in DNA preservation. To this point, no studies have employed ATR-FTIR on human skeletal remains processed in this way (24–26). From this launching point, detailed analysis will be completed of the variance in DNA preservation and accessibility across a single, recent individuals' skeletal remains. This analysis into the number of starting molecules for mitochondrial, autosomal, and Y chromosomal DNA, as well as the ability to obtain a complete CODIS profile, will allow for understanding how differential DNA presence, and therefore accessibility, can be measured across the post-crania.

This research also opens an opportunity to expand the toolkits utilized in both forensic and aDNA studies by examining the riddle of differential DNA preservation across bony elements and tissue types. This is a question which has lingered in the background of many studies across forensic and biological anthropology. Perhaps most important of all, it affords the opportunity to assist forensic DNA analysts in the pursuit of identification of unknown human skeletal remains. Unfortunately, complete sets of human skeletal remains are rarely recovered. Usually, all that is recovered are disarticulated elements or sets of elements; or worse yet, mere fragments. In order to

obtain identification, investigators have to rely on forensic anthropologists and DNA extractions from whatever skeletal material is available. Without thorough understanding of DNA preservation across elements, identification of the deceased can be elusive. This is not a hypothetical problem. According to the National Missing and Unidentified Persons (NAMUS) database and the National Crime Information Center (NCIC), there are approximately 90,000 cases of missing persons in the U.S. at any given time and approximately 4,000 new cases of skeletal remains from unknown individuals were located by law enforcement in 2018 (31,32). With those alarming numbers in mind, creation of a more accurate and reliable sampling method, focusing on post-cranial elements, allows forensic anthropologists and DNA analysts to quickly identify which elements are the best for DNA extraction; specifically, where on a particular element is the optimal extraction site and, if applicable, whether the dense cortical or the inner cancellous bone tissue is optimal. Biological anthropologists will also benefit greatly from a more precisely targeted and minimally destructive sampling ability.

Hypothesis 1 (H1): Due to the presence of multinucleated osteoclasts and the concomitant proliferation of active osteoblasts involved in the repair and maintenance (homeostasis) of living bone, there will be higher concentration of both nuclear and mtDNA present in samples taken from sites on long bones and flat bones where homeostatic bone activity (resorption) is most prevalent. These sites will occur near articular points and any place where ante-mortem trauma has occurred.

Null hypothesis: Due to cellular apoptosis and/or the enzymatic actions involved in autolysis after organismal death, there will be no increase in the nuclear DNA found in sites involving *in vivo* homeostatic bone activity.

Test Expectations: If this hypothesis is supported, then the extractions sites on, or adjacent to, articular surfaces will yield more complete genetic profiles of all DNA types than mid-diaphyseal extraction sites or those sites away from articular points on flat bones.

Hypothesis 2 (H2): In the long bones, trabecular bone tissue is directly involved with the formation of blood cells and osteoclastogenesis. Across all element groups, trabecular bone has a higher surface area (43,45) and thus has the potential to trap more genetic material in the charged hydroxyapatite crystals than does the dense, outer, cortical layer.

Null hypothesis: Due to the porosity of trabecular bone, there will be no noticeable increase, and there may even be a marked decrease, in the amount of genetic material found in bone tissue closer to the medullary cavity.

Test Expectations: Because both **H2** and **H3** are so closely related in both theory and practice, test expectations for the two hypotheses are combined and elucidated below.

Hypothesis 3 (H3): During differentiation from mature osteoblasts, both bone lining cells and osteocytes lose most of their mitochondria and experience a marked reduction in their nuclei (62). Due to these cellular processes, samples taken from osteonal, or lamellar, tissue in the large, load-bearing elements will not yield as much genetic material.

Null hypothesis: There will be no difference in the amount or quality of the genetic material extracted from osteonal tissue sites of the large, load-bearing bones versus the cortical and trabecular surfaces.

Test Expectations for H2 and H3: If these hypotheses are supported, then extraction sites involving trabecular bone will consistently yield more complete genetic profiles of both nuclear and mtDNA, than will extractions from either the cortical or osteonal layers. Additionally, very little genetic material will be obtained at all from samples taken from the osteonal layer of the large long bones.

Hypothesis 4 (H4): Mundorff and Davoren (2014) and Obal (2019) indicate significant success obtaining genetic material from the bones of the hands and feet. Therefore, it is hypothesized that due to increased osteoclastic activity, bone groups which are subjected to a significant degree of lifetime rates of remodeling, will consistently yield more complete genetic profiles than skeletal elements whose primary functions are more structural than load-bearing.

Null hypothesis: According to a 2004 study by Pearson and Lieberman, Wolff's Law (the premise that bone experiences remodeling as a function of its role in life) is not always true (33) . Therefore, there will be no noticeable difference in the number of complete profiles generated from the DNA extracted from load-bearing bone groups versus that which is extracted from structural or non-load bearing groups.

Test Expectations: If this hypothesis is supported, then extractions from load-bearing bones and bone groups such as the vertebrae, tarsals/metatarsals, etc., will yield more complete genetic profiles of both nuclear and mtDNA than will structural elements or groups such as the ribs and scapulae.

This project is designed to make a significant contribution to the process of forensic victim identification, the ethical concerns that arise from destructive analysis of human bone tissue, and to the preservation of ancient specimens. This can be done by designing a sampling method that begins with mindful recognition of cell populations and bone biochemistry, and proceeds through the creation of a “heat map” that clearly shows the best sampling sites for mitochondrial, autosomal, and Y- chromosomal DNA, if any can be found. The results of this study will be beneficial across numerous professions and may well retain its rigor into forthcoming technologies such as forensic genetic genealogy (FGG).

The following chapters will delve into the history and current theories and methods of forensic DNA analysis including a focused account of the literature of DNA extractions from human bone. Following that is a detailed reexamination of what we know about bone biology and biochemistry. Then comes a thorough look into the processes of molecular taphonomy and diagenesis. All of these topics weave in and through one another as a way to address the knowledge that was necessary for the project as a whole. Once the background has been covered, the methods used in this project will be covered in detail and that is followed by the results of the experiment, in- depth discussion of those results, and finally, some thoughts on where to go from here.

CHAPTER 1: BONE CELLULAR BIOLOGY

HISTORY

A basic understanding of the history of bone biology is foundational because it illuminates the research leading up to current trends and practices. It also shows where there are potential gaps that invite contemporary research, such as this project. This brief section mirrors much of the history of the biological sciences, in that a new discovery appears, followed by a period of relative quiet until sufficient technology is developed that allows for further advancement.

In 1691 Clopton Havers published the first known work on the microstructure of bone (Havers 1691). The canals that carry blood, nutrients, and biochemical messages through bones are named after him. Due to technological limitations, however, he was unable to see the cells themselves. For the purposes of this project, the story truly begins with a publication by Goodsir and Goodsir in 1845, in which the authors reported the ability to see osteoblasts. The authors believed that they may be responsible for bone formation. This was supported by the works of Tomes and DeMorgan in 1853 and Muller in 1858. In 1864 the term “osteoblast” was officially coined and was grounded in the hypothesis that these cells were of mesenchymal origin (34). In 1873 a German anatomist named Albert Kölliker discovered a previously unknown type of cell, the osteoclast (nee:

osteoklast), that seemed to be responsible for the destruction of old or damaged bone (35). As of 1916, what would eventually be known as the osteon was observed and noted (36), yet it didn't appear in the literature as anything other than the literal translation of the Latin word for bone. Fourteen years later, in 1930, Weidenreich observed that the bone tissue surrounding what we now know as osteocytes, being shot through with Haversian canals, was different than the bone on either the periosteal or endosteal surfaces and the trabecular bone in the medullary cavity. He could see the concentric rings and distinct lines of demarcation between them and used the term "osteon" to describe them, but he could not yet ascertain their significance. With the advent of scanning electron microscopy (SEM), osteocytes were finally observed as distinct cells. Little was known about osteonal modeling or remodeling until the 1980's (37,38). And according to Bonewald, it has only been since about the year 2000 that we've known much about what these cells really are, what they do, and how they are formed.

For the almost 300 years between Clopton Havers' observation and the technological explosion of the late 20th century, new information about the structure or function of the different bone cell types came in small bursts, a decade or two apart. There was debate, which primed the intellectual pump, but the histochemical technology to detect the hormones, enzymes, and other chemical factors that play an integral role in bone growth and re-growth simply were not available. Experiments such as using Plutonium as a stain that showed that osteoclasts do absorb the bone matrix, or Cartier's 1951 study that confirmed osteoblastic role in bone matrix production (which had been originally posited by Goodsir and Goodsir 100 years prior and then discounted) were the hallmarks of progress for much of the 20th century (39,40). That is, of course, until

technology advanced enough to show that osteoblastic communication with hematopoietic cells is necessary to induce osteoclastogenesis (41) and allowed investigators to detect the presence of biochemical factors such as Parathyroid hormone (PTH), tumor necrosis factor (TNF), and osteoprotegerin (OPG) in the late 1990's, and the discovery of receptor activator of nuclear factor κ B ligand (RANKL) in the early 2000's (37).

The discovery of the osteoclast revolutionized scientific understanding of bone growth and re-growth. The echoes of Herr Kölliker's discovery, coupled with modern histochemical analytical methods, and an emerging picture of the communicative role played by osteocytes, have led to the realization that bone cell types and functions are not independent of one another. In fact, we now know that bones play vital roles in the endocrine, immune, and the circulatory systems and are far from being static pieces of biological lumber(38,42–44). For most of the 20th century, biological and forensic anthropologists primarily used cellular knowledge of bone structure in qualitative paleopathological studies until DNA was discovered and extracted from bone in the 1980's (45,46).

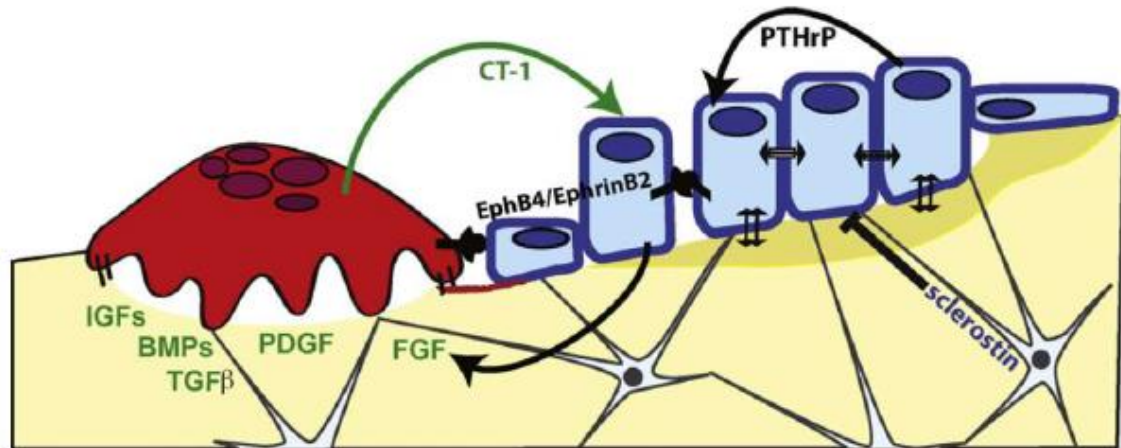


Image 1- From Sims and Gooi 2008-Included here to show the complex biochemical interactions between cell types during resorption. Osteoclasts (red) pave the way for bone lining cells (flatter blue rectangles) which derive from osteoblasts (tall blue cells). Osteocytes are the black dots in white, stellate, lacunae. If one of the osteoblasts is programmed for differentiation into an osteocyte, it would be the middle of the three in order to allow the surrounding cells to encase it within the unmineralized osteoid.

For most of the history of bone biology, it was assumed that because osteoclasts operate on bone, they must derive from the same lineage. Today, we know that osteoblasts derive from mesenchymal stem cells, which are also responsible for the development of chondrocytes and other tissue progenitor cells. Osteocytes are differentiated osteoblasts that have shed their mitochondria, become completely ensconced within the bone matrix, and taken on a new role (14,15,38,47). Additionally, we know that osteoclasts derive from hematopoietic progenitor cells of the monocyte-macrophage lineage rather than those of mesenchymal lineage (11,37,43). This is relatively new information that only became available when technology was sufficiently advanced to detect the biochemical pathways involved with macrophage differentiation into other immunological and hematopoietic cells.

Now that science has a solid foundational knowledge, and the technological capacity to detect, measure, and experiment with bony tissues outside of the human body (*in vitro*), much of the recent research being performed in this field deals with pathology and trauma. Conditions such as osteoarthritis (OA), osteoporosis (OP) and osteopetrosis are being investigated further. With the discovery of tumor necrosis factor (TNF) related to osteoclastic activity, there is much research focused on how various tumors influence, and are influenced by, osteoblastic and osteoclastic activity. These tumors and cancers are not only limited to the bones; since osteoclasts derive from hematopoietic cells, their biochemical signals and pathways are systemically pervasive and can be found in disorders involving smooth muscle cells, lung cancers, and kidney diseases, just to name a few.

Despite the current state of our understanding of bony tissue, most forensic anthropological research is not concerned with which cell types are yielding DNA and the question of *why* their results emerge as they do are addressed simply in terms of taphonomy. In the majority of studies there is no cellular examination to help elucidate why the sample did not produce any viable DNA or, perhaps, produced only limited amounts. Those studies that do involve cellular components or processes (outside of genetic analyses) primarily involve human/non-human comparisons, the differentiation of osseous or dental material from wood or non- biological material (48,49) or are looking at biochemical signatures of burned remains such as the Ubelaker (2009) study (50). Most of the introductory level textbooks in forensic anthropology do address the different cell types and their respective roles, but little is said beyond a brief introduction (51–55).

Ever more targeted approaches to forensic analyses, especially those involved in the identification of unknown remains, characterize the state of the research today. Even as costs decrease somewhat from the earlier years of DNA analyses, financial concerns still dictate a good portion of workflow in law enforcement (LE) offices, crime labs, and so on. The ability, therefore, to target a small bone or portion of a bone for optimal DNA analysis is a worthwhile goal. And the dissemination of this knowledge to current and forthcoming generations of forensic anthropologists is an important aspect in our cooperative efforts with LE officials, Medical Examiners (ME's), coroners, and crime labs. Increasingly stringent rules of admissibility of scientific evidence and expertise in courts also demand more accurate and targeted scientific understandings.

BONE TISSUE TYPES

It is well understood that bone is both composed of, and responsible for, the storage and homeostasis of molecular nutrient essentials such as calcium and phosphate. Current characterization of bone tissue types varies between two or three categories, depending on the goal of the material, whether investigative or descriptive; and the names of each type may also vary. For example, some authors prefer the term “cancellous” or even “spongy” rather than “trabecular”. For the purposes of this study, it useful to break up bone tissues into three types and the following terms, listed in order from exterior to interior will be used: the term Cortical here refers to the very outer layer that is just below the periosteum; Osteonal refers to the layer (found exclusively in major long bones) that is developed in concentric rings with Haversian and Volkmann's canals; and Trabecular which refers to the inner- most layer of most elements, contains hematopoietic cells, and is outside of the endosteum. A fourth type of bone, diploic, is found only in the cranium,

and because this project does not involve DNA extraction sites from the cranium or mandible, this bone type is not thoroughly discussed. Furthermore, since this project focuses on adult skeletal tissue, immature or woven bone is addressed only as a reference in the section on skeletal ontogeny.

Cortical Bone

For the purposes of this study, “cortical bone” is used to refer to the circumferential layer just below the periosteum. Often lumped together with lamellar bone, it is created in layers of opposing direction to make it the hardest, outer layer of the bones. It is what offers the greatest protection from most types of trauma and it is the site of anchorage for the muscles, tendons, ligaments, cartilage, and periosteum. Structural failure of the cortical layer results in a wide array of pathological conditions, most of which are characterized by element deformation (19,56,57) and/or fragility. Damage to the cortical layer often results in damage to the periosteum. This can result in various infections such as periostitis, osteomyelitis, and so on. Not surprisingly, then, the cortical layer is the first layer to be repaired in traumatic injury. Evidence of healing can be seen in as little as 2-3 days after the traumatic event (17,19,43,58–63). Even in cases of trauma, osteoclastic activity is stimulated to remodel the bone surface around the area to prepare it for the osteoblasts to deposit new osteoid and allow for fresh hydroxyapatite mineralization. A more detailed examination of the healing process of bone is included in a later section that deals with the specific trauma and pathology found on the skeletal material used in this study. Specific cellular activity is also detailed more thoroughly in the sections below.

Osteonal Bone

For this project, the thick layer of bone between the cortical layer and the medullary cavity/ trabecular layer is referred to as osteonal bone. As noted above, this tissue is often called lamellar and is not always conceptually separated from the outer, cortical layer. This tissue is laid down in concentric rings delineated by cement lines and shot through longitudinally with Haversian canals, and latitudinally with Volkmann's canals. Osteons are sometimes referred to as "Haversian systems." Also characteristic of osteons are the presence of osteocytes in their lacunae and the dendritic process extending from them through canaliculi. Trauma to the osteonal bone is the last tissue to be healed once both outer and inner tables have regained structural integrity. Osteoclastic activity in the osteons is much slower, both in initial response time and in progression due to the energy involved in reaching the resorption site(s). See the sections on osteoclasts and osteocytes for further specifics on cellular anatomy, processes, and pathology.

Trabecular Bone

Trabecular bone tissue is found in the medullary cavities and is the primary bone tissue type at the proximal and distal ends of the long bones. It also makes up the majority of all the bony tissue in the hands and feet. Often referred to as "spongy" bone because of its porous appearance, trabecular bone is the site of blood cell formation in the medullary cavities and is thus the site of osteoclastogenesis (the formation, or birth, of osteoclasts). Starting as rapidly and chaotically formed woven bone during ontogeny, trabecular bone goes through extensive and continual remodeling during youth and adolescence, becoming more organized and structurally functional (64). The epiphyses and metaphyses of the long bones are primarily trabecular bone covered in a cortical shell

which allows for dramatic growth of the element(s) from birth until full skeletal maturity when the cartilaginous growth plate that joins the epiphysis to the metaphysis is completely ossified (40,65,66).

BONE CELL TYPES

Traditionally, bone is described in the forensic anthropological literature in terms of three (or even four) distinct cell types. It is actually somewhat misleading, and nearly incorrect, to separate bone cell types so much since two of the three (osteoblasts and bone lining cells) are nearly identical and osteoclasts are more akin to immunological cells than bone cells. Mostly, this taxonomic segregation is carried out by describing the primary function of each cell type. However, the interdependence of the cell types cannot be overstated. Indeed, understanding of this interdependence led researchers to coin the term “Basic Multicellular Unit” or BMU. Still, it may be argued that, 1) due to their hematopoietic origin (meaning that they are actually derived from the same stem cells that produce blood cells), osteoclasts are not truly bone cells at all, 2) that because both bone lining cells and osteocytes are actually transformed osteoblasts, that 3) there is really only one type of bone-specific cell (osteoblasts) which performs multiple inter-related functions. However, for the purposes of this project, the traditional distinction between the bone cell types will be utilized, with the exception that bone lining cells are herein classified with osteoblasts. Each individual cell type will be discussed in relevant detail from genesis through apoptosis. The biochemical pathways involved in the communication between the cell types will be only generally addressed, as the detailed specifics of them are outside the scope of this project.

OSTEOBLASTS

Osteoblasts originate from mesenchymal stem cells (MSC's) found in the periosteum and the endosteum. MSC's also give rise to fibroblasts, chondroblasts, and other cells responsible for the production of tendons, ligaments, and cartilage (15,16,20). Osteoblasts are principally responsible for the deposition of bone matrix, making them essential for bone formation, growth, and remodeling. This also means that they are of primary interest in pathologies of hyper- or hypo- trophic bone development, such as osteopetrosis and osteoporosis, Paget's disease, hyperparathyroidism, etc.

Beginning as preosteoblasts, these cells are irregularly shaped and produce collagen types I, II, and III precursor molecules. Working with other biochemicals such as alkaline phosphatase and osteonectin, the preosteoblast then differentiates into a mature osteoblast and begins producing the bone matrix, or osteoid (67). Mature osteoblasts are cuboidal in shape, contain a distinct nucleus, mitochondria, rough endoplasmic reticulum, well- defined Golgi apparatus, and secretory vesicles. Normal osteoblasts typically produce about 0.5 μm of bone matrix per day and persist for up to 100 days, depending on the need. After this period osteoblasts may undergo one of four possible changes. They may differentiate into bone lining cells, differentiate into osteocytes, they may succumb to programmed apoptosis, or undergo metaplasia and transdifferentiate into chondroblasts (16,20,22,67,68). According to the 2006 study by Franz-Odenaal, et al., there are multiple factors (including: species, sex, overall organismal health, bone type, and many others) which play a role in determining what proportion of osteoblasts follow each of the above trajectories. Estimates vary widely and range from 50- 80% that undergo apoptosis. Parfitt's 1990 study suggests that only about

30% of osteoblasts differentiate into osteocytes. These numbers are hard to pin down in living organisms and are not conserved among taxa or bone types. (16,67,69).

If differentiation into bone lining cells occurs, the cells flatten and lose much of their cytoplasm, mitochondria, and other organelles. If they come into contact with sufficient parathyroid hormone (PTH), bone lining cells shrink even further, excreting enzymes that remove a thin layer of osteoid from the surface of the mineralized bone matrix and prepare it for resorption by osteoclasts (11,15,42,56,70). This shrinkage, loss of cytoplasm and organelles, and bone surface preparation also act as a biochemical “runway” for the osteoclasts which were activated by biochemical signaling from osteocytes or other factors (37,43). Under normal conditions, apoptosis of osteoblasts on bone surfaces acts as an inhibitory signal to osteoclasts when bone remodeling and osteoid apposition need to stop, slow down, or change direction. This is different than the inhibitory signals which modulate bone remodeling and apposition in osteonal units. Those signals come from neighboring osteocytes (71,72). The reason for this is simply that most osteocytic dendrites run through canaliculi that are parallel to the bone shaft and thus intersect more with other osteonal BMU’s than with those on the surfaces of the bones. There are dendrites that do reach the bone surfaces via canaliculi that run transversely, or perpendicular to the long axis of the bone, and osteocyte communication with the bone lining cells occurs at those syncytia or gap junctions. The biochemical signals are then passed from bone lining cell to bone lining cell. Data varies regarding the number of osteoblasts that differentiate into bone lining cells but most studies seem to agree that it is the least common outcome, once primary osteoblastic functions have been fulfilled.

If an osteoblast is signaled to differentiate into an osteocyte, it will cease production of bone matrix while the neighboring cells continue to do so, effectively burying it (38,67,73). The rates at which this occur vary depending on the location of the cells (intramembranous, or osteonal, vs peri- or endosteal), the type of bone being constructed or reconstructed (woven vs lamellar), and the bony element in question. Construction and repair of the inferospinous portion of the scapula, for example, will occur differently and at a different rate than that of diaphyseal femur tissue or cranial bones. After the initial deposition of osteoid is in place, other osteoblasts literally line up along the bone spicule and deposit more osteoid which encapsulates the differentiating cell (74). This process effectively means that osteoblasts of different developmental stages are nearly always present along the surface of bones (67,75,76). Polarization of the osteoblasts, which influences the directionality of osteoid secretion/ matrix production, along with the sex, age, and other organismal factors, as well as bone type, element type, and element specific location, all influence which osteoblasts will differentiate and the rates at which the process occurs. This has the potential for drastic implications in forensic and ancient DNA extraction. Because of this cellular behavior, sites immediately adjacent to peri mortem trauma should be the primary target of forensic DNA extraction since multiple cell types would be active there. Often, these injury sites are conserved for descriptive or educational purposes and their forensic importance is limited to photographs. The same premise holds for sites of *in vivo* remodeling such as the pubic symphysis and the auricular surface.

OSTEOCYTES

The transition from osteoblast to osteocyte is not yet fully understood. Several studies have uncovered multiple genetic factors that play a major role systemically, but the actual process of differentiation is still difficult to visualize, especially *in vivo* (22,38,71,73). What is known is that significant alterations to the cell begin to occur very early in differentiation. Development of dendritic processes are one of the first observable changes to the cell as it becomes encased in osteoid. Other changes that occur are reduction in the amount of cytoplasm and the quantity and activity of other organelles; most notably the mitochondria. These changes are apt, given the immobile nature and communicatory function of osteocytes. From the main lacunae, osteocytic dendrites extend in all directions from the cell through tunnels known as canaliculi. These tunnels and tentacles are the lines through which the cells draw nutrients and exchange biochemical signals.

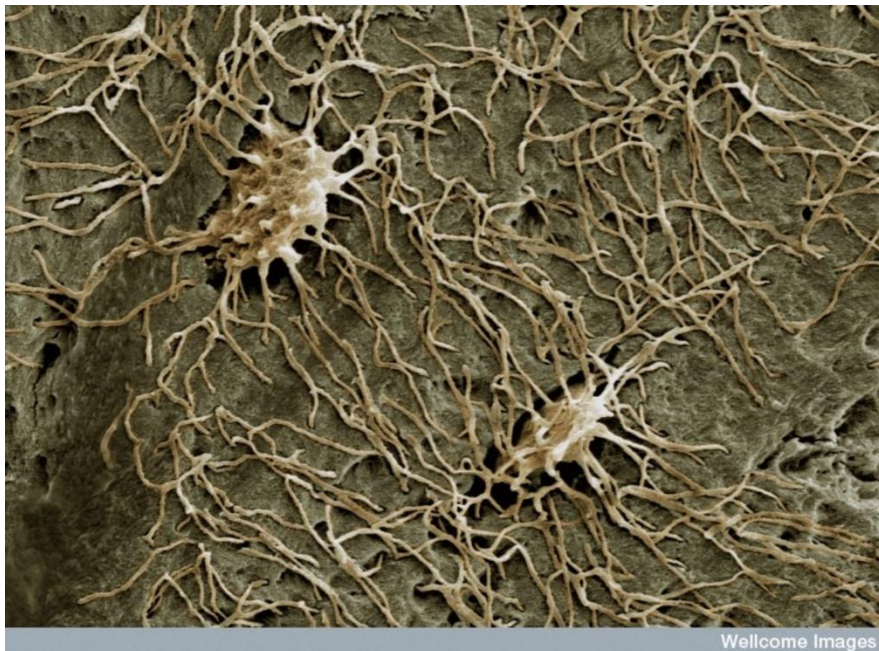


Image 2- Osteocytes in their lacunae. Image sourced from google.

Osteocytes are the longest lived of the bone cells, surviving for many decades before programmed apoptosis. Primarily, they serve as mechanosensors for the bones but also perform some endocrine functions such as phosphate regulation and systemic calcium availability. During pregnancy and lactation, osteocytes in mice and rats have been observed to remodel their own lacunae and canaliculi. Using the same methods as osteoclasts, they dissolve bone matrix to release Ca^+ into the blood (15,20,38). Most of the time, however, osteocytes serve as coordinators of skeletal homeostasis. In his 2008 article, Skerry disputed the mechanosensory model of osteocyte involvement, noting that normal strain and loading on bones does not show a direct response from osteocytes to indicate that they are responsible for bone formation. However, it has been shown that growth, remodeling, and healing are more akin to a complex, biochemical, conversation between all cell types in the BMU rather than a single set of instructions given by one cell type with no feedback from the others (37,38,44,60,67,73).

Trauma to the bone can cause osteocytes to initiate remodeling in different ways. If traumatic apoptosis occurs, RANKL (receptor activator of nuclear factor kappa- β ligand) is released which stimulates the development and proliferation of osteoclasts as well as signaling mesenchymal stem cells to differentiate into osteoblasts. Microtrauma, or trauma that does not result in osteocytic apoptosis, will still stimulate the above biochemicals, but in smaller, timed, dispersals to allow for more targeted direction of osteoclast and osteoblast proliferation. In cases of programmed apoptosis, depending on multiple organismal factors (age, overall health, etc.), the lacuna may or may not remodel. In healthy individuals, often empty lacuna are refilled with osteoid during the

healing process, which is the construction of a secondary osteon. Much the way a brick wall is built, the building of secondary osteons, which often overlap the primary osteons that were constructed in juvenile osteogenesis, allows for maintenance of full element stability (22,66,71). However, in older individuals, or those who suffer from certain pathologies, the empty lacuna left after osteocytic apoptosis may not be refilled. This leads, in time, to fragility in the element and contributes to OP as well as OA. Conversely, filling an empty lacuna without the construction of a secondary osteon can contribute to osteopetrosis, even in an organism that does not exhibit this condition overall; this is known as micro osteopetrosis.

Several older studies indicate that osteocytes make up approximately 90% of all cells in any given element (14,15,20,71,73). This may lead to the assumption that they would account for any nuclear DNA that may be extractable from bone and the possible reason for a lack of mtDNA in certain elements such as the femur and the humerus, especially if the sample is taken from the osteonal layer between the periosteum and the endosteum, as most mid- diaphyseal extractions of long bones are. However, Parfitt in 1990 stated that osteoblast population in a BMU is greater than the sum of osteocytes + bone lining cells. This would indicate that genetic material extracted from bone would most likely be of osteoblastic origin and might account for any success in mtDNA extractions. It is not well characterized, however, whether Parfitt's model of cellular populational ratio holds true in elements that are not experiencing any major remodeling at the time of, or immediately prior to, DNA extraction. In either case, as mentioned previously, osteocytes do undergo programmed apoptosis as well as traumatic apoptosis in life and enzymatic apoptosis at organismal death, and thus it is not a foregone

conclusion that these cells are responsible for yielding any genetic material. This could be especially true in cases of elderly individuals or extractions from sites of OA or OP.

Notably, according to the 2000 study by Martin, trabecular bone tissue BMU's exhibit a weaker inhibitory signal from osteocytes, indicating that in these specific sites, genetic material may be osteoblastic, or even osteoclastic, in origin (71,77). This is consistent with some aDNA studies that have favored the otic region of the petrous portion of the temporal bone for their extractions (78,79).

OSTEOCLASTS

Osteoclasts are terminally differentiated, multinucleated, cells that derive from the monocyte/ macrophage lineage of hematopoietic stem cells. This means that, unlike osteoblasts, they will not differentiate into any other cell type. Additionally, despite earlier suspicions to the contrary, it has been shown that they are derived from the same lineage of stem cells that are responsible for blood cells. While the exact number of nuclei in any given osteoclast may vary depending on a multiplicity of factors, they are generally characterized by having at least 2 nuclei and as many as 20 have been recorded in *in vitro* experiments (11,12,23,39,80–83). Osteoclasts are generally oblong or rounded in shape, especially during resorption activity, and contain multiple mitochondria. Once resorptive activity begins, the osteoclast changes shape even further. Polarization occurs and three distinct regions become apparent: a functional secretory domain (FSD) appears at the rounded apex of the cell opposite the surface of the bone being resorbed, a sealing zone (SZ) appears circumferentially that creates a tight seal and a ruffled border (RB) extends into the resorptive pit, known as a Howship's lacuna. Actual resorption occurs by secretion of hydrochloric acid (HCL) which dissolves the inorganic HA^+ crystals and

then the enzymes tartrate- resistant acid phosphatase (TRAP), cathepsin- K, and matrix metalloproteinase- 9 (MMP-9) degrade the organic collagen materials (16,23,80). The metabolites are then endocytosed into the osteoclast and transcytosed to the FSD where they are excreted into the extracellular matrix.

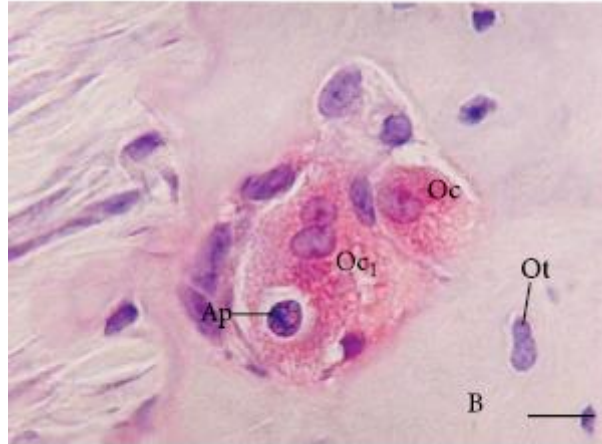


Image 3- From Florencio- Silva, et al 2015- Osteoclasts (Oc & Oc1) in Howship's lacunae. Note the apoptotic cell (Ap) in a vacuole of Oc1. B = bone tissue. Ot = Osteocyte.

Osteoclast recruitment, that is, the biochemical signals which induce osteoclastogenesis, is not of primary relevance to this project. What is relevant, however, is the strong evidence indicating that not all populations of osteoclasts are identical. The 2011 study by de Souza Faloni, et al., showed that osteoclast populations differed in small, yet notable ways between mouse mandibular bone versus tibial bone tissue; “...osteoclasts at different bone sites appear to differ and the existence of bone site-specific osteoclast heterogeneity has been proposed” (80). These cell populations differed in nuclear number, time between osteocytic RANKL secretion resulting in osteoclastogenesis, and the specific biochemical recipe used in resorption. This heterogeneity extends to other skeletal elements, as well, including the calvarium and the

femur. Primary ossification in different skeletal groups occurs in different ways; that is, they do not all ossify in identical directions at identical rates. In fact, the blueprint for long bone ossification, for example, is quite different than that of cranial or facial bones. Biochemically, this means that the matrices are inherently different between the calvarium and the humerus, for example, or the sphenoid and the clavicle. Therefore, the osteoclasts populations responsible for maintaining those elements must be able to adapt to the specific matrix of the element they are working on. This is not only true of different bony elements, but it applies to cortical versus trabecular bone tissues, as well.

This heterogeneity in osteoclast populations indicates another potential reason for differential degrees of success in DNA extraction. Skeletal elements which exhibit osteoclastic populations with fewer nuclei or mitochondria or those elements/sites where osteoclastogenesis occurs more slowly may not yield the same amount or quality of DNA. Multiple studies have shown that the frontal bone, for example, does not perform well in DNA analysis (3,4,6,84,85). Assuming that osteocyte populations vary only in number between skeletal elements, and that osteoblastic involvement in quiescent, or non-resorbing, tissue will be minimal, then the failure to yield adequate genetic material may very well be due to the specific population of osteoclasts that operate on or within that element.

The application of the idea of osteoclast populational heterogeneity and elemental site specificity may be shown in another example. Mostly, osteoclastogenesis in the long bones occurs in the periosteum, the endosteum, or in the marrow itself, depending on the location of the section of bone that needs remodeling. Peri- and endosteal osteoblast populations morphologically differ somewhat from marrow- derived populations. In the

femoral head, however, osteoclastogenesis occurs from stem cells residing in the connective tissues that surround and penetrate the joint. It is logical then, to consider that perhaps DNA extractions involving the femoral head will be more productive in samples taken from the inner trabeculae, rather than the external cortical matrix. The same processes and reasoning also extend to the humerus and humeral head. Since all osteoclasts are hematopoietic in origin, it also stands to reason that populations in closer proximity to marrow or the endosteum, may potentially provide better, more complete, results in genetic tests. This application of osteoclastic heterogeneity is surely operative in all other post- cranial elements and may account for the recent popularity of various tarsal bones in forensic analysis (1,3–5). The function and primary ossification of the element to be tested must be taken into consideration in forensic DNA analysis.

OSSIFICATION & ONTOGENY

Human skeletal ossification is well characterized, but a brief review is warranted because of the site- specific nature of this project. Not all elements develop and ossify through identical pathways and the specifics of the process may mirror osteoclastic population heterogeneity, and osteoblastic and osteocytic proliferation. Additionally, any structural differences in ontogenetic construction may play a role in the way in which, and the extent to which, DNA survives in specific sites on specific skeletal elements. In order to address the pattern of post- mortem DNA survival in skeletal tissues, then as many factors as possible should be probed, which means understanding whether intramembranous versus endochondral ossification allows for better DNA preservation. The following section is divided into the two primary methods of ossification in the human skeleton. Most elements follow either one or the other design, but some elements

exhibit both and those constitute a third group. Since this project does not test samples from the cranium, mandible, or teeth, those elements are mentioned only as reference points.

ENDOCHONDRAL OSSIFICATION

Primarily occurring in the long bones (including the phalanges) endochondral ossification occurs as the cartilaginous blueprint for the element is replaced with osteoid and hydroxyapatite crystals. MSC's proliferate in the perichondrium (the cartilaginous equivalent of the periosteum) and usually, just before birth, chondroblasts yield as the MSC's begin to differentiate into osteoblasts at the primary ossification centers located in the mid- diaphyseal regions (86,19,56,51,66). Secondary sites at the proximal and distal ends of the elements follow the same process, as do the metaphyses and epiphyses which ossify from the cartilaginous growth plate.

Since ossification begins at the outer table of the element, penetrative vascularization of the ossifying element commences and a bony ring is formed (66). Through this vascularization, the ring is thickened and becomes dense from the periosteum through the cortical tissue to the inside where the endosteum will eventually reside, once the marrow and inner trabecular bone is adequately formed. This inner tissue, and all trabecular bone, begins as unorganized, woven bone to give preliminary strength to the element and as a platform for remodeling to occur. Similarly, primary osteons laid down in the early stages of ontogeny will be resorbed and rebuilt into secondary osteons in the mature bones. The marrow itself begins as "red marrow", primarily involved with production of blood and immunological cells, including the macrophages and monocytes involved in osteoclastogenesis. Remodeling occurs on or

within all bony tables even during ontogeny, to allow for growth in length while still maintaining structural integrity. This occurs at the flared ends of these elements as well, so they can grow in thickness and length.

INTRAMEMBRANOUS OSSIFICATION

Flat bones and diploic bones primarily ossify from two membranes that build bone between them. This occurs appositionally as the bone is laid down from the periosteum, much the way remodeling occurs on the cortical surfaces of all elements. Skeletal structures that develop intramembranously begin as a sandwich with two perichondrial membranes and cartilaginous material between them. The change from perichondrium to periosteum occurs in the same way as in endochondral ossification, with centers that begin the process. As the perichondrium differentiates into a periosteum, MSC's differentiate into osteoblasts. In the cranium, ossification begins in the base of the occipital to build structural support for the cranial vault as well as for protection for the brain stem and the spinal cord. The sphenoid is the primary center of ossification for the bones of the face, and also serves to build structural integrity for the sensory nerves and the developing brain. Other elements that ossify from an intramembranous blueprint include the sternum and manubrium and the patella.

INTRAMEMBRANOUS + ENDOCHONDRAL OSSIFICATION

Some elements ossify by utilizing a combination of the above schemes. Denser aspects of these elements, mostly those involved in articulation with elements whose functions require a high degree of mobility in life, ossify from a cartilaginous model (endochondral), while the more gracile aspects ossify intramembranously. The anterior

and lateral aspects of the mandible for example, ossify intramembranously to allow for the development of the bony crypts which hold the developing dentition, but the rami and coronoid processes develop endochondrally. The clavicle ossifies intramembranously in the diaphysis, and endochondrally at the medial and lateral ends. It is one of the first bones to begin ossification and is usually the last to complete the process (87). This combination occurs in the scapula and the ilium, as well.

HYDROXYAPATITE

Hydroxyapatite (HA^+) is the inorganic, mineral, aspect of bone tissue. While the chemical formula, $\text{Ca}_{10}(\text{PO}_4)_6(\text{OH})_2$, has been known for decades, hydroxyapatite formation and deposition is not definitively characterized (15,16,56,64,77). However, recent research has indicated that osteoblasts, during osteoid production, also produce matrix vesicles containing high concentrations of calcium (Ca^{2+}) and phosphate (PO_4^-) ions that are the constituent components of HA^+ that are not found in high enough concentrations in the extracellular matrix to satisfy the mineral requirement for bone mineralization. After filling, these vesicles separate from the osteoblasts and rupture, thereby “dumping” their mineral components onto the newly deposited osteoid. The OH constituent of HA^+ is found in high enough concentrations in the extracellular matrix so that the cells need not produce it themselves. The addition of this part of the molecule completes the formation of the hydroxyapatite crystals, which mineralizes and spreads by accretion, joining together from the foci of deposition from other osteoblasts (64). The resulting hydroxyapatite has a positive charge.

It is thought that HA^+ crystals maintain their charge long after organismal death and it may be this charge that attracts, binds, and preserves negatively charged DNA molecules (88–90). Like the process of bone mineralization, this charge retention is not definitively characterized, but may contribute to the explanation of why some bony elements perform better in forensic (and ancient) DNA extractions than others. Elements or bone types with higher cell populations may potentially contribute more genetic material to the HA^+ upon apoptosis or lysis after organismal death. Additionally, this charge retention may combine with higher surface area to account for better DNA preservation in trabecular than cortical bone tissue. However, the density of the outer cortical layer may prove more resilient in charge retention, if cortical samples are shown to outperform trabecular samples in forensic DNA analysis. There is also the possibility that while the cortical layer may be stronger in original charge retention, due to exposure to environmental conditions, it may lose its hold on DNA earlier than the protected, trabecular, tissues, thus accounting for differences in older samples or those exposed to certain taphonomic factors

CHAPTER 2: FORENSIC DNA ANALYSIS

In Chapter 1, human skeletal cellular biology was explored in depth with references made to forensic DNA analysis. This section flips the lens and examines the field of forensic DNA analysis, drawing pertinent lines of connection to human skeletal biology. Different approaches to the forensic application of DNA analysis are examined through time leading up to contemporary practices and briefly discussing potential future research. While the construction of the “heat map” is primarily focused on autosomal

DNA, forensic casework often employs mitochondrial DNA (mtDNA) for its unique properties and information, so there is discussion of such in this section. Likewise, both X and Y chromosomal analysis is pertinent to forensic applications and will be addressed. To a limited extent, ancient DNA (aDNA) studies are discussed as some of the limitations encountered, methods employed, and reasons for differential DNA preservation, extraction, and quantitation are relevant to modern forensic contexts. Additionally, because this project is focused on the cellular components of bone as potential reasons underlying the differential preservation of DNA, what happens to the cells and the genetic material they hold after death needs to be understood. Therefore, the taphonomic forces which influence the differential preservation and extractability of DNA across the human skeleton are discussed in this section, focusing on the cellular, biochemical and biomineral characters at play during and after decomposition.

HISTORY & THEORY

The idea that biological traits can be examined to identify an individual, whether deceased or alive, has been explored, discussed, written about, and published on, for centuries. Much like Clopton Havers' early observations of bone cells, the very first cases of forensic victim identification come from Europe during the Enlightenment Period of the 17th and 18th centuries. During this time, there was a growing belief in Biological Determinism. That is, that perpetrators of crime (whether actual or only potential) could be identified by various morphological traits and victims of said crimes could be similarly identified. Despite a resurgence in popularity during the eugenics movement in the early 20th century, Biological Determinism, as a paradigm, has slowly lost favor over the years. The influence of environment on behavior has become better understood and

more widely accepted, supported by acknowledgement from the scientific community that genetics cannot always explain *why* an individual acted in a certain way or whether genetics played a role in victimization. In forensics, this coalesced to an extent in the Supreme Court ruling that forensic evidence must meet an objective, peer-reviewed, scientific standard (Daubert v. Merrell Dow Pharmaceuticals, Inc. 1993). As time, science, and culture have advanced, the methods used have come under greater and greater scrutiny by the criminal justice community, and indeed, by society at large. In the waning decades of the 20th century, the use of DNA to establish identity of both victims and perpetrators was invented and has become the standard against which all other methods are compared.

In forensic science, most evidence has both class characteristics and individual characteristics, and human genetic material is no exception. Class characteristics are those which are similar across typologies and allow for generalized identifications (for example a projectile may exhibit class characteristics that identify it as a bullet fired from a rifle, but not the specific make or model of rifle). In forensic genetics, mtDNA and both X- and Y- chromosomal DNA are informative on a genealogical or phylogenetic level, but they lack the discriminating characteristics required to identify a specific individual. The data gathered from mtDNA can be, and is, used to make familial matches in cases where the decedent is unknown. And Y- chromosomal analysis is similarly effective in cases where paternity or paternal lineage is needed. For example, if an unknown decedent is profiled as male and the nearest potential relative is the father, then the Y- chromosomal analysis is necessary since the two males would have different mtDNA. If the nearest potential relative is a brother, then mtDNA would be useful (assuming they

have the same mother) and the Y-chromosome would be useful as a confirmation of relation (assuming the siblings had the same father).

Non- sex-linked autosomal DNA is what can identify individuals or maintains the individual characteristic. Returning to the illustration of the bullet and the gun, the barrel of a particular rifle, the firing pin, and the ejection port will all leave unique indicators on bullets and shell casings as they are fired and allow that specific projectile to be linked back to that specific weapon. Regardless of manufacture, no two firearms are exactly the same and (except in cases of identical twins) no two humans have exactly the same autosomal DNA, regardless of parentage. Therefore, in cases where a victim must be identified to an extremely high degree of probability, or a specific perpetrator must be linked to a specific location or piece of evidence, it is that individual's unique autosomal genetic profile that must be obtained.

In the United States, a rigorous benchmark has been set for the identification of a perpetrator of crime using DNA, and victim identification investigations strive to live up to the same standards. Using short tandem repeats (STR's) which will be discussed in more detail below, the genetic profile of a suspect must match at least 20 points, known as *loci*, to the DNA left behind at a crime scene in order to be considered a "positive match." This is discussed in more detail below. The greatest goal would be to match a complete genome from crime scene to suspect and from victim to reference sample. But, for a multiplicity of reasons, that goal is very rarely achieved. The benchmark for criminal prosecution is rightly very high and victim identification efforts should be no less rigorous.

So, the question at hand is how do we obtain the greatest accuracy in our attempts at victim identification? If there is a presumptive identification (a driver's license, for example, is considered a presumptive ID), then it is far easier to obtain familial reference samples for DNA comparison, medical and dental records, and so on to try and match the remains to an individual identity. If there are no other overt indicators of identification, however, then investigators must rely on forensic anthropologists, odontologists, and hope that DNA analysis results match up to records in a national database such as the violent criminal apprehension program (VICAP) or the Armed Services database.

ACRONYM SOUP

The field has evolved over the last 30 years, becoming more accurate, less expensive, and faster. In the beginning, long, repeating, fragments called Variable Nucleotide Tandem Repeats (VNTR's) were used in both victim ID and in prosecutorial endeavors (91). VNTR testing was expensive and not nearly as reliable as modern methods, given that genome-wide frequencies of the nucleotides being examined did not exist at the time. The very name itself also gives a clue to this method's greatest shortcoming: *variable*. The repeat units being employed in this method vary too widely across populations and there was no effective way to reduce allele drop-out which is a common source of error in genetic data analysis, even today (46).

The next method that was developed involved the use of Restriction Fragment Length Polymorphisms (RFLP's). RFLP analysis requires the use of restriction enzymes and probes, and typically focuses on a specific gene. This method, while effective at discriminating variation between individuals, is laborious, time-consuming, subject to a significant degree of human error, and is prone to other issues that are specific to

polymerase chain reaction (PCR) amplification methods, known as inhibitors (46,92–94). While RFLP's are more consistent across populations, and thus more reliable than VNTR's, today's amplification and sequencing technology is sufficiently advanced that this technique is no longer necessary. Additionally, RFLP analysis is not ideal in cases or situations where the DNA is already, or is assumed to be, highly fragmented.

Single Nucleotide Polymorphisms (SNP's) are, as the name implies, very small polymorphisms that occur due, primarily, to mutations. The primary drawback to using SNPs in a forensic setting is the number of specific SNPs which are needed to identify an individual. In the last ten years, several studies have been published about the possibility of using SNPs in forensic settings and while there are SNPs that can be individualizing (iiSNPs), most are still in the realm of ancestry-informative, or aiSNPs (95–99). While SNPs and Indels (insertions or deletions of small chunks of base pairs) have a lower rate of mutation than STRs, all studies have still found that a large number, between 40 and 150, are required to even approach the same genetic information gleaned from 13- 20 STRs. The consensus is that SNPs are extremely useful in confirmatory roles, but still lack the individualizing power of discrimination required in forensic contexts. The final consideration that keeps SNPs and Indels from overtaking STRs in forensic settings (for the moment, anyway) is that there are already large databases of reference STRs from victims, perpetrators, and average citizens against which investigators can compare their samples. However, research into the forensic utility of SNPs and Indels is gaining considerable momentum and offers a wealth of future research potential.

The discovery of Short Tandem Repeats (STRs) in the early 1980's greatly increased the reliability of forensic DNA analysis and replaced VNTR's in the 1990's.

Multiple STRs occur throughout the human genome and knowledge of these allowed for the creation of standards, as well as the ability to generate identification with degraded or fragmented DNA. While a SNP could occur anywhere in the genome or get lost in either populational redundancy during analysis or in taphonomic degradation, the ability to predict, and thus amplify STRs was one of the defining features that led to the rise of this method at that time. STR analysis quickly replaced all previous methods and have been adopted by both the FBI and European forensic and law enforcement agencies. In 2017, the FBI, aided by investigatory task forces from multiple scientific endeavors, expanded the minimum number of STR loci to be used in criminal cases from 13 to 20. The nature and utility of STRs is well characterized in the literature (46,84,92,100–103) and this has become the standard method for forensic DNA analysis globally. Shewale and Liu's 2014 textbook lays out the structure, history, and contemporary use of STR's in detail and is an invaluable reference for anyone interested in the topic.

FORENSIC STR ANALYSIS

STRs occur on every chromosome in the human autosomal genome. While some of the repeating motifs in STRs are as short as 2 bp's and some are hundreds of bp's long, those most useful in forensic casework, and thus the ones employed in CODIS, mostly consist of 4 non-coding bp's that repeat a certain number of times at a given locus. Some CODIS STR's are only 3 bp's long and some are 5, but most are 4 bp's long and are commonly referred to as *tetranucleotides*. The number of repetitions vary from just over a dozen to several dozen. Some of those that only involve a few repeats, known as *MiniSTR's*, are extremely useful in cases of degraded DNA (94,104). Commercially available kits have been, and continue to be, developed that reduced the number of

necessary PCR cycles, increased the number of samples that can be tested simultaneously (multiplexing), and incorporate the newer loci which include sex- discriminating STR's (93,102,105). Capillary electrophoresis (CE), the method used in this project and discussed in greater detail in the methods section, is still a highly effective, and decreasingly expensive, method of STR profile construction.

Against a backdrop of human genomes, STR “matches” are calculated simply by multiplying the populational percentages of each STR in the sample. For example, an individual's STR profile is obtained from a buccal swab and the percentage of people exhibiting the same allele at the CSF1PO locus are multiplied by the percentage of people also exhibiting the same allele at the remaining 19 loci. The probability of multiple people within a given population exhibiting the identical STR profile is a magnitude of $1:1 \times 10^{-n}$. where n is the number STR loci employed. The more loci that match, obviously, the lower the probability of a duplicate. With the addition of the 7 new loci by the FBI, those probabilities are in the trillions to quadrillions (93). Image 1 lists the STR loci used in the Combined DNA Index System (CODIS).

In early 2015, the FBI announced that the validation project for additional CODIS Core Loci had been completed and that an additional seven loci would be added to the CODIS Core effective January 1, 2017.³ The additional seven loci—D1S1656, D2S441, D2S1338, D10S1248, D12S391, D19S433 and D22S1045—along with the original 13 loci, will comprise the new CODIS Core Loci. Below is a listing of the 20 CODIS Core Loci.

- CSF1PO
- D3S1358
- D5S818
- D7S820
- D8S1179
- D13S317
- D16S539
- D18S51
- D21S11
- FGA
- TH01
- TPOX
- VWA
- D1S1656 (effective January 1, 2017)
- D2S441 (effective January 1, 2017)
- D2S1338 (effective January 1, 2017)
- D10S1248 (effective January 1, 2017)
- D12S391 (effective January 1, 2017)
- D19S433 (effective January 1, 2017)
- D22S1045 (effective January 1, 2017)

Image 4 - STR loci used in forensic DNA analysis. Reproduced from the CODIS website: fbi.gov.

Y- AND X- CHROMOSOME STR'S

The STR's listed above, those typically used in both perpetrator and victim ID cases, are located on the 22 autosomal chromosomes of nuclear DNA. For the most part, sex-linked STRs, found on the X and Y chromosomes respectively, do not have the individuation power that the others have and are better used for general kinship, evolutionary, and haplotype/ haplogroup studies. Forensically speaking, these markers are used almost exclusively in paternity testing and in cases of sexual assault.

New studies of STRs found on both of the sex chromosomes, however, are beginning to show promise of the ability to confirm individuation made by other means.

Rapidly mutating Y- STRs have been found which will, no doubt, enhance the utility of these markers in forensic casework (106,107). Newer studies of STRs on the X chromosome are showing similar potential. Although the studies are still primarily populationally specific, their ability to confirm or refute identity has the definite potential for future expansion into other avenues of forensic casework (108,109).

This project does involve extraction and amplification of the Y-chromosomal DNA in tandem with the major focus of differential DNA preservation across the human post-cranial skeleton. In keeping with the overall goal of the project and the relative utility of the male chromosome in forensics, Y-STR analysis in this study is primarily research oriented with a secondary goal of haplogroup analysis and potential kinship reference material. Sex confirmation in this case is a tertiary concern since visual analysis of the individual at autopsy and subsequent forensic anthropological analysis both concluded the individual was male.

MITOCHONDRIAL DNA (MTDNA)

Albert von Kölliker, the same German microbiologist who first described osteoclasts, was also the first to describe the mitochondria in 1857. Originally coined “bioblasts” by Kölliker, they were renamed some 40 years later by Carl Benda. It wasn’t until the 1950’s, however, that their role as energy producers was uncovered and the term “powerhouse of the cell” applied by Philip Siekevitz. As research progressed, it was discovered that mitochondria were once part of a bacterium that was endocytosed by another prokaryotic cell and developed a symbiotic relationship trading energy (in the form of ATP) for protection. That relationship, possibly the longest standing one in Earth’s history, survived through the development of eukaryotes and into today. Medical

and microbiologists had also learned, by the mid- 20th century, that during fertilization of a human egg by a sperm cell, the mitochondria (located solely in the tail of the spermatozoa) were excluded from entering the egg. This dovetailed nicely with the discovery that mtDNA moved only along the maternal lineage. Utilizing this information, plus the discovery that mtDNA has a much higher mutation rate than nuclear DNA, scientists found they were able to trace human maternal lineages a long way back into the past. In 1987 groundbreaking works were published about the utility of mtDNA in human evolutionary studies with concepts about the molecular clock and mitochondrial Eve, respectively (110,111).

In the 30+ years since those articles, biological anthropologists have successfully extracted and typed whole mitochondrial genomes of modern humans, Neanderthals, and Denisovans. As our technology continues to improve, phylogenetic studies continue to become more detailed and our understanding of the human diaspora across the Earth has come into sharper focus. Unlike nuclear DNA, mtDNA occurs in much greater numbers within the mitochondria of a cell. This high copy number in the cells, its somewhat protected location within the mitochondria, and its circular shape, often allows mtDNA to survive in bone tissue better than does nuclear DNA (112–114). All of the factors contribute to its utility in studies dealing with extremely old or degraded samples. In forensics, we often analyze mtDNA when the autosomal material is too fragmented, or in cases where limited skeletal elements prevent nuclear STR profiling. While it does not have the power to identify an individual, mtDNA is useful in forensics as a means of excluding a potential suspect or victim, and it is useful as an aid to forensic anthropological assessments of ancestry. In cases of unknown remains, often times

mtDNA can lead to a familial match with a mother or sister or even a daughter. At that point, other means of individuation are utilized to confirm the identity of the deceased.

ANCIENT DNA

Ancient DNA (aDNA) was originally a term indicating a general age of the origin of a given sample. It has become, however, an umbrella term in genetic casework referring to DNA extractions and analyses where the long, double-stranded autosomal DNA is broken, or fragmented. This is usually because the biological tissues or fluids the samples are taken from are less than perfectly preserved. A more detailed discussion of the specifics of DNA fragmentation and degradation is provided in the following chapter. Since most of the skeletal remains that are surrendered to ME's or Coroners offices have been subjected to unknown (and presumably less than ideal) taphonomic influences for an unknown amount of time, the *de facto* assumption is that any genetic material recovered from the samples will be degraded, or fragmented, to some extent. Working under this assumption compels investigators to follow more stringent protocols and allows us to be happily surprised if the results are better than expected. Further discussion of such taphonomic processes is provided subsequently.

Ancient DNA (aDNA) studies are relevant to forensic casework because of what has been, and continues to be, learned about genetic fragment analysis and DNA survivability through time, across different skeletal elements, and in spite of (or perhaps, because of) various taphonomic environments and processes. The ability to extract DNA from megafaunal skeletal remains as old as 400,000 years (115,116) and fossil hominin DNA as old as 45,000 years (117,118). have helped propel modern forensic DNA extraction techniques and technologies. Finding consistently reliable results from aDNA

extractions from teeth as well as the otic portion of the tympanic region of the temporal bone (9,79,119,120) has informed forensic investigators on the where to look for reliable sources of genetic material, as well as how to chemically extract the DNA from bone tissue in order to facilitate amplification. Indeed, the protocol documented by the Dabney, et al study from 2013 is one of the methods used in this project and is discussed further in the methods section.

The otic region of the tympanic portion of the temporal bone is made up of trabecular bone surrounded by a layer of cortical bone that lies within the cranial vault. It houses and protects the delicate bones of the inner ear and plays a vital in hearing. As such, the otic region undergoes a high degree of lifetime remodeling. The cellular processes and the general location of the region most probably account for the high level of DNA survivability written about by biological anthropologists, specifically documented in the Pinhasi, et al (2015) study. The teeth are the other primary sources of aDNA due to the well documented protection afforded by layers of dentin and enamel. Teeth survive for an extremely long time post-mortem and protect DNA from taphonomic process that normally degrade genetic material (119,121–123).

Proteomics are becoming more and more popular in studies of ancient organisms. This is a kind of reverse- engineering whereby, the proteins that remain in bone samples, or even fossilized bones, are used to reconstruct the genes that coded for them. Once the organism's proteome has been established, some further reverse- engineering leads to a tentative genome. In this way, investigators have been able to learn a surprising amount from bones well over 100,000 years old (124,125). These methods, though not widely

used in forensics as of yet, have the potential to make a huge contribution to the science in general, not just in cases of DNA degradation.

Chapter 3: MOLECULAR TAPHONOMY

Taphonomy of osseous tissues has been, and continues to be, a topic of paramount importance in forensic anthropology. This is both a process- based understanding of how and at what time intervals these changes occur, as well as an appreciation for what implications these changes and processes have on the macroscopic morphology, the microstructural composition, and the condition of endogenous DNA within the bones. Studies of taphonomic process are abundant in the forensic anthropological literature; historically focusing on macroscopic changes that may alter traditional forensic anthropological construction of the biological profile. More recent studies have focused on whether and how certain taphonomic processes and maceration techniques affect DNA in bones. The newer taphonomic studies focus on the soil around the body at the time of deposition or burial. Mostly, the factors examined in such studies include soil composition, moisture and pH levels, as well as microbial constituents or other environmental degradative agents. Maceration studies have focused on the chemicals involved and the temperature of the solution in which the bones are processed; as both of these certainly have some effect on the quality (strand length) of endogenous DNA when forensic analytical methods (such as STR and SNP panels) are to be employed.

For this project, the taphonomic factor most at play is the maceration technique employed to separate the soft tissue from the osseous. Recently, some studies have hinted

at an internal taphonomic players such as the individual's age and relative bone density at the time of death. Though this project does not delve into this factor, there is a great deal of potential future research in such a proposition. While the impact of maceration techniques on endogenous DNA in bone tissue is documented to a greater extent than the internal factors, in neither case is there adequate understanding of the *how* or *why*. For example, the popular opinion for some time was that, because they are embedded within the bone tissue, osteocyte populations are responsible for the DNA that is recovered from bone tissue. However, this is unproven and does not fit with the results obtained in studies of differential DNA preservation patterns across the skeleton (1,2,12,113,126–128) and also does not take into account attrition of osteocyte populations as the individual advances in age (9,12,22,43,129). And while it was originally assumed that chemicals such as bleach would have a negative impact on endogenous DNA levels, studies such Steadman et al 2006 indicate that temperature has a greater effect than detergents or chemicals. Nearly all studies today, including but not limited to those listed above, acknowledge a lack of understanding about which cellular components of bone are responsible for contributing to the genetic material recovered bone, as well as what biochemical/biophysical properties of bone tissue are involved with the preservation of DNA in spite of the various degradative processes. It is therefore crucial to understand the types, processes, and patterns of DNA degradation.

TYPES OF DAMAGE

Base Degradation

Hydrolysis, defined as the breakdown of a compound due to interaction with water, is the most common degradative process to which DNA is subjected. Hydrolytic

damage causes deamination, whereby a cytosine is changed to a uracil, adenine is converted into hypoxanthine, or guanine is converted to xanthine. These switches are known as “transitions.” Hydrolytic deamination lesions are usually repaired in life, though such post- mortem changes can be misdiagnosed as *in vivo* mutations, rather than taphonomic alterations. However, hydrolytic deamination of 5-methylcytosine to thymine at the 5’ end CpG site converts the G to T and cannot be repaired *in vivo*, resulting in a lasting mutation.

Hydrolysis also causes depurination which manifests as the elimination of either an A or a G resulting in an abasic, or apurinic, site. Depurination also occurs at T and C sites, although at a much slower rate. Even though the pyrimidines (Cytosine and Thymine) are subject to this type of damage, it is known as “depurination” simply because it occurs more quickly and easily at the purine (Adenine and Guanine) sites. Post-mortem depurination is easier to recognize as being taphonomic than are the deamination transitions noted above.

Most maceration methods involve the use of water, often with added solvents. Thus, hydrolysis is the primary degradative agent encountered in studies where the bones have been artificially defleshed. However, it is not solely the water itself that raises concerns, but also the temperature of the water used. Increased heat has the positive effect of increasing efficiency when removing soft tissue but the negative effect of also increasing depurination/deamination of the DNA inside the bones. For illumination of the damage inflicted by high temperature and high humidity, one need only look at a globe. It is well documented that bones recovered from latitudes between the tropics of Cancer

and Capricorn rarely yield the same quantity or quality of DNA as those recovered from cooler climates at higher latitudes (130).

Another agent of base pair degradation is oxidative damage. Similar to deamination/ depurination by hydrolysis, oxidation causes transversions from G:C → T:A. Oxidation is caused mostly by exposure to radiation or chemical ions, known as radicals, such as OH[•], a hydroxyl radical (131), or CO₃^{•-}, a carbonate radical (132). While an in-depth discussion of the specific chemical reactions that cause these radicals to occur are outside the scope of this project, it is pertinent to understand that they occur in much higher frequency in living tissue and the damage to living DNA is usually repaired, though oxidative damage can be carcinogenic. This is the primary form of base pair damage encountered in bone tissue recovered in drier climates. Which, while understudied, could be due to persistent exposure to solar and cosmic radiation, differential microbial activity, and/or chemical reactions in the soil and the immediately adjacent atmosphere (133). This also accounts for the slower pace of oxidative damage compared to hydrolysis. Studies such as those by Antinick and Foran (2019) and Misner, et al (2009) seek to correlate remaining endogenous DNA to weathering patterns found in skeletal material from various depositional environments. Yet nearly all studies indicate that skeletal weathering is rarely a valid indicator of the conservation of DNA quality (strand length) or quantity (copy number). Buried bone exhibited greater damage levels than did those deposited on the surface, further indicating the possibility that oxidative damage is a greater threat to living bone than it is taphonomically important (134). Therefore, it is important to realize that the visual appearance of weathering, be it

bleached from subaerial exposure or stained by soil and water, may lead to erroneous assumptions about the preservation of DNA within the elements.

Structural Degradation

Structural damage to DNA may be a more serious detriment even than oxidative or hydrolytic degradation. Cross-linking is a form of damage that occurs when DNA is subjected to UV radiation. It causes the double-helix strand to twist and “kink up” on itself, like an old strand of Christmas lights. The sugar-phosphate backbone of the DNA strand will bind in places where it normally would not. Strands that have undergone this type of damage will not amplify in laboratory settings, and thus UV light is an effective method for preventing contamination in aDNA labs. Cross-linked DNA is the primary reason for low copy number data in genetic profiling. Essentially, if the sample has undergone an extensive degree of this type of damage, no DNA will be analyzable because once the strand is knotted up, it can’t be untangled.

Probably the easiest form of post-mortem damage to work around is strand breakage, at least with more recent analysis methods. Strand breakage occurs by hydrolysis or oxidation and is, quite simply, breaks in the DNA strand. Modern primers are designed to adhere to the broken ends of the strands in the sample DNA and allow researchers to amplify the remaining genetic material for analysis. This was not always the case and in the early days of gel slab electrophoresis, it was seen as a dire limitation, even though researchers could see that some DNA remained in their samples. Today, in samples where the taphonomic damage to DNA is unknown, or is thought to be severe, the assumption of widespread strand-breakage simply prompts researchers to design primers that will bind to the smaller, broken, fragments in the sample. This allows for

greater success in PCR amplification whether the ensuing steps are geared toward complete genomic assembly or, in projects such as this, STR profile generation.

Each of these different types of DNA degradation, depurination by hydrolysis, oxidation, cross-linking, and strand breakage, require mitigation measures in the lab when attempting extractions. Ergo, the *a priori* assumption for this project is that all types of extractable DNA have undergone a level of degradation such that the methods employed in aDNA studies are necessary to establish a baseline of the quantity (physical amount, or copy number) and quality (strand length, number of lesions, etc.) of whatever genetic material may remain in the bones. The Pääbo, et al (1989) article outlines the issues and difficulties encountered in very old specimens and these are the same conditions that are assumed to be operative when dealing with samples of unknown provenience. By treating the specimens as though they had undergone more extensive damage than may be the case allows for a more thorough investigation of all DNA types across all skeletal elements and thus affords the opportunity to ascertain the cellular components that are contributing their genetic material and the biochemical factors that are protecting the DNA from degradation.

Rate and Patterns of Decay

Much of what is known regarding the rates and specific steps in the degradation of DNA, whether mitochondrial or nuclear, comes from *in vitro* studies, or studies involving DNA extractions taken from soft tissue. Since soft tissue decomposition progresses through several distinct and well-documented phases, it is known that the DNA recovered from soft tissue is subjected to damage that is not identical to the processes that damage the DNA recovered from osseous tissue. Studies that do

investigate the patterns and rates of DNA degradation from bone often encounter issues (especially in terms of establishing correlation, causation, and/or statistical significance) directly related to a number of factors such as: small sample size, varied depositional environments, extreme (and often widely ranging) post-mortem intervals (PMI's), and extinct and/or non- human species (2,88,135–137).

While some of these studies do offer some insight into the rates (kinetics) of DNA degradation, there are still more variables that prevent accurate model building. For example, there are kinetic differences between mtDNA and nuclear DNA degradation (135), and differences in decay have also been shown in mtDNA extractions between different dental substances (9). Brundin et al published a study in 2013 which showed *in vitro* DNA molecules that are bound to hydroxyapatite crystals survive significantly longer than those DNA molecules which are not bound to hydroxyapatite in 3 substrates (water, sera, and DNase I). All these studies do hint at unknown cellular and biochemical factors and the common thread is that what is still unknown makes it virtually impossible to predict the quantity (how many chunks of base pairs) or quality (strand length, number of lesions) of endogenous DNA that will be conserved in any given skeletal element outside of a laboratory. Due to widely ranging depositional environments, this also means that it is extremely difficult to ascertain a constant rate of genetic decay in specimens outside of a laboratory setting.

Furthermore, from Pääbo's early work in the late 1980's through today, attempts to obtain genetic material from ancient specimens has advanced our understanding of not just the types or even the rates of genetic degradation, but also the patterns of how these processes typically play out in the natural world. Modern biomedical studies of both *in*

vivo and *in vitro* samples and aDNA studies from long dead samples have provided us with the beginnings of an understanding that, while subject to a wide array of factors and a significant degree of stochasticity, there may be more of a pattern to DNA damage than originally feared. It has been shown that *in vivo* DNA strands more commonly break at certain locations and some base pair transitions, or misincorporations, occur more commonly at 3' ends and others at 5' ends, that an overabundance of cytosines in certain locations is indicative of post- mortem transition, and so on (9,88,130,131,135,138–140). To that end, a computer program called mapDamage was designed that scans genetic data for these patterns and help researchers to distinguish between what is endogenous to the sample and what is most likely a contaminant contribution from outside sources, and to a lesser extent, post- mortem versus ante- mortem change (141). A thorough investigation of bioinformatic methods such as this is beyond the scope of this project. However, even the best chemical primers, computer programs, and bioinformatic pipelines cannot repair taphonomic damage or perfectly distinguish between post-mortem changes and *in vivo* mutations.

Because it is impossible to predict the extent and nature of post-mortem damage to DNA contained in every specific bone sample, there is need for methods that will allow researchers an insight prior to the destructive processes of DNA extraction. Modern extraction methods are far less destructive than in years past, due in large part to improvements in primers, dNTP's, and other chemical components of the extraction, PCR, and library preparation steps. However, even more insight would be useful. If only a tiny amount of bone powder could give researchers an indication of whether the element (or fragment) was to be useful or should be preserved as is, more fragments or

elements could be preserved and efficiency would increase. It is for this reason that this project uses Attenuated Total Reflectance Fourier Transform Infrared (ATR-FTIR) tests to measure the chemical bonds within each element. Samples that indicate chemical bonds consistent with those found in DNA can then be confidently used for extraction purposes (24–26). While this test is still yet to be widely employed, preliminary results are encouraging.

Because of the assumption of the primacy of depositional environment and, secondarily, whatever decomposition or maceration may have occurred on the condition of endogenous DNA in skeletal tissue, combined with the understanding that the physical tools, chemicals, and temperatures used to remove any lingering soft tissue, there is growing appreciation of aDNA extraction and amplification methods. Indeed, the term “aDNA” itself no longer refers merely to the age of the sample, but the condition of the DNA within. Some of the methods are being used even in modern forensic settings when the endogenous genetic material has experienced unknown degrees of degradation due to strand breakage, depurination, etc. And while analytical tools such as mapDamage continue to improve the interpretation of genetic material by scanning read sequences for signatures of specific damage types, it is no longer sufficient to understand merely that some bones persist better than others through time, that different soil types have different macrostructural effects, or merely that DNA degrades in certain ways. Contemporary studies must be deeply involved with answering questions of *why* these phenomena occur the *way* they do and *what*, exactly, is involved on a cellular and microstructural level.

Methods

The methods used in this study were chosen for their ability to effectively test the underlying hypotheses that extractable and amplifiable DNA from the human post-cranial skeleton will be highly dependent on cellular populations and activity and the biochemical properties of that bone tissue. These methods were also chosen for their applicability, as the project is keenly interested in reducing the amount of destruction to human bone tissue necessary for STR profile construction.

Sample Selection

One of the primary goals of the project has been to develop and test a more targeted approach to sample collection for the purposes of DNA extraction and analysis. This involved applying the knowledge of bone cell types, their position on the elements as indicated by both knowledge and visual assessment, and an understanding of the biochemical properties of the different bone tissue types. Thus, samples were taken in a very strategic manner (table 1). Flowing from the overarching hypotheses of the study, the samples used in this analysis were selected based on the following criteria:

- 1) Visible bony changes to the cortical layer indicative of ante- or perimortem cellular activity
- 2) Bone tissue type
- 3) Notable sites or elements in the known literature on forensic DNA extraction

Since the project focuses on the post-cranial skeleton, multiple samples were taken from every element wherever possible. Due to their small size, samples taken from the carpals, tarsals, sesamoids, 1st metacarpals, 1st metatarsals, and phalanges were collected

irrespective of tissue type. The 3rd metacarpals/ metatarsals were robust enough to provide distinction between cortical and trabecular tissue. Additionally, since the mechanical action of drilling into bone tissue occasionally leads to some amount of bone powder being propelled away from the collection boats, in an effort to reduce waste, any dispelled powder was collected and created an extra sample that is a combination of tissue types.

Additionally, because it is well established that the petrous portion of the temporal bone and the teeth are excellent repositories of endogenous DNA, samples were also taken from both of the petrous regions and the right maxillary 1st molar (RM₁) for comparative purposes. Furthermore, ancient samples were obtained from elements that had not yielded good results in DNA quantitation efforts in another study. These allowed a baseline for biochemical analyses and will be discussed further in the ATR/FTIR section below.

Element	Site I	Site II	Site III
Manubrium	Clavicular notch (C)	Ventral surface (C,T)	N/A
Sternum	1 st costal notch (C)	5 th costal notch (C)	Ventral surface (C,T)
Xiphoid	Entire (C)	N/A	N/A
Clavicle	Sternal end (C,T)	Lateral end (C,T)	N/A
Scapula	Coracoid process	Acromion process	Glenoid fossa (C,T)

	(C,T)	(C,T)	
Humerus	Intertubercular sulcus (C,T)	Deltoid tuberosity (C,O,T)	Trochlea (C,T)
Ulna	Olecranon process (C,T)	Brachial tuberosity (C,O,T)	Extensor carpi ulnaris groove (C,T)
Radius	Head (C,T)	Radial tuberosity (C,O,T)	Ulnar notch (C,T)
Carpals	Radial/Ulnar articular surfaces (C)	Entire Pisiform (T)	Metacarpal articular surfaces (C)
Metacarpals	Prox. articular Surfaces (C)	Mid-diaphyseal (C,T)	Distal articular Surfaces (C,T)
Phalanges	Prox. Articular surfaces (C,T)	Distal articular surfaces (C)	Entire distal phalanges (C)
Ribs	Head (C)	Tubercle (C)	Sternal end, where applicable (C)
Vertebrae	Inferior aspect of vertebral body (T)	Anterior aspect of vertebral body (T)	Posterior aspect of vertebral body (T)
Sacrum	Sacral promontory (T)	Auricular surface (C)	Transverse lines (C,T)

Ilium	Auricular surface (C)	Posterior inferior iliac spine (C)	Iliac crest (C)
Ischium	Ischial spine (C)	Ischial tuberosity (C,T)	Inferior ischial ramus (C,T)
Pubis	Pubic symphysis (C,T)	Dorsal surface (C)	Ventral surface of the pubic face (C)
Femur	Fovea capitis (C,T)	Linea aspera (C,O,T)	Intercondylar fossa (C,T)
Patella	Medial articular facet (C,T)	Lateral articular facet (C,T)	N/A
Tibia	Tibial plateau (C,T)	Interosseus surface (C,O,T)	Malleolar groove (C,T)
Fibula	Styloid process (C,T)	Interosseus crest (C,O,T)	Fibular groove (C,T)
Tarsals	Sustentaculum tali & calcaneal tuberosity of the calcaneus (C,T)	Talar dome & head of talus (C,T)	Anterior & posterior articular surfaces of other tarsals (C,T)
Metatarsals	Proximal (Tarsal) articular surfaces (C,T)	Distal articular surfaces (C,T)	N/A

Phalanges	Prox. Articular surfaces (C,T)	Distal articular surfaces (C,T)	Entire distal phalanges (C)
Element	Site I	Site II	Site III
Manubrium	Clavicular notch (C)	Ventral surface (C,T)	N/A
Sternum	1 st costal notch (C)	5 th costal notch (C)	Ventral surface (C,T)
Xiphoid	Entire (C)	N/A	N/A
Clavicle	Sternal end (C,T)	Lateral end (C,T)	N/A
Scapula	Coracoid process (C,T)	Acromion process (C,T)	Glenoid fossa (C,T)
Humerus	Intertubercular sulcus (C,T)	Deltoid tuberosity (C,O,T)	Trochlea (C,T)
Ulna	Olecranon process (C,T)	Brachial tuberosity (C,O,T)	Extensor carpi ulnaris groove (C,T)
Radius	Head (C,T)	Radial tuberosity (C,O,T)	Ulnar notch (C,T)
Carpals	Radial/Ulnar articular surfaces (C)	Entire Pisiform (T)	Metacarpal articular surfaces (C)
Metacarpals	Prox. articular Surfaces (C)	Mid-diaphyseal (C,T)	Distal articular Surfaces (C,T)
Phalanges	Prox. Articular surfaces (C,T)	Distal articular surfaces (C)	Entire distal phalanges (C)
Ribs	Head (C)	Tubercle (C)	Sternal end, where

			applicable (C)
Vertebrae	Inferior aspect of vertebral body (T)	Anterior aspect of vertebral body (T)	Posterior aspect of vertebral body (T)
Sacrum	Sacral promontory (T)	Auricular surface (C)	Transverse lines (C,T)
Ilium	Auricular surface (C)	Posterior inferior iliac spine (C)	Iliac crest (C)
Ischium	Ischial spine (C)	Ischial tuberosity (C,T)	Inferior ischial ramus (C,T)
Pubis	Pubic symphysis (C,T)	Dorsal surface (C)	Ventral surface of the pubic face (C)
Femur	Fovea capitis (C,T)	Linea aspera (C,O,T)	Intercondylar fossa (C,T)
Patella	Medial articular facet (C,T)	Lateral articular facet (C,T)	N/A
Tibia	Tibial plateau (C,T)	Interosseus surface (C,O,T)	Malleolar groove (C,T)
Fibula	Styloid process (C,T)	Interosseus crest (C,O,T)	Fibular groove (C,T)
Tarsals	Sustentaculum tali & calcaneal tuberosity of the calcaneus (C,T)	Talar dome & head of talus (C,T)	Anterior & posterior articular surfaces of other tarsals (C,T)
Metatarsals	Proximal articular surfaces (C,T)	Distal articular surfaces (C,T)	N/A
Phalanges	Prox. Articular	Distal articular	Entire distal phalanges

	surfaces (C,T)	surfaces (C,T)	(C)
--	----------------	----------------	-----

Table 1- List of drilling sites. Applies to both LEFT and RIGHT sides. Bone tissue type from each site is listed as: C = cortical, T = trabecular, and O = osteonal.

Sample Preparation

In an effort to reduce the risk of DNA contamination, a semi-sterile room devoted exclusively to the purpose of bone sample collection was established (142,143). The room is as environmentally isolated as possible and rules for the use of the room incorporate many of the published recommendations for facilities designed for aDNA studies (CITE). Prior to sampling, the drilling area itself was wiped down with either a 3.75% enzyme-based bleach solution or DNAway®. All tools were likewise decontaminated. Investigators wore masks, eye protection, and nitrile gloves (also decontaminated with bleach or DNAway®). The bones were cleaned with 3.75% enzyme-based bleach (sodium hypochlorite) and allowed to soak for 15 minutes. They were then rinsed 2-3x with distilled water and allowed to air dry overnight in a drawer lined with UV sterilized paper towels.

Between each drilling session, all tools were wiped with DNAway® or bleach solution and metal components were then autoclaved at 250°F for 25 minutes. Plastic components such as microcentrifuge tubes and weigh boats were placed in a crosslinker and subjected to UV-C light for 5 minutes. The room itself was decontaminated with UV-C light for 30 minutes. Because the room is not fully climatically independent from the rest of the Social Sciences building on the University of Montana campus, precise control of the temperature of the room was not possible. However, relative humidity levels were

adjusted by the use of evaporators or humidifiers, depending on the need. It was discovered that the optimal climactic environment for drilling was approximately 60-65°F and approximately 45% relative humidity. In these conditions, there was enough humidity to prevent static electricity from causing the bone powder to “float” inside of the plastic collection tubes while also being dry enough to exclude excess environmental moisture from the samples. Either extreme caused mismeasurement of sample weights and added extra effort and time to the work of sample collection.

Sample Collection

All bone tissue samples were taken using either a rechargeable, handheld, Dremel® 7760 or an air-powered BienAir® Station S001 dental drill with a 1mm dental burr. Power settings with both machines were deliberately kept as low as possible to avoid any potential damage to the endogenous DNA that might occur as a result of heat generated by the machines or their action on the bones (144). The Dremel was set to the second power setting and the dental drill, through the use of an air pressure regulator, was kept at or below 40psi.

Collection of cortical bone tissue samples was performed by running the drill over the surface of the targeted region. All attempts were made to minimize the area of necessary sampling, while still maintaining accuracy of cortical bone. In other words, since the actual cortical layer of bone is very thin on most elements, only very light manual pressure was applied in collection of these samples, and they are generally no larger than 1 cm². For the osteonal samples (limited only to mid- diaphyseal drilling sites on the humerus, radius, ulna, femur, and tibia), more pressure was applied at the same location

of the cortical sampling in order to ensure that only the osteonal tissue was being collected. On bony elements or drilling sites where osteonal tissue was not available, cortical sampling penetrated just deep enough to allow access to the trabecular tissue within. At all sites, extreme care was taken to limit the size of the holes that were drilled. In nearly all cases, the holes were no larger than 3 mm in diameter and in many cases, cortical surface collection sites are nearly unrecognizable to the untrained eye.

The result of these drilling techniques is a powder, the particles of which are generally uniform in size and quite small. This method precludes the need for any additional homogenization; a step that is included in some DNA extraction protocols where the samples are collected by scalpel or other methods. Theoretically, particle size homogeneity is recommended by Promega and other manufacturers as it allows for less stochasticity in actual DNA extraction across samples. The small particle size provided by the drilling method allowed for maximization of surface area with which the chemicals can interface during the extraction phase (145)

All bone powder was collected into UV sterilized plastic weigh boats and transferred to 2ml microcentrifuge tubes which had also been subjected to UV light in a crosslinker. The samples were then weighed on an electronic scale adjusted for the weight of the tube itself, and labeled with the side of the body, the element, and drilling location. A colored sticker indicated the tissue type. Red stickers were for cortical samples, green for trabecular, yellow for osteonal tissue, blue for the dental sample and those samples which were an amalgamation, received no color delineation. Because ATR/FTIR testing requires so little powder, those samples were collected concurrently and placed in 0.2 ml PCR tubes. All samples were then stored at 13°C in the refrigerator in the drilling room.

ATR/FTIR

Attenuated Total Reflectance Fourier Transform Infra-Red (ATR/FTIR) analysis is a method used in biochemistry to visualize chemical components of a substance. The technology is not new but is gaining in popularity due to its simplicity, the small amount of sample required, the speed of the analysis, and low cost. It is sometimes used in triage medicine to determine chemical components of blood samples and has applications in other disciplines where such characterizations are instructive. Either liquids or solids may be analyzed, and no fixation of solid samples is required. The equipment and software are easy to learn, and most university chemistry departments, hospital pathology labs, and forensic toxicology labs already have the equipment. Total testing time varies by the number of scans per sample, but it is possible to run many samples in a very short amount of time (approximately 5-10 minutes).

The technology fires a laser through a sample and measures the amount of IR light that is either absorbed or reflected by the component chemicals in the sample, depending on what analysis is desired. In this experiment, a ThermoScientific Nicolet iS5 with an id7 ATR attachment was used. OMNIC 9.3.3.2 software was used, and the machine was set to absorbance, with 64 scans and 4 wave resolution.

The test required approximately 1mg of bone powder and, as mentioned, no further treatment or fixation was necessary. A background collection was run prior to adding bone powder as a control for any background chemicals that may be on the surface of the plate or diamond. This test followed the protocol as set forth in studies published by

Leskovar et al in 2020. Because a total of 64 scans were performed on each sample, each sample took approximately two minutes to test.

Since the purpose of this test was to characterize both the chemical constituents of the sample, as well confirm or refute DNA quantitation methods, an aqueous DNA sample, that is, synthetic DNA in water, was run prior to testing bone powder. This was informative as to where on the IR spectrum (wavelength), DNA would be found, since the water is easily identified and subtracted from the results of the scan. The ancient samples mentioned in the sample collection section above were tested with ATR/FTIR to obtain a baseline indication of what DNA negative bone sample would look like on the IR spectrum. This was also informative regarding the diagenetic changes that occur to bone over a long (800+ years) post-mortem interval which may impede or preclude DNA extraction. The results of all the tests were then compared to the results of DNA quantitation methods as well as STR analysis which implicitly involves DNA amplification by polymerase chain reaction (PCR) and is instructive of chemical impediments thereto. The phosphate and carbonate groups shown in Figure 1 are anticipated, as they are major chemical constituents of bone tissue. However, their relative concentrations and ratios to one another can be indicative of diagenetic changes that may inhibit or preclude DNA extraction and amplification. This is discussed in greater detail in the Results section. Fatty acids, which are often found in bone tissue, may be problematic for DNA extraction and PCR amplification. In small amounts, the purification phase of DNA extraction can wash fatty acids out of the sample, but in too large a concentration, they can effectively block the lysis buffer used in DNA extraction

and/or overwhelm chemical wash steps in the purification phase and be detrimental to downstream analyses.

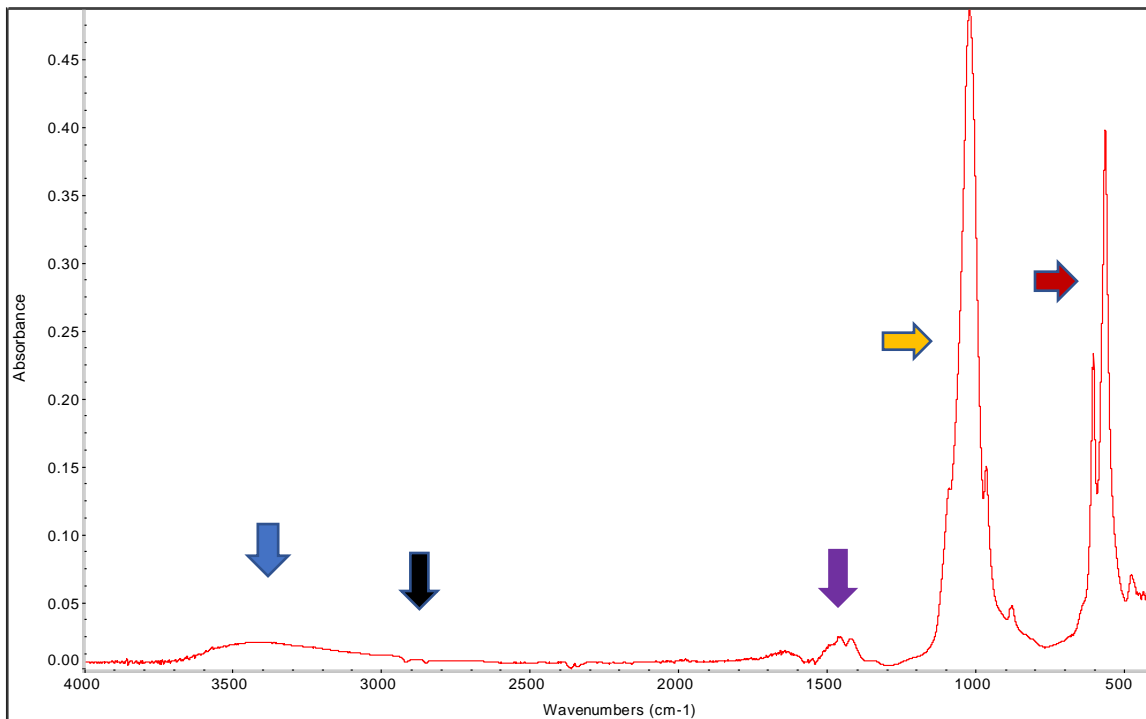


Image 5- Example of ATR/FTIR scan results. This was one of the ancient samples. The PURPLE arrow indicates where DNA should be. The YELLOW arrow indicates phosphate group and the RED arrow indicates a sulfate group. Fatty tissue, which could inhibit PCR amplification of DNA, is absent from this sample but would be found at the BLACK arrow. Water, also absent from this sample, is marked by the BLUE arrow.

DNA Extraction

This project used customized extraction kits provided by Promega® for preprocessing and the Promega DNA IQ® system for purification. Chemical extraction methods use demineralization buffers to dissolve the hydroxyapatite and release the DNA into solution. This also releases unwanted contaminants into the solution and those must be “washed” away in the purification phase to allow for a cleaner DNA free of chemicals that will inhibit downstream quantitation and amplification. However, because this

project is interested in the optimization of methods for forensic DNA extraction from human bone tissue, especially that which is potentially contaminated or of unknown quality, several modifications were made to the published protocol.

Whereas the protocol calls for 100 mg of bone powder, this project used significantly less than that. Sample weights varied between 55-75mg. Additionally, the protocol called for the use of a vortexing incubator which both heats and agitates the samples by shaking. Since such a device was not available, a Benchmark RotoTherm mini® was used instead. This machine both inverts and agitates the samples within a closed, heated, chamber. Each sample tube was closed and sealed with Parafilm immediately prior to heating/agitation to further prevent any loss of sample. The time of incubation/agitation was also decreased significantly as the RotoTherm mini uses more agitation than a regular incubating vortexer. All other steps in the manufacturer's protocol were followed as published.

The first step in the extraction/purification phase was the creation of a lysis cocktail which was made up of 400µL demineralization buffer, 40µL Proteinase K, and 10µL 1-Thioglycerol. The amounts listed are for 1 sample, so the actual amounts were multiplied by the number of samples being run +2 to accommodate for pipetting error or spillage. Next, 400µL of the cocktail was added to each tube of bone powder and vortexed for 10 seconds. The tubes were then sealed with parafilm and added to the incubator that was set to 56°C. Samples were incubated and agitated for 30-45 minutes. The samples were then vortexed again for 10 seconds and added to a centrifuge set to 13,000 x g for 5 minutes to pellet any remaining powder.

Upon removal from the centrifuge, the supernatant was carefully transferred by pipette to new sterile 1.5mL tubes. The tubes containing the remnants of the extracted bone powder were discarded. Next, a second lysis cocktail was prepared which consisted of 990 μ L Lysis buffer and 10 μ L 1-Thioglycerol. 800 μ L of this cocktail was added to the supernatant from the prior step and vortexed for 10 seconds.

The purification phase began with the addition of 15 μ L of DNA IQ® Resin magnetic beads to each tube. Tubes were vortexed for 5 seconds and allowed to rest at room temperature for 5 minutes, vortexing every 2 minutes. The tubes were then placed in a magnetic rack which attracted the beads to one side. The supernatant was removed and discarded. A final step of lysis was performed by adding 100 μ L of the second lysis buffer and vortexing for 5 seconds. The tubes were placed back on the magnetic rack and the supernatant was once again pipetted off and discarded. The beads holding the DNA were then cleaned with a buffer solution that was a cocktail of 30 μ L 2xWash Buffer, 15mL isopropyl alcohol and 15 mL 95% ethanol. The wash step, adding 100 μ L of the wash buffer to the beads was repeated three times, with the supernatant being discarded after each cleanse. Once all three washes were complete, 50 μ L of Elution buffer was added to the tubes with the beads, vortexed for 5 seconds, and incubated with no agitation at 65°C for 5 minutes. The tubes were again vortexed for 5 seconds and placed back in the magnetic stand. The eluted DNA solution was pipetted into new sterile 1.5 mL tubes and stored at 4°C.

DNA Quantitation

Immediately following extraction and purification, each sample was subjected to initial quantitation using an Invitrogen 1x dsDNA HS Assay Qubit Fluorometric Quantification® system following manufacturer's published protocols. This method provides a tentative assessment of the initial molecular weight, or quantity, of DNA contained in each sample down to the ng/μL level. However, since samples may contain amplifiable amounts of DNA that Qubit fluorometry cannot measure, or non-target specific DNA such as microbial or bacterial, additional quantitation of target DNA is desired.

Therefore, real-time, or quantitative, polymerase chain reaction, or qPCR, testing was also performed. This analysis allows for amplification of the target DNA within each sample and is a truer measure of the starting amount of DNA that may be further analyzed. Quantitative PCR also allows for a degree of quantification of the degree or amount of degradation that has occurred to the DNA; usually based on varying sizes of DNA fragments that are amplifiable and detectable with the individual kits or protocols.

Autosomal & Y- Chromosomal DNA

This project utilized the Plexor HY System® by Promega for qPCR analysis. This product was selected for its ability to quantify as little as 6.4pg of DNA. The kit also utilizes internal positive and negative controls, as well as employing melt curve analysis which allows for visualization of the change in fluorescence at a given temperature range. Failure of a sample to provide melt curve data indicates that the DNA in that sample did not amplify with the fluorescent primers or that a contaminant prevented quenching of the fluorescent dye at that temperature range.

This kit was also selected for its ability to discriminate between starting molecular weights of autosomal and Y- chromosomal DNA. Forensically, this is important in cases of potentially mixed samples, paternity testing, or biological sex determination. In cases where the pelvis is not present for forensic anthropological analysis, or the sex determination of the pelvis is not definitive, the ability to extract and quantify Y- chromosomal DNA from other elements may be an invaluable asset. Even though the presence of Y- chromosomal DNA does not necessarily definitively characterize the biological sex or gender of the individual, it may exclude certain individuals in the set of missing persons reports against which the DNA data is compared. Additionally, since qPCR testing is followed by more complete genomic analysis, the presence of Y- chromosomal DNA in qPCR results with an STR profile which does not indicate the presence of such, may be a sign of sample contamination. However, if downstream STR analysis does indicate the presence of a Y-chromosome in conjunction with 2 X chromosomes, then the list of missing persons against which the results are compared is narrowed that much more.

All qPCR analysis requires running several standards along with the experimental samples. The Plexor HY® kit requires 7 standards of known DNA concentrations ranging from 50 ng/μL at the most concentrated to 0.0032 ng/μL at the most diluted. These are duplicated for a total of 14 standards for every experiment. To enable visualization of potential contamination, two negative controls are also run on every experiment. During the analysis phase, these known concentrations of DNA provide a standard curve against which sample results are compared.

Setup for qPCR amplification and quantitation began with the creation of the standards against which the samples would be compared. Using undiluted concentrate, dilutions were made using 40 μL of Promega TE⁻⁴ Buffer and 10 μL of the next most concentrated solution. For example, for the 10 ng/ μL dilution, 10 μL of undiluted concentration was added to 40 μL of TE⁻⁴ buffer. For the next dilution, 10 μL of the 10 ng/ μL dilution was added to 40 μL of TE⁻⁴ buffer, and so on to arrive at concentrations of 50, 10, 2, 0.4, 0.08, 0.016, and 0.0032 ng/ μL respectively. A negative control was also created using the TE⁻⁴ buffer and amplification grade water in order to attempt to detect potential contamination to the reagents.

The reaction mix for the analysis began with the formulation of a cocktail containing 10 μL Plexor® HY 2x Master Mix, 7 μL amplification grade water, and 1 μL Plexor® HY 20X Primer/IPC Mix. As in the extraction and purification stage, the actual amounts of chemicals were multiplied by the number of samples to be run +2 to account for pipetting error or loss. The cocktail was vortexed for 10 seconds and then 18 μL of the cocktail was added to each well along with 2 μL of sample DNA or TE⁻⁴ buffer which created an NTC, or No- Template Control. Two NTC wells were run with every plate.

The plate was then taken to the UM Genomics Core for analysis on the Stratagene Mx3000P® Quantitative PCR System. The experimental design was input into the software following manufacturer's recommendations. For full details, see Promega TM294.

Mitochondrial DNA

Because mtDNA is carried within the mitochondria of the cell, is circular in shape, and is generally more plentiful in the cells than nuclear DNA, quantitative analysis of mtDNA differs from nuclear DNA quantitation in a few practical ways. The theoretical underpinnings and the processes of activation, denaturation, annealing and extension are the same, but the molecules themselves are different enough that different primers and dyes are employed. Quantitative analysis of mtDNA is important to this project as it helps determine the nature of cell types present at the sampling sites at the time of death.

For this project, PowerUp®SYBR Green system from Applied Biosystems was used as it is amenable for visualization on the MX3000P Genetic Analyzer at the UM Genomics Core, because the kit allows for the use of customized standards for sample comparison, and finally, because The PowerUp® SYBER® Green kit also allows investigators the option of integrating a dissociation curve into the qPCR, just as there is with the Plexor®HY nuclear DNA kit from Promega. This is helpful for the current project because it aids in determining the degree of degradation sustained by the DNA molecules. In this experiment, GBlocks® from Integrated DNA Technologies were created for use as standards against which the experimental samples were compared. A GBlock®, just like the standards used in autosomal and Y-chromosomal quantitation, is an artificially created sequence of DNA with a one base pair difference from normal human mtDNA found in the hypervariable region 1 (HVR1) of the mitochondrial DNA molecule. The GBlock® standards in this experiment ranged from 3.35nM at the most concentrated to 0.000000335nM at the most diluted.

Mitochondrial DNA quantitation followed the manufacturer's published protocol for 10µL volumes and began with creation of a loading cocktail. The cocktail called for 5µL

PowerUp®SYBR® Green Master Mix, 1µL each of forward and reverse primers and 2µL of amplification grade water. Actual amounts were multiplied by the number of reaction wells in each run plus 2 to account for pipetting error or environmental loss. The cocktail mix was vortexed for 10 seconds and spun in a microcentrifuge to eliminate air bubbles. Nine (9) µL of the cocktail were added to each of the reaction wells followed by 1µL of either sample DNA or GBlock® artificial DNA as standards. Every plate was accompanied by a no template control (NTC) well which substituted an additional 1µL of amplification grade water for either the sample or control DNA. The NTC was used to visualize any potential contamination. Both the thermal cycling and dissociation set-ups followed the manufacturer's published protocols for standard cycling mode (primer $T_m < 60^\circ$).

DNA Analysis

Since the primary goal of this study has been to develop a sampling method that will aid forensic DNA analysts and other investigators involved in the identification of unknown human post-cranial skeletal remains, the primary method of analysis lies in the establishment of an STR profile which can be uploaded into CODIS and NaMUS and compared to other known profiles. To that end, the eluted and purified DNA samples were taken to the Montana State Crime Lab for STR analysis. The Qiagen Investigator 24Plex QS kit was used with the following specifications (PCR was performed prior to CE injection following the manufacturer's protocol):

Injection on the Applied Biosystems 3500 CE with run specs:

Application Type: HID

Capillary Length: 36cm

Polymer: POP4

Dye Set: Qiagen BT6

Run Module: HID36_POP4

Protocol Name: Qiagen 24 Plex_1.2kV30sec_DEFAULT

Oven Temp (°C): 60

Run Voltage (kVolts): 13.0

PreRun Voltage (kVolts): 15

Injection Voltage (kVolts): 1.2

Run Time (sec): 1550

PreRun Time (sec): 180

Injection Time (sec): 30

Data Delay (sec): 1

Statistical Analysis

PAST 4.03 was utilized as the analysis software for this project. This software was chosen due to experience with it as well as the general ease of use. One- way analysis of variance, or ANOVA, was employed when comparing the results of the three types of DNA, as well as the three tissue types, in both inter- and intra- element comparisons. ANOVA testing in PAST 4.03 automatically incorporates several tests concurrently, including Levene's test of homogeneity of variance and Welch's F. One of the known limitations of ANOVA is its assumption of homogeneity of variance within the sample population (146–151). In this project, that was often not applicable as the numbers themselves could have anywhere from two decimal places to 11 depending on the sample types. For example, ATR/FTIR analyses involved IR wavelength measurements which were in the hundreds, if not thousands. Results of mtDNA quantitation, on the other hand, were several decimal places in the opposite direction. Thus, since Welch's F does not make the assumption of data normality, it was often the more accurate and dependable of the tests. The Kruskal- Wallis test of medians is also included in the PAST software ANOVA analysis, as is Turkey's Pairwise and Dunn's post- hoc. While the former is not instructive for data of the type used in this study, the latter two tests were often useful to determine where the variance actually was when ANOVA or Welch's F indicated significance (152–155).

During comparisons of ATR/FTIR results to either tissue type or DNA type, correlation tests were performed. This was carried out in an effort to determine if it was possible to ascertain if/whether the biochemical components of bone tissue types influenced DNA extractability. PAST 4.03 allows for several types of correlation tests to

be run depending on what kind of data is being analyzed. Because this project deals exclusively with interval/ratio data, Pearson's R and Spearman's Rho were compared. It was quickly evident that, in most cases, Pearson's R was less desirable as it is a test of linear correlation and the data simply did not fit that assumption. However, because Spearman's Rho is designed more for ordinal data than interval data, it was decided that Pearson's R was the more logical choice (156–160).

In order to determine which sites on which elements are best to use for DNA analysis, both inter- and intra- element comparisons were performed. Inter- element group testing provided a picture of whether there is a significant difference between the DNA quantities obtained from, for example, the legs versus the arms, or the ribs versus the vertebrae. Intra- element testing, then, allowed for determination of where on each bone is the optimal site. This proceeded along each side, where applicable, and then the elements or groups from each side were combined.

Statistical analysis proceeded from the broad to the more specific. Initially, all tissue type data and element group data were combined and only the DNA type was specified. For example, all data from the bones of the right arm were compared by DNA type to all the bones from right leg. Then, all cortical tissue samples from each side were compared to all trabecular tissue samples and all osteonal tissue samples for each DNA type. Then, where applicable, proximal sites were compared to mid- diaphyseal and distal sites on each element and compared by both tissue and DNA type.

Using starting molecular weight data obtained from qPCR testing, inter- group variability testing was performed to assess the significance, if any, between the different bone groups. Both sides of the body were tested in this way. Groups were assigned based on anatomical position of the bones. In other words, the bones of the arm, starting with the humerus and then proceeding inferiorly to the ulna and radius were compared to the legs from femur through tibia and fibula. Similarly, the clavicles and the scapulae were compared to the sternum and manubrium. The vertebrae were compared to the sacrum, the wrists and hands compared to the ankles and feet, and the patellas were compared to the other sesamoid bones. Due to their unique anatomical positions, the os coxae were compared to each other and the sacrum.

In order to further enhance understanding of the actual cellular contributions to endogenous DNA preservation, it was necessary to compare data taken from at least 2 sampling sites on each element to each other. For example, cortical bone tissue samples from the proximal ends of all of the long bones were compared to mid- diaphyseal sites as well as to distal sampling sites. This was repeated for trabecular and osteonal (where possible) tissues. Furthermore, this was done for all 3 types of qPCR data as well as the percentage of complete STR profiles. This was repeated in intra- element testing. Meaning that all cortical and trabecular samples from a single bone were compared to themselves and then to each other for all DNA types. In this way, we can begin to see if, and to what extent, cellular populations differ within each sampling point and across element groups as well as each individual bone. Since only 1 sample of osteonal bone tissue was taken from each relevant bone, those samples were compared by element by

side (right humeral osteonal samples compared to each other) and then to those from other elements as well as the mid- diaphyseal cortical and trabecular sample data.

Results

The tables included in this section show which tests indicated significant differences or variation. Because the study is focused on finding the optimal sites for DNA extraction and not generalizations of DNA preservation, ANOVA read- outs showing no significant differences are omitted. However, results of all testing can be found in Appendix 1. As indicated in the Methods section, the alpha level for all testing was set at $p < 0.05$.

While all samples were tested with ATR/FTIR spectroscopy, and statistically analyzed for significant variance within or between samples those samples that exhibited low starting molecular weight of any or all DNA types, and/or failed to produce at least 75% of the STR loci of a full forensic profile, were further scrutinized for potential biochemical reasons for the low performance. As discussed in the background section, lack of amino acid presence, overabundance of either phosphate or carbonate ions, or the presence of PCR inhibitors such as fats or humic acids, are all possible reasons for a sample's failure to provide adequate DNA in qPCR or fragment analysis (161,162).

At the end of this section is a table showing the highest DNA yielding location for each bone by 1) tissue type and 2) DNA type. The specific drilling site for each bone is included. In this way, those interested in real-world questions of where to sample for DNA analysis can find the data quickly.

Inter- Group Variability

All Tissue Types

First, only autosomal DNA data was compared between drilling locations. Then the Y-chromosome data only, and then the mtDNA data only. Following this, each DNA analysis type was compared to each other type. This was repeated for both sides of the body. Lastly, the percentage of full STR profile construction was compared to the starting mtDNA molecular weight.

APPENDICULAR SKELETON

LEFT SIDE

Left Side Element Group Comparisons

First, averages were taken of the qPCR raw scores from sampling sites on each element for each DNA type alone. In this way, all of the autosomal, Y chromosome, and mtDNA data from each element could be compared to other elements irrespective of the tissue type. Then, each DNA type average was taken for each particular tissue type.

Comparison between the element groups involved raw qPCR data, rather than averages of such. No significance was noted on the starting DNA quantification values of the left side between any element groups other than the hands and feet. In other words, there was no statistically significant difference between the arm and the leg, but ANOVA testing did show significant difference between the means of the left hand (the carpals, metacarpals and phalanges) and the left foot (tarsals, metatarsals and phalanges) in raw

qPCR values for autosomal and Y-chromosomal DNA. No significant difference was found in mtDNA data. In the outputs from PAST 4.03 which follow, relevant *p* values are highlighted in yellow.

Autosomal DNA:

LEFT hand versus LEFT foot:

	Sum of sqrs	df	Mean square	F	p (same)
Between groups:	0.246507	1	0.246507	6.398	0.01873
Within groups:	0.8861	23	0.0385261		Permutation p
(n=99999)					
Total:	1.13261	24			0.01514

Components of variance (only for random effects):

Var(group):	0.0168816	Var(error):	0.0385261	ICC:	0.304679
omega2:	0.1776				

Levene's test for homogeneity of variance, from means p (same): 0.106

Levene's test, from medians p (same): 0.1208

Welch F test in the case of unequal variances: F=7.315, df=20.91, p=0.0133

Y- Chromosome

	Sum of sqrs	df	Mean square	F	p (same)
Between groups:	0.0224674	1	0.0224674	7.418	0.01211
Within groups:	0.0696592	23	0.00302866		Permutation p (n=99999)
Total:	0.0921265	24			0.00255

Components of variance (only for random effects):

Var(group):	0.00157782	Var(error):	0.00302866	ICC:	0.342521
omega2:	0.2043				

Levene's test for homogeneity of variance, from means p (same): 0.006095

Levene's test, from medians p (same): 0.02025

Welch F test in the case of unequal variances: F=9.483, df=13.32, p=0.008572

In these cases, the Bonferroni corrected p values were identical to the raw p values. Despite homogeneity of variance in the autosomal DNA tests, there is significant difference between the hand and foot samples at $p < 0.05$. The averages of raw data from the groups are shown in the table below. Note that the tarsals outperformed the carpals in all three analyses, while the metacarpals outperformed the metatarsals in autosomal and mtDNA, but not in Y-chromosome analysis. The phalanges of the foot outperformed

those of the hand in both autosomal and Y- chromosome analysis, but not in mitochondrial DNA. **STR results**

	Autosomal	Y- Chromosome	Mitochondrial
Carpals	0.08179	0.01650	5.95E-05
Metacarpals	0.14257	0.00988	8.52E-04*
Phalanges	0.02854	0.00699	3.24E-05
Tarsals	0.42633*	0.09376*	2.50E-04
Metatarsals	0.09758	0.01799	5.13E-07
Phalanges	0.34852	0.08249	1.393E-07

Table 2- Raw qPCR data scores for the left hands and feet. Asterisks indicate highest performing element groups.

Tissue Type Comparisons

When combining all the data from each tissue type and then comparing each to the others, no statistically significant difference was found between the averages of autosomal or Y- chromosomal DNA.

Mitochondrial DNA comparisons across tissue types on the left side, however, did indicate some statistical significance in Dunn's post-hoc testing, (shown below) which can be useful in tests of small sample size like this one. Especially since it makes no assumption of normality and because ANOVA is known to be prone to error in tests of small sample populations. In this case, the greatest variance was seen between starting DNA molecular weights of mtDNA between cortical and osteonal tissue across the whole of the left side of the skeleton.

	<u>Cort Mito</u>	<u>Trab Mito</u>	<u>Osteo Mito</u>
Cort Mito		0.116	0.0152
Trab Mito	0.116		0.236
Osteo Mito	0.0152	0.236	

Table 3- Post hoc testing results. Significant variance is highlighted in yellow.

It is when the three DNA types were compared within the tissue types that the greatest amount of difference is seen statistically. This testing is the most important for this project because it is the most indicative of differential cellular populations at the time of death in the post-cranial skeleton.

ALL left side Cortical Tissue: Autosomal vs Y- Chromosome vs mtDNA

Test for equal means

	Sum of sqrs	df	Mean square	F	p (same)
Between groups:	1.1279	2	0.56395	5.417	0.009805
Within groups:	3.12315	30	0.104105		Permutation p (n=99999)
Total:	4.25105	32			1E-05

Components of variance (only for random effects):

Var(group):	0.0418041	Var(error):	0.104105	ICC:	0.286507
omega2:	0.2112				

Levene's test for homogeneity of variance, from means p (same): 0.01556

Levene's test, from medians p (same): 0.1201

Welch F test in the case of unequal variances: F=8.445, df=13.33, p=0.004271

Given the lack of homogeneity of variance seen in Levene's test, Welch's F is more likely the truer test since it makes no assumption of normality. Welch's F detected a significant difference at $p < 0.05$.

	Cortical A	Cortical Y	Cortical Mito
Cortical A		0.03427	4.179E-07
Cortical Y	0.03427		0.003243
Cortical Mito	4.179E-07	0.003243	

Table 4- Post hoc testing. Significant variance, in yellow, was most pronounced between cortical autosomal and cortical mtDNA scores.

Post- hoc testing shows that the variance is most pronounced between autosomal and mtDNA in the cortical tissue. The next most pronounced degree of variation occurred between the Y- chromosome and mtDNA. The least, though still significant, was between autosomal and Y- chromosome data.

ALL left side Trabecular Tissue: Autosomal vs Y- Chromosome vs mtDNA

Test for equal means:

	Sum of sqrs	df	Mean square	F	p (same)
Between groups:	0.150962	2	0.0754811	14.23	4.948E-05
Within groups:	0.15385	29	0.00530516		Permutation p
(n=99999)					
Total:	0.304812	31			0.00018

Components of variance (only for random effects):

Var(group): 0.00658543 Var(error): 0.00530516 ICC: 0.553835
 omega2: 0.4526

Levene’s test for homogeneity of variance, from means p (same): 0.000337

Levene’s test, from medians p (same): 0.004344

Welch F test in the case of unequal variances: F=15.74, df=12.63, p=0.0003716

Again, since there was no homogeneity of variance, Welch’s F test is more reliable than ANOVA. It detected significant difference at $p < 0.05$.

	<u>Trabec A</u>	<u>Trab Y</u>	<u>Trab Mito</u>
Trabec A		0.05322	8.808E-07
Trab Y	0.05322		0.002235
Trab Mito	8.808E-07	0.002235	

Table 5- Post- hoc testing. As with cortical bone tissue, trabecular tissue varied most between autosomal and mtDNA scores.

Post- hoc testing showed the highest variance, again between autosomal and mtDNA in the trabecular tissue, followed by Y- chromosome versus mtDNA. The difference between the variance of Y- chromosome and autosomal DNA was nearly significant.

LEFT side tissue types by location

Cortical Tissue

Statistically significant difference was noted in autosomal DNA levels between cortical samples from the proximal versus distal ends as well as between the mid-shaft versus distal ends of long bones.

	L Prox Cort	L Mid Cort	L Dist Cort
	Auto	Auto	Auto
L Prox Cort Auto		0.6653	0.004926
L Mid Cort Auto	0.6653		0.01735
L Dist Cort Auto	0.004926	0.01735	

Table 6- Post- hoc testing showed the variance was most pronounced between proximal and distal sampling sites among cortical tissue samples.

Post- hoc testing shows that the most significant variance in qPCR data scores lies between cortical tissue samples from the proximal and the distal ends of the long bones. The next most significant degree of variance was between mid-diaphyseal and distal cortical samples. It's not that the scores themselves were variable, per se, but that there was significant difference (or, variance) between 1-scores from the proximal and distal sites and 2- between the mid- diaphyseal and distal sites. Essentially meaning that the distal sites were either statistically better or worse (ANOVA doesn't distinguish between higher and lower) than the proximal sites and the mid- diaphyseal sites, but there wasn't much difference between proximal and mid- diaphyseal.

Comparison between cortical levels of Y- Chromosomal DNA also showed significant difference between proximal and distal samples.

	L Prox Cort Y	L Mid Cort Y	L Dist Cort Y
L Prox Cort Y		0.3042	0.01735
L Mid Cort Y	0.3042		0.1764
L Dist Cort Y	0.01735	0.1764	

Table 7- Post- hoc testing showed significant variance between proximal and distal sampling sites.

There was no significant difference detected in mtDNA levels between cortical samples from proximal, mid- shaft, and distal samples of the long bones.

Trabecular Tissue

No significant difference was detected in autosomal, Y-chromosomal, or mitochondrial DNA results from trabecular tissue samples of the proximal ends versus midshaft versus distal ends of the long bones from the left side of the body.

Osteonal Tissue

Because there was only one osteonal sample taken from the mid-diaphyseal regions of each long bone, the results of such are included here, rather than in the intra-element testing section.

	Sum of sqrs	df	Mean square	F	p (same)
Between groups:	0.244599	2	0.1223	3.844	0.05126

Within groups: 0.381764 12 0.0318136 Permutation p
(n=99999)

Total: 0.626363 14 0.00527

Components of variance (only for random effects):

Var(group): 0.0180972 Var(error): 0.0318136 ICC: 0.362591

omega2: 0.275

Levene's test for homogeneity of variance, from means p (same): 0.03314

Levene's test, from medians p (same): 0.06082

Welch F test in the case of unequal variances: F=3.707, df=5.333, p=0.09794

Given the small sample size and heterogeneity of variance, the lack of significance shown by Welch's F and the near significance of ANOVA may be the result of a type II error.

	Osteo Auto	Osteo Y	Osteo Mito
Osteo Auto		0.1791	0.0008893
Osteo Y	0.1791		0.04771
Osteo Mito	0.0008893	0.04771	

Table 8- Post- hoc testing shows significant the most variance occurred between autosomal and mtDNA scores.

Post- hoc testing shows the greatest variance occurs between autosomal and mtDNA in the osteonal tissue and lends credibility to the idea that a false negative may have

occurred. However, given the nature of the data, it is not surprising that a significance may have been detected between autosomal DNA and mtDNA. Whether or not this is the case, further study with larger sample population is warranted.

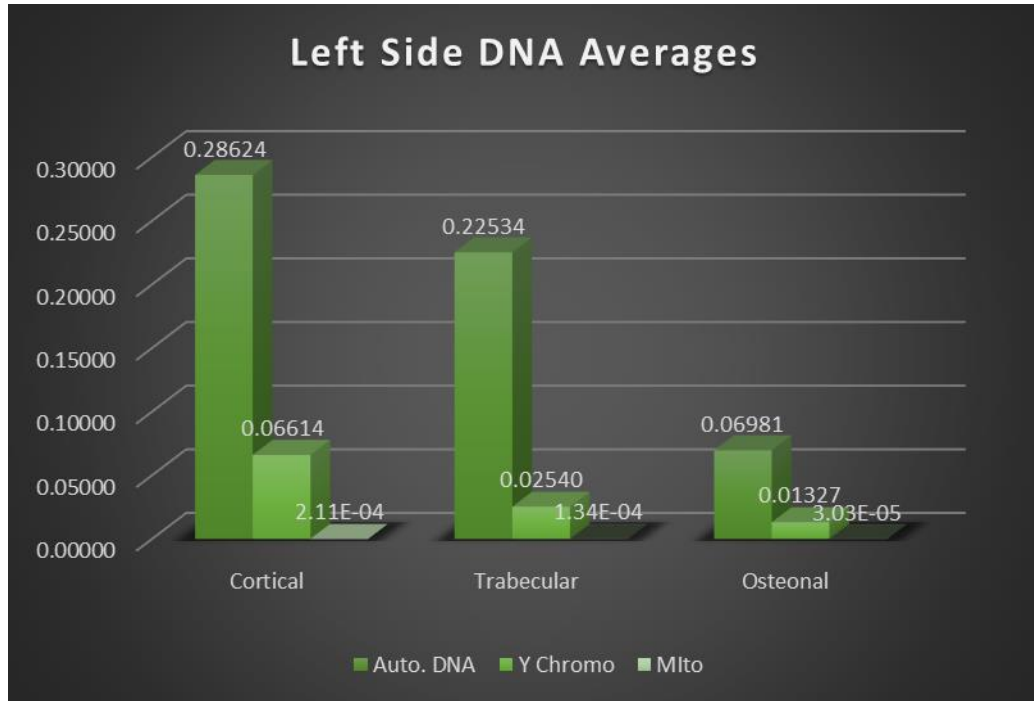


Figure 1- Averages of the three DNA types across the tissue types on the left side of the body. Y- axis is DNA levels in ng/uL.

RIGHT SIDE

Element group comparisons

Right Arm versus Right Leg

No significance was detected between the elements of the right arm (humerus, ulna and radius) and the right leg (femur, tibia, and fibula) in autosomal DNA. However, significant difference was found between the right arm and leg in Y chromosome analysis.

	R Hum Y	R Rad Y	R Ulna Y	R Fem Y	R Tib Y	R Fib Y
R Hum Y		0.6244	0.7312	0.01763	0.1799	0.89
R Rad Y	0.6244		0.8712	0.0596	0.3945	0.5301
R Ulna Y	0.7312	0.8712		0.03506	0.2977	0.6267
R Fem Y	0.01763	0.0596	0.03506		0.3019	0.01202
R Tib Y	0.1799	0.3945	0.2977	0.3019		0.1391
R Fib Y	0.89	0.5301	0.6267	0.01202	0.1391	

Table 9- Post- hoc testing indicated that significant variance occurred between the right femur and fibula, the right ulna, and the right humerus.

Dunn's post- hoc shows the difference between the means from the humerus & femur, the femur & ulna, and the femur & the fibula.

Additionally, a significant difference was detected between mitochondrial DNA means of the elements of the right arm and the right leg.

	R Hum mtDNA	R Rad mtDNA	R Ulna mtDNA	R Fem mtDNA	R Tib mtDNA	R Fib mtDNA
R Hum mtDNA		0.2464	0.1928	0.5622	0.6368	0.1566
R Rad mtDNA	0.2464		0.9161	0.08211	0.1028	0.01001
R Ulna	0.1928	0.9161		0.05732	0.07345	0.005685

mtDNA						
R Fem mtDNA	0.5622	0.08211	0.05732		0.9145	0.4025
R Tib mtDNA	0.6368	0.1028	0.07345	0.9145		0.345
R Fib mtDNA	0.1566	0.01001	0.005685	0.4025	0.345	

Table 10- Post- hoc testing indicating the majority of variance occurred between the right fibula and ulna for mtDNA scores.

Dunn's post- hoc shows the variance is mostly between the radius and fibula and between the ulna and the fibula.

Right Hand vs Right Foot

ANOVA and post-hoc testing show the greatest variance is between the carpals and the metatarsals. As with the same elements on the left side, raw data indicates that the bones of the foot outperformed those of the hand in both autosomal and Y- chromosomal DNA and mtDNA generally, although the metatarsals underperformed in this DNA type.

	Autosomal DNA	Y-Chromosome	mtDNA
Carpals	0.01777	0.00768	9.39E-05
Metacarpals	0.08750	0.01006	1.02E-05
Hand Phalanges	0.23162	0.03139	1.39E-05
Tarsals	0.42073	0.05237	6.08E-04*
Metatarsals	0.04518	0.01330	1.98E-06

Foot Phalanges	1.24256*	0.12397*	4.62E-04
----------------	----------	----------	----------

Table 11- Raw qPCR score averages from the right hands and feet. Asterisks indicate the highest performing groups.

Right Shoulder (Clavicle vs Scapula)

Comparisons of the upper elements of the right arm (the scapula, clavicle, humerus, radius, and ulna) yielded no statistically significant differences across DNA types.

Right Side Tissue Type Comparisons

Cortical versus Trabecular versus Osteonal- Autosomal DNA

ANOVA detected significant difference in DNA starting molecular weight variance between tissue types. However, in spite of heterogeneity of variance, Welch's F did not. Dunn's post- hoc, below, shows that the variance is primarily between the cortical and the trabecular and the cortical and the osteonal samples. Raw data seems to indicate that it is more likely a type II error in Welch's F, rather than a type I error in ANVOA.

	Cortical Auto.	Trabecular Auto.	Osteonal Auto.
Cortical Auto.		0.009264	0.004876
Trabecular Auto.	0.009264		0.2888
Osteonal Auto.	0.004876	0.2888	

Table 12- Post- hoc testing showing greatest variance between cortical vs trabecular and cortical vs osteonal tissue. This is most likely a type II error in Welch's F test.

Cortical versus Trabecular versus Osteonal- Y- Chromosome

As with autosomal DNA scores, ANOVA detected significant difference between the variance in Y- Chromosome data.

	Cortical Y	Trabecular Y	Osteonal Y
Cortical Y		0.002045	0.00375
Trabecular Y	0.002045		0.4125
Osteonal Y	0.00375	0.4125	

Table 13- Post- hoc testing showing greatest variance between cortical vs trabecular and cortical vs osteonal tissue.

Post- hoc testing shows that the variance is greatest between the cortical and trabecular, followed by the cortical versus osteonal tissues.

No significant difference was detected between the tissue types by mtDNA data.

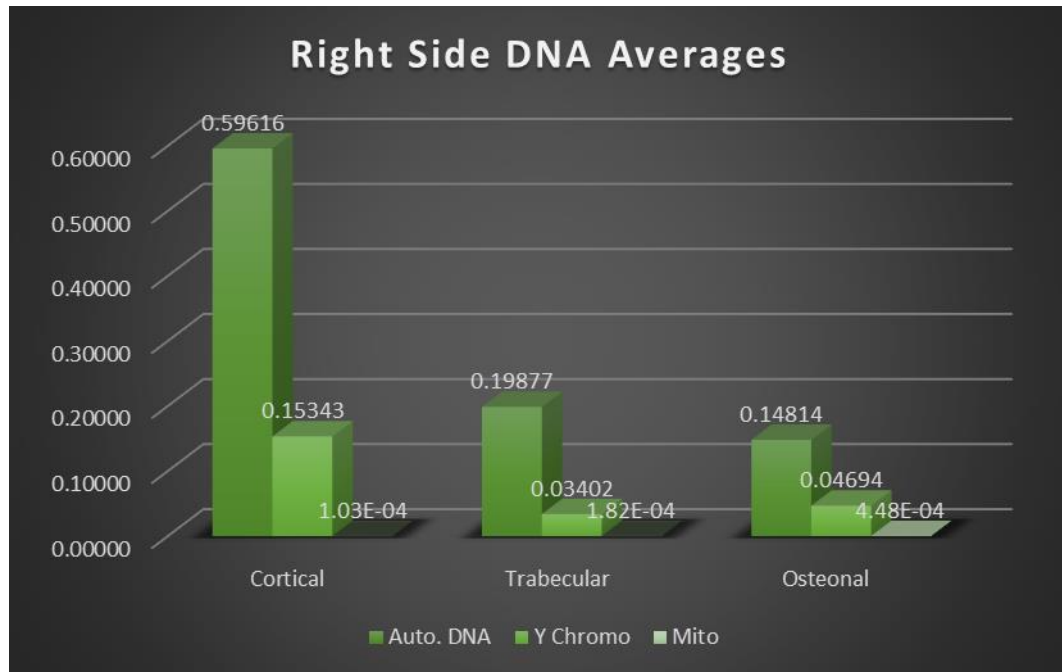


Figure 2- Averages of the three DNA types in each of the three tissue types across the right side of the body. DNA amounts are in ng/uL.

Right side tissue type by location

No statistically significant difference was detected in comparative analyses of the proximal, mid- diaphyseal, and distal ends of the long bones across all tissue and DNA types.

THE AXIAL SKELETON

One-way ANOVA testing did not detect any significant difference between the ribs of either side and the sternum and manubrium. Note that there is no trabecular sample from the clavicular notch, nor a cortical sample from the inferior articular margin.

The reason is that the bone tissue at these locations was not conducive to sampling in that manner.

Sample	Autosomal DNA	Y- Chromosome	mtDNA
Clavicular Notch Cort.	0.84411*	0.22409*	0.00E+00
Inferior Articular Margin Trab.	0.53527	0.12502	7.01E-04*
Prox. Corpus Sterni Cort.	0.13609	0.03377	1.33E-04
Prox. Corpus Sterni Trab.	0.01181	0.00105	9.77E-06
Dist. Corpus Sterni Cort.	0.00292	0.00266	0.00E+00
Dist. Corpus Sterni Trab.	0.45001	0.05253	3.17E-03

Table 14- Raw qPCR averages from the sternum and manubrium. Asterisks indicate highest perform sites.

It should also be noted that there were significant outliers in the data in autosomal and Y-chromosomal DNA in cortical samples taken from the 8th ribs bilaterally, but most especially on the right side. Additionally, five of the samples taken from the right ribs failed to yield any mtDNA, whereas only one sample from the left failed.

Sample	L Ribs Auto.	L Ribs Y Chromo.	L Ribs mtDNA		R Ribs Auto.	R Ribs Y Chromo.	R Ribs mtDNA
Rib 1 Cort.	0.04506	0.03737	2.92E-04		0.11375	0.03888	0.00+E00

Rib 1 Trab.	0.00961	0.00387	2.11E-05		0.01686	0.00870	2.41E-05*
Rib 4 Cort.	6.06043	0.60374	0.00+E00		0.26937	0.09781	0.00E+00
Rib 4 Trab.	0.01070	0.00254	6.58E-05		0.00734	0.00171	5.25E-06
Rib 4 Frag. Cort.	0.30980	0.06586	2.41E-04		0.07765	0.01092	0.00E+00
Rib 4 Frag. Trab.	0.01180	0.00122	7.67E-07		0.05148	0.01220	6.38E-09
L Rib 8 Cort.	1.73860*	0.78290*	6.10E-04*		6.28993*	1.9013*	0.00E+00
L Rib 8 Trab.	0.19730	0.03754	3.46E-06		1.29446	0.07055	0.00E+00

Table 15- Raw qPCR averages for the ribs. Asterisks indicate highest performing elements.

Vertebrae vs Sacrum vs Os Coxae

Statistical comparison of the three vertebral types indicated no statistical differences in autosomal or Y- chromosomal DNA. However, because the lumbar

vertebrae failed to yield any mtDNA whatsoever, ANOVA analysis of all three tissue types failed. ANOVA analysis is inherently a measure of variance and if all samples from one group = 0, then there is no variance to compare. Comparison of the cervical and thoracic vertebrae by mtDNA indicated no statistically significant difference. Nor was there any significant difference found in comparisons of the cervical and thoracic vertebrae to the sacrum, and either/both Os Coxae.

Intra- Group Variability

Intra-group variability testing was performed by combining left and right-side data for each for each sampling location (proximal, mid-diaphyseal, and distal) on each element and comparing the data for each DNA type. In other words, all of the data from the sampling sites at the proximal ends of the long bones were combined and compared against all of the data from the mid-diaphyseal, and distal sampling sites on each element individually. Since there were very few actual data points to compare (four each), and because the osteonal data was included in the inter-element comparisons, raw data scores may be more instructive. In fact, some ANOVA calculators require at least five data points and in tissue type comparisons, there were only two for each sampling location. Shapiro-Wilk tests of normality were run along with ANOVA, simply as a measure of certainty and visualization of the data.

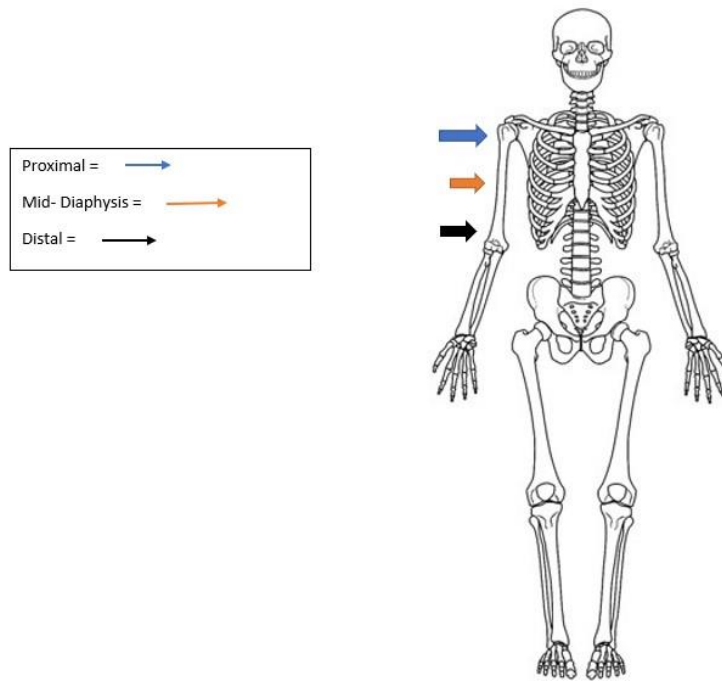


Image 6- Fun picture illustrating some of the relevant anatomical directions used in the study.

Humeri:

Autosomal DNA:

	Prox. Hum Cort.	Prox. Hum Trab.	Mid Hum Cort.	Mid Hum Trab.	Dist. Hum Cort.	Dist. Hum Trab.
Right	0.0231	0.2662	0.0297	0.0415	4.6646*	0.1145
Left	0.0267	0.0340	0.1507	0.0457	1.0905*	0.1637

Table 16- Raw autosomal qPCR averages of the humeri by sampling site and tissue type. Asterisks indicate highest performing sites.

Most likely due to small sample size, one-way ANOVA and Welch's F both failed to detect any statistical significance in the variance of the humeri. However, the table above clearly shows a marked difference between the raw autosomal DNA qPCR data scores of the cortical samples taken from the distal humeri versus all of the others. Not surprisingly, this pattern repeated for the Y- chromosome.

Y- Chromosome:

	Prox. Hum.	Prox. Hum.	Mid. Hum.	Mid. Hum.	Dist. Hum.	Dist. Hum.
	Cort.	Trab.	Cort.	Trab.	Cort.	Trab.
Right	0.00898	0.05601	0.08978	0.00832	0.15056*	0.01086
Left	0.00411	0.01474	0.06603	0.00483	0.14296*	0.02493

Table 17- Raw Y- Chromosome averages for the humeri by sampling site and tissue type. Asterisks indicate highest performing sites/tissues.

mtDNA:

	Prox. Hum.	Prox. Hum.	Mid. Hum.	Mid. Hum.	Dist. Hum.	Dist. Hum.
	Cort.	Trab.	Cort.	Trab.	Cort.	Trab.
Right	2.68E-05	5.21E-08	1.98E-05	2.70E-05*	0.00E+00	2.11E-05
Left	7.29E-05	4.07E-07	3.49E-04*	7.84E-05	1.74E-04	3.82E-05

Table 18- Raw mtDNA qPCR averages for the humeri by sampling site and tissue type. Asterisks indicate highest performing sites.

Generally, the left humerus outperformed the right in mtDNA scores, and interestingly, the sampling site which the best for autosomal and Y-chromosome, was the worst for mtDNA. Cortical samples from the distal humerus were the highest in

autosomal DNA and Y- chromosome, while the mid- diaphyseal cortical and trabecular were the highest in mtDNA.

Ulnae:

	Sum of sqrs	df	Mean square	F	p (same)
Between groups:	0.603911	2	0.301955	4.971	0.02898
Within groups:	0.668179	11	0.0607436		Permutation p (n=99999)
Total:	1.27209	13			0.02745

Components of variance (only for random effects):

Var(group): 0.0527651 Var(error): 0.0607436 ICC: 0.464855
 omega2: 0.362

Levene's test for homogeneity of variance, from means p (same): 0.01221

Levene's test, from medians p (same): 0.01651

Welch F test in the case of unequal variances: F=6.663, df=4.551, p=0.04446

Both ANOVA and Welch's F detected significance at $p < 0.05$.

Post-hoc testing showed the greatest variation occurred between the mid- diaphyseal and distal sampling sites. The outliers in this case were the proximal trabecular sample from the right ulna at the high end and the mid- diaphyseal trabecular samples from both sides at the low end.

	L Ulna Prox Auto	L Ulna Mid Auto	L Ulna Dist Auto
L Ulna Prox Auto		0.05187	0.5541
L Ulna Mid Auto	0.05187		0.009534
L Ulna Dist Auto	0.5541	0.009534	

Table 19- Post- hoc testing shows greatest variance between distal and mid- diaphyseal sites.

No significant difference was detected between sampling sites for either the Y- chromosome or mtDNA.

Radii:

Autosomal DNA

	Sum of sqrs	df	Mean square	F	p (same)
Between groups:	0.629961	2	0.31498	5.156	0.02632
Within groups:	0.672	11	0.0610909		Permutation p
(n=99999)					
Total:	1.30196	13			0.02984

Components of variance (only for random effects):

Var(group): 0.0555383 Var(error): 0.0610909 ICC: 0.476196

omega2: 0.3725

Levene's test for homogeneity of variance, from means p (same): 0.1594

Levene's test, from medians p (same): 0.2369

Welch F test in the case of unequal variances: $F=3.446$, $df=5.892$, $p=0.1021$

ANOVA detected significance, whereas Welch's F did not.

Post- hoc testing indicates that the greatest variance, as with the ulnae, occurs between the mid- diaphyseal and distal sampling sites. However, given the results of Levene's and Welch's F, the ANOVA results may well be a type I error. Outliers in this case occurred on the right side with highest scores being the distal sites and nearly equally low scores from the mid- diaphyseal sites.

	Prox Rad Auto	Mid Rad Auto	Dist Rad Auto
Prox Rad Auto		0.8774	0.09097
Mid Rad Auto	0.8774		0.04486
Dist Rad Auto	0.09097	0.04486	

Table 20- Post- hoc testing shows greatest variance between distal and mid- diaphyseal sites of the radius.

No significant difference was detected between either Y- chromosomal or mtDNA among sampling sites of the radii.

Femora

Despite the lack of any mtDNA from several sites in the femora, no significant difference was detected between sampling sites across the three DNA types. The raw data from the femora is more instructive.

Sampling Site	Left Autosomal	Left Y-Chromosome	Left MtDNA	Right Autosomal	Right Y-Chromosome	Right mtDNA
Fovea Capitis Cort.	0.15387	0.04409	4.21E-05	1.31470	0.53454	0.00E+00
Fovea Capitis Trab.	0.24068	0.03996	7.09E-05	1.98432	0.52505	0.00E+00
Nutrient Foramen Cort.	0.16600	0.08380	4.83E-05	0.60443	0.34736	0.00E+00
Nutrient Foramen Ost.	0.28897	0.02743	4.66E-10	0.56923	0.20587	1.97E-03
Nutrient Foramen Trab.	0.03646	0.00441	9.37E-06	0.12636	0.09317	0.00E+00
Inter Condylar Fossa Cort.	0.47736	0.16870	4.98E-06	1.53072	0.63708	1.69E-03
Inter Condylar Fossa Trab.	0.04574	0.01794	5.47E-06	0.00337	0.00000	3.95E-06

Table 21- Raw qPCR averages from the femora. Note the lack mtDNA and Y- chromosome data from the right side.

Also of note is the discrepancy between the mtDNA values from the osteonal sampling sites between sides.

Tibias

No statistically significant difference was detected in the tibias across DNA type and sampling site. However, raw qPCR data for these elements looks very similar to that of the femora with several sites from both sides failing to produce any mtDNA data.

Sampling Site	Left Autosomal	Left Y-Chromosome	Left Mito	Right Autosomal	Right Y-Chromosome	Right Mito
Tibial Plateau Cort.	0.06259	0.02534	1.31E-05	1.41029	0.37741	2.56E-06
Tibial Plateau Trab.	0.00380	0.00147	0.00E+00	0.09577	0.02189	3.90E-06
Mid-diaph. Cort.	0.05063	0.00880	7.85E-06	0.98559	0.44617	2.42E-03
Mid-diaph. Ost.	0.07628	0.01914	0.00E+00	0.05901	0.02012	4.84E-06
Mid-diaphy Trab.	0.04214	0.02384	0.00E+00	0.01769	0.01161	0.00E+00
Malleolar Groove Cort.	0.66057	0.07306	8.25E-09	0.29396	0.12147	6.15E-06
Malleolar Groove Trab.	0.05711	0.01195	0.00E+00	0.21526	0.05322	0.00E+00

Table 22- Raw qPCR averages from the tibias. Note the lack of mtDNA data from trabecular samples on both sides and the osteonal sample on the left.

Fibulas

ANOVA detected significance between the scores of sampling sites on the fibulas. However, this may be another type I error due to small population size. Welsch's F is nearly significant, but this also indicates support for the above statement. Post- hoc testing shows the greatest variance was between proximal and distal sites. This is consistent with the raw data which shows higher performance of distal samples than proximal with intermediate performance of mid- diaphyseal samples.

	Prox Fib Auto	Mid Fib Auto	Dist Fib Auto
Prox Fib Auto		0.2807	0.01423
Mid Fib Auto	0.2807		0.1698
Dist Fib Auto	0.01423	0.1698	

Table 23- Post- hoc testing shows greatest variance between proximal and distal sampling sites of the fibulae.

No significant difference was detected in Y- Chromosome or mtDNA between the proximal, mid- diaphyseal, and distal fibula samples.

Irregular Bones

No statistically significant differences were noted within in the clavicles or scapulae or the os coxae. The qPCR data from the clavicles indicates that the medial end performed better than the lateral end on both sides. Data from the scapulae were mixed and showed no clear pattern.

Sampling Site	Left Autosomal	Left Y-Chromosome	Left MtDNA	Right Autosomal	Right Y-Chromosome	Right mtDNA
Clavicles						
Medial End Cort.	0.52210	0.15167	6.36E-03	1.60835	0.55749	2.05E-04
Medial End Trab.	0.34800	0.01471	0.00E+00	0.06831	0.00492	5.59E-09
Lateral End Cort.	0.13830	0.06363	0.00E+00	0.64781	0.24278	2.62E-05
Lateral End Trab.	0.08975	0.01548	8.88E-09	0.03534	0.00466	4.39E-05
Scapulae						
Glenoid Fossa Cort.	0.27374	0.14407	1.64E-04	0.73983	0.19428	0.00E+00
Glenoid Fossa Trab.	0.01384	0.00474	2.60E-05	0.03607	0.06603	0.00E+00
Acromion Process Cort.	0.01805	0.18988	4.05E-10	0.71162	0.15759	4.83E-08
Acromion Process Trab.	0.56170	0.05292	1.37E-04	0.18870	0.03741	2.65E-05

Table 24- Raw qPCR averages for the clavicles and scapulae

While no statistically significant difference was detected between the right and left Os Coxae, examining the raw data may be more instructive as to which sampling sites are optimal for DNA extraction. The auricular surface and the cortical tissue of the pubic symphysis yielded the highest amounts of autosomal DNA, and the pubic symphysis was among the best for mtDNA, as well. Results from trabecular samples from the os coxae were mixed across DNA types.

Sampling Site	Left Autosomal	Left Y-Chromosome	Left mtDNA	Right Autosomal	Right Y-Chromosome	Right mtDNA
Iliac Crest	0.11510	0.02488	4.81E-04	0.17752	0.02880	1.72E-05
Auricular Surface	2.12180	0.06066	0.00E+00	0.25182	0.06008	0.00E+00
Posterior Inferior Spine	1.44270	0.00092	0.00E+00	0.01534	0.00142	8.08E-07
Ischial Spine	0.02870	0.00091	2.97E-05	0.01074	0.00111	8.92E-06
Ischial Tuberosity Cort.	0.04316	0.01206	4.06E-05	0.03402	0.00868	5.24E-08
Ischial Tuberosity Trab.	0.05825	0.00547	5.55E-06	0.04727	0.00732	3.74E-08
Ischio-Pubic Ramus Cort.	0.05030	0.00552	8.58E-05	0.03751	0.00456	1.15E-05
Ischio-Pubic Ramus Trab.	0.61590	0.00244	0.00E+00	0.01148	0.00086	2.55E-08
Pubic Symphysis Cort.	0.61088	0.09139	7.49E-05	0.75087	0.08042	3.59E-05
Pubic Symphysis Trab.	0.01283	0.00278	1.61E-05	0.00756	0.00086	5.26E-06
Dorsal Surface	0.43939	0.00548	1.48E-09	0.09917	0.00682	5.97E-07
Ventral Surface	0.35614	0.02571	0.00E+00	0.23351	0.05299	0.00E+00

Table 25- Raw qPCR averages for the os coxae.

ATR/FTIR

ANOVA testing of ATR/FTIR results were first run by the absorbance levels of amino acids, phosphates and carbonates by tissue type, irrespective of DNA type. No statistically significant differences were noted. Then, ANOVA was run by tissue type and showed no statistically significant difference in amino acid absorbance across tissue type. The tissue types did, however, exhibit some significant differences in phosphate and carbonate absorption. With these results in mind, correlation tests were conducted first in aggregate, then across tissue type, for all DNA types.

Phosphate Absorbance by tissue type

	Sum of sqrs	df	Mean square	F	p (same)
Between groups:	0.0716473	2	0.0358237	4.676	0.01357

Within groups: 0.398369 52 0.00766094 Permutation p
(n=99999)

Total: 0.470016 54 0.01307

Components of variance (only for random effects):

Var(group): 0.00170027 Var(error): 0.00766094 ICC: 0.18163

omega2: 0.1179

Levene's test for homogeneity of variance, from means p (same): 0.1731

Levene's test, from medians p (same): 0.252

Welch F test in the case of unequal variances: F=4.343, df=15.1, p=0.03237

ANOVA and Welch's F both detected significance at $p < 0.05$.

Dunn's post- hoc indicates the greatest variance is between the phosphate absorbance levels in the trabecular and the osteonal tissues.

	Ph Abs (Cort)	Ph Abs (Trab)	Ph Abs (Ost)
Ph. Abs. Cort.		0.01195	0.6593
Ph. Abs. Trab.	0.01195		0.03407
Ph. Abs.Ost.	0.6593	0.03407	

Table 26- Post- hoc testing shows greatest variance between phosphate absorbance levels of the trabecular vs cortical samples with somewhat less between trabecular and osteonal samples.

Carbonate absorbance by tissue type

Sum of sqrs	df	Mean square	F	p (same)	
Between groups:		0.0787873	2	0.0393936	6.413 0.003239
Within groups:		0.319402	52	0.00614234	Permutation p (n=99999)
Total:		0.398189	54		0.00318

Components of variance (only for random effects):

Var(group):	0.00200749	Var(error):	0.00614234	ICC:	0.246323
omega2:	0.1645				

Levene's test for homogeneity of variance, from means p (same): 0.2217

Levene's test, from medians p (same): 0.284

Welch F test in the case of unequal variances: F=6.353, df=15.13, p=0.009933

Both ANOVA and Welch's F detected significance at $p < 0.05$.

Post- hoc testing in this case shows that the greatest variation in Carbonate absorbance is between the cortical and the trabecular tissue with only somewhat less variance between trabecular and osteonal tissue.

	Car. Abs. Cort.	Car. Abs. Trab.	Car. Abs. Ost.
Car. Abs. Cort.		0.003059	0.6693
Car. Abs. Trab.	0.003059		0.01615
Car. Abs. Ost.	0.6693	0.01615	

Table 27- Post- hoc testing shows greatest variance between carbonate absorption in the trabecular vs cortical tissue with somewhat less between trabecular and osteonal tissue.

Correlation Testing

In an effort to ascertain more details about the nature of the variance seen in ANOVA testing, correlation testing was performed between DNA concentration values and the ATR results. First, phosphate absorption was run against carbonate absorption and the results indicate a strong, linear, correlation with a $p = 4.087E-40$ where $\alpha = 0.05$.

Then, aggregate correlation testing, that is, comparing all phosphate and carbonate absorption scores to all scores from each DNA type suggested a weak, negative, monotonic, correlation between phosphate absorption and autosomal DNA. Both Y-chromosome and mtDNA were weakly, positively correlated. Pearson's R, shown in the table below, indicated that none of the p values were statistically significant. As with the ANOVA data, relevant p values are highlighted in yellow and relevant correlation coefficients are in blue.

	Phosphate	Autosomal		Phosphate	Y Chromo		Phosphate	Mito
Phosphate		0.19305	Phosphate		0.80702	Phosphate		0.71717
Autosomal	-0.17819		Y Chromo	0.033702		Mito	-0.049962	

Table 28- Pearson's R Correlation test results of phosphate absorption by DNA type. None of the p values (yellow) showed significant correlation. Correlation coefficients (blue) indicated negative relationships.

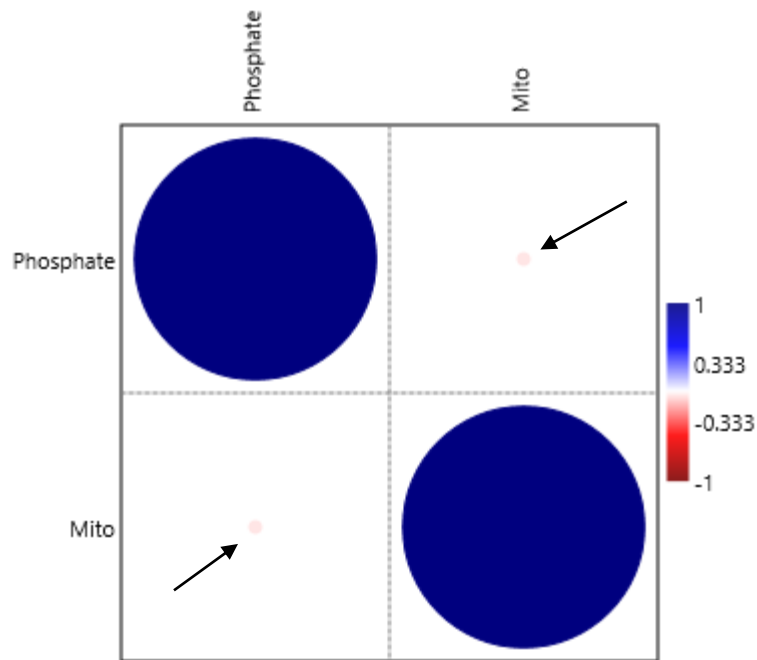


Figure 3- Example of an output from PAST 4.03 showing correlation strength/weakness between Phosphate absorbance levels and mtDNA Arrows point to the small, pink, circles indicating a very weak, negative, correlation.

Cortical Bone Tissue

Pearson's R detected a weak, negative, monotonic, correlation between amino acid absorption and autosomal DNA ($p = 0.13701$). A weak, positive correlation was

detected between amino acid absorbance and both Y-chromosome data ($p = 0.69626$) and mtDNA ($p = 0.24743$).

Both phosphate ($p = 0.15592$) and carbonate ($p = 0.14663$) were weakly, negatively, correlated with autosomal DNA and Y-chromosome data. A weak, positive correlation was detected between both phosphate ($p = 0.47651$) and carbonate ($p = 0.47651$) absorbance and mtDNA.

	Ph Abs	Y Chromo			Car Abs	Y Chromo
Ph Abs		0.51472		Car Abs		0.49512
Y Chromo	-0.13668			Y Chromo	-0.14306	

Table 29- Correlation testing results between phosphate and Y chromosome and carbonate and Y chromosome DNA.

Trabecular Bone Tissue

	Amino Acid	Auto		Amino Acid	Y Chromo		Amino Acid	mtDNA
Amino Acid		0.79112	Amino Acid		0.77478	Amino Acid		0.93026
Auto.	-0.058437		Y Chromo	-0.063123		mtDNA	-0.019325	

Table 30- Correlation testing results comparing amino acid absorption levels by DNA type in trabecular tissue.

	Phos.	Auto		Phos.	Y Chromo		Phos.	mtDNA
Phos.		0.34747	Phos.		0.31151	Phos.		0.88409
Auto.	-0.20525		Y Chromo	0.22072		mtDNA	-0.032186	

Table 31- Correlation testing results comparing phosphate absorption levels by DNA type in trabecular tissue.

	Car.	Auto.		Car.	Y Chromo		Car.	mtDNA
Car.		0.29079	Car.		0.30894	Car.		0.77917
Auto.	-0.23013		Y Chromo	0.22186		mtDNA	-0.06186	

Table 32- Correlation testing results comparing carbonate absorption levels by DNA type in trabecular tissue.

While none of the p values met the requirements for significance, there was a more consistently negative relationship between biochemical properties of trabecular tissue and DNA.

Osteonal Bone Tissue

	Amino Acid	Auto.		Amino Acid	Y Chromo		Amino Acid	mtDNA
--	---------------	-------	--	---------------	-------------	--	---------------	-------

Amino Acid		0.2423	Amino Acid		0.94658	Amino Acid		0.68898
Auto.	0.50996		Y Chromo	-0.03148		mtDNA	0.18643	

Table 33- Correlation testing results comparing amino acid absorption by DNA type in osteonal tissue.

	Phos.	Auto.		Phos.	Y Chromo		Phos.	mtDNA
Phos.		0.73005	Phos.		0.82899	Phos.		0.42004
Auto.	0.16109		Y Chromo	-0.10125		mtDNA	0.35714	

Table 34- Correlation testing between phosphate absorption by DNA type in osteonal tissue.

	Carb.	Auto.		Carb.	Y Chromo		Carb.	mtDNA
Carb.		0.47619	Carb.		0.88054	Carb.		0.51452
Auto.	0.14168		Y Chromo	-0.07054		mtDNA	0.29918	

Table 35- Correlation testing between carbonate absorbance by DNA type in osteonal tissue.

With the exception of Y-chromosome data, which was negative in all three correlation tests, osteonal tissue was more positively correlated with amino acid, phosphate, and carbonate levels.

To elaborate on the relationship between carbonate and phosphate levels and DNA, those samples which displayed the lowest levels of mtDNA were combined in a table with the ancient samples that were run through ATR/FTIR analysis as a baseline. Since there were only four ancient samples, with only mtDNA results in an unrelated study, no correlation or other statistical analysis could be run on those samples. Raw data does not appear to support, or be supported by, the findings from the correlation tests. This could well be due to smaller sample size, but whatever the reason, the raw data table are provided below.

Sample	Tissue Type	Amino Acid Absorbance	Phosphate Absorbance	Carbonate Absorbance	Mito
LTIB 6	1	0.098	0.331	0.300	0.00E+00
LTIB 2	2	0.093	0.370	0.329	0.00E+00
R2A	1	0.088	0.310	0.266	0.00E+00
MAN 1	1	0.084	0.330	0.340	0.00E+00
C2A	1	0.083	0.207	0.193	0.00E+00
C2B	2	0.068	0.120	0.107	0.00E+00
LRib 2A	1	0.066	0.191	0.181	0.00E+00
R3A	1	0.062	0.148	0.129	0.00E+00
L2B	2	0.062	0.135	0.110	0.00E+00
C4A	1	0.060	0.351	0.340	0.00E+00
C1A	1	0.059	0.235	0.241	0.00E+00
LFP 4	1	0.043	0.160	0.162	0.00E+00
L2A	1	0.042	0.138	0.136	0.00E+00
LTIB 5	2	0.039	0.145	0.150	0.00E+00
LTAR 1	1	0.029	0.156	0.134	0.00E+00
LSC 3	1	0.143	0.409	0.354	4.05E-10
LFEM 4	3	0.064	0.237	0.225	4.66E-10
LRad 5	2	0.045	0.153	0.152	6.81E-10
T10B	2	0.060	0.700	0.510	0.00E+00
Ancient A	2	0.03	0.5	0.39	0.00E+00
Ancient B	2	0.05	0.75	0.5	0.00E+00
Ancient C	2	0.05	0.85	0.64	0.00E+00
Ancient D	2	0.05	0.8	0.56	0.00E+00

Table 36- Samples with zero, or E-10 mtDNA results are listed alongside Amino Acid, Phosphate, and carbonate levels as measured by ATR/FTIR spectroscopy. The bottom 4 samples are the ancient samples which were run as a baseline for the ATR/FTIR analyses.

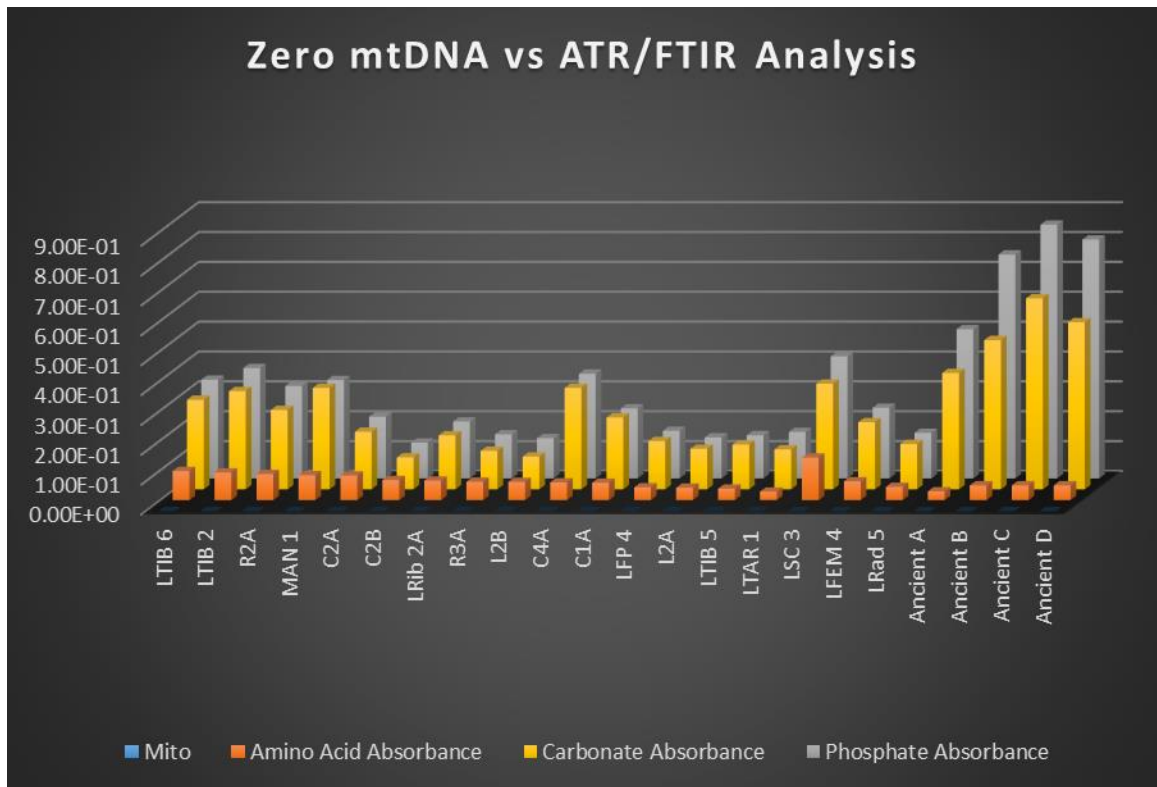


Figure 4- Graph of mtDNA in relation to Amino Acid, Phosphate, and Carbonate absorbance.

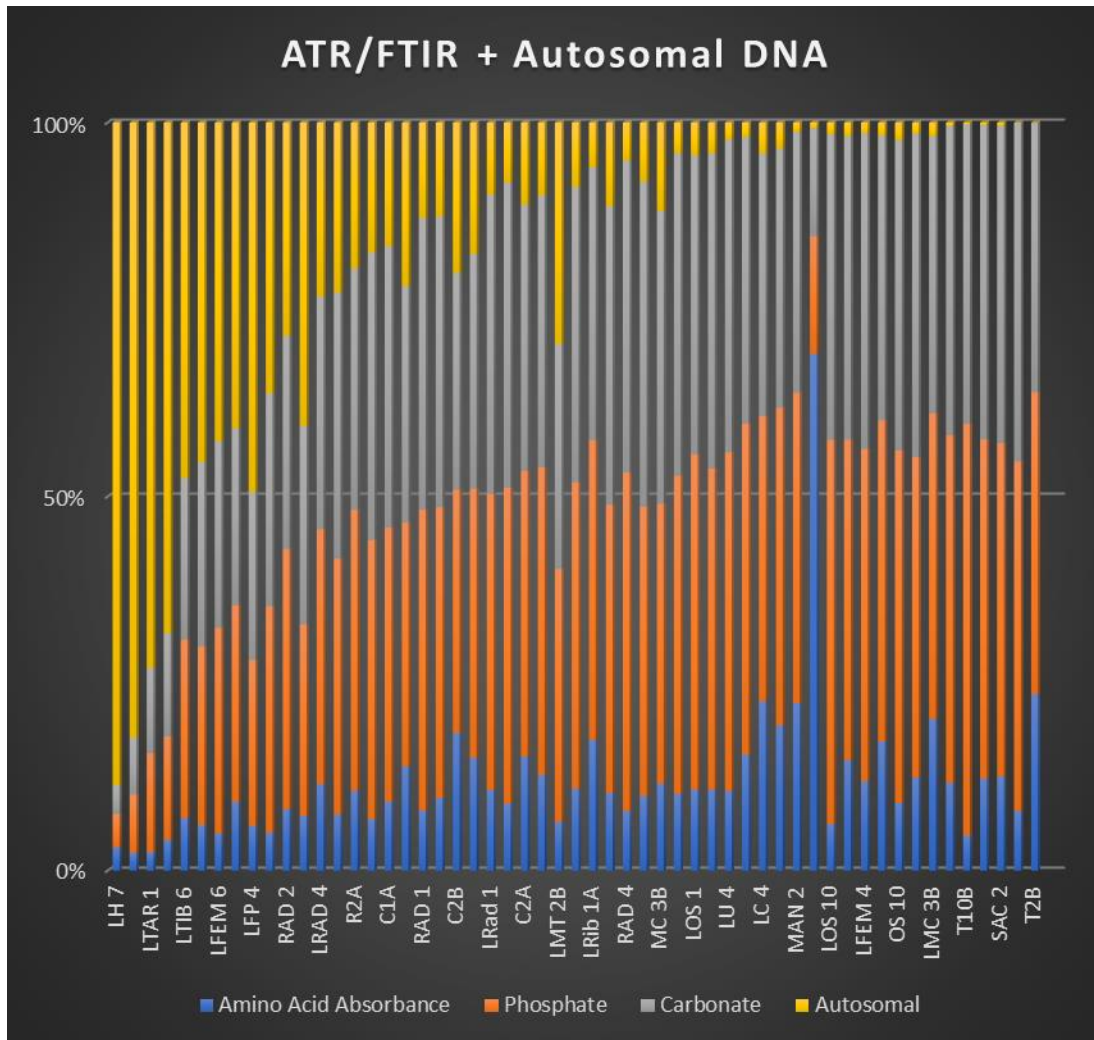


Figure 5- Graph showing the correlation between amino acid, phosphate, and carbonate absorbance from ATR/FTIR testing and autosomal DNA.

STR Results

Due to budgetary restraints, only 62 of the samples were run through CE for fragment analysis and STR profile construction. While this may seem to be a serious limit to the study, it is illustrative of real- world issues facing forensic DNA analysts. The samples that were chosen for fragment analysis were selected to be a truly representative

subset of the overall sample population. The criteria used were 1) tissue type, 2) skeletal element grouping, and 3) the highest, middle, and lowest performing samples by qPCR data. The samples were taken to the Montana State Crime Lab and testing was performed by Joe Pasternak. Ten of the eluted DNA samples had evaporated beyond the point that re- hydration with deionized water was possible. Results from the remaining 51 are as follows:

Sample	# Loci	% Profile		Sample	# Loci	% Profile
LOS1	23.0	100%		MAN2	23.0	100%
LOS7	11.0	48%		MC3B	9.0	39%
LP	23.0	100%		MC3A	8.5	37%
LMC3A	14.0	61%		MC1B	3.5	15%
LMC1B	16.0	70%		MC1A	5.0	22%
LMC1A	0.0	0%		RAD6	3.0	13%
LH4	0.0	0%		RAD1	23.0	100%
LH1	23.0	100%		U6	23.0	100%
R4B	23.0	100%		U1	23.0	100%
R4A	0.0	0%		HUM4	11.5	50%
R1B	7.0	30%		HUM2	22.0	96%

R1A	23.0	100%		HUM1	11.0	48%
L1B	0.0	0%		FEM2	14.0	61%
L1A	0.0	0%		FEM1	23.0	100%
T1B	5.0	22%		OS9	21.0	91%
T1A	3.0	13%		OS7	12.0	52%
C1B	10.5	45%		OS2	17.0	74%
C1A	23.0	100%		OS1	23.0	100%
MT1B	19.0	83%		STE2	6.5	28%
MT1A	14.0	61%		STE1	23.0	100%
TAR4	0.0	0%		TIB3	22.0	96%
TAR3	23.0	100%		TIB1	19.0	83%
TAR2	23.0	100%		FEM6	23.0	100%
TAR1	22.0	96%		FEM5	23.0	100%
TIB7	22.0	96%		FEM4	23.0	100%
TIB6	23.0	100%		TIB4	22.0	96%

Table 37- Fragment analysis indicating the # of STR loci for each sample and the % of complete profile represented. A profile is considered complete that contains all 23 of the CODIS loci. Red = cortical tissuesamples, green = trabecular, and yellow = osteonal.

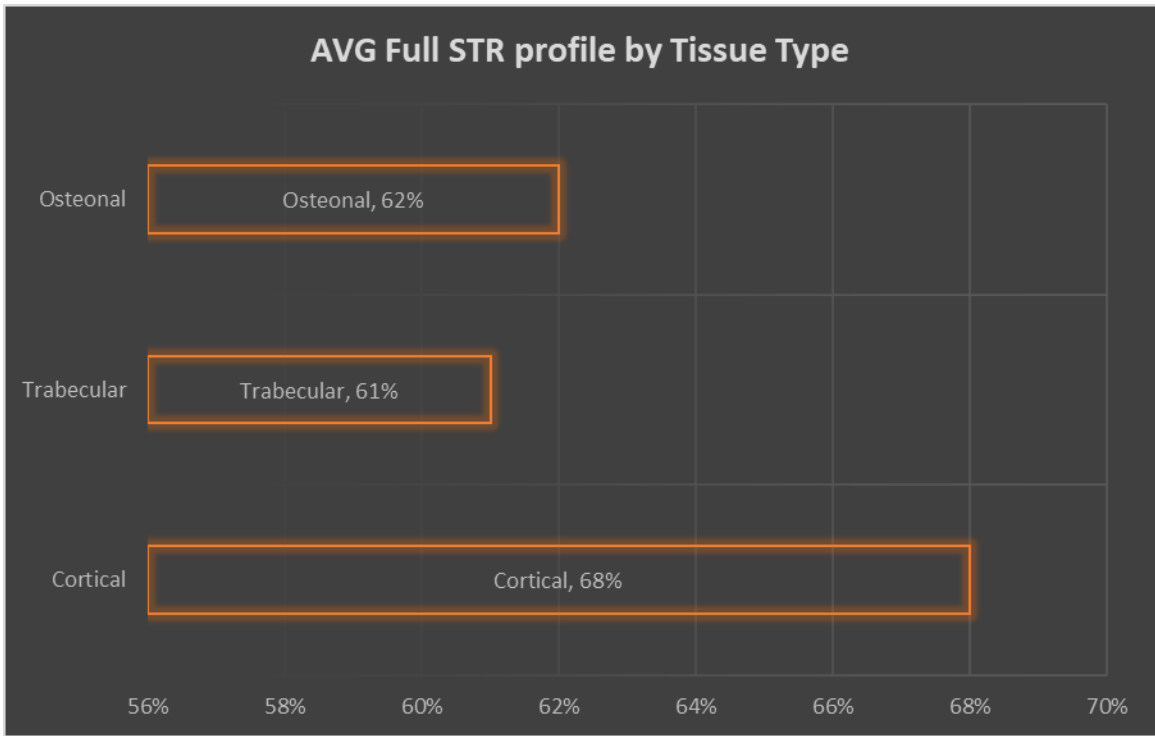


Figure 6- Average percentage of complete STR profiles by tissue type.

Sample	# Loci		Sample	# Loci		Sample	# Loci
LOS1	23.0		FEM1	23.0		TAR3	23.0
LOS7	11.0		OS9	21.0		TAR2	23.0
LMC3A	14.0		OS7	12.0		TAR1	22.0
LMC1A	0.0		OS2	17.0		TIB6	23.0
LH1	23.0		OS1	23.0		FEM6	23.0
R4A	0.0		STE1	23.0		HUM1	11.0
R1A	23.0		MC3A	8.5		FEM1	23.0
L1A	0.0		MC1A	5.0		OS9	21.0
T1A	3.0		RAD6	3.0		OS7	12.0
C1A	23.0		RAD1	23.0		OS2	17.0
MT1A	14.0		U6	23.0		OS1	23.0
TAR4	0.0		U1	23.0			

Table 38- # STR loci by cortical samples.

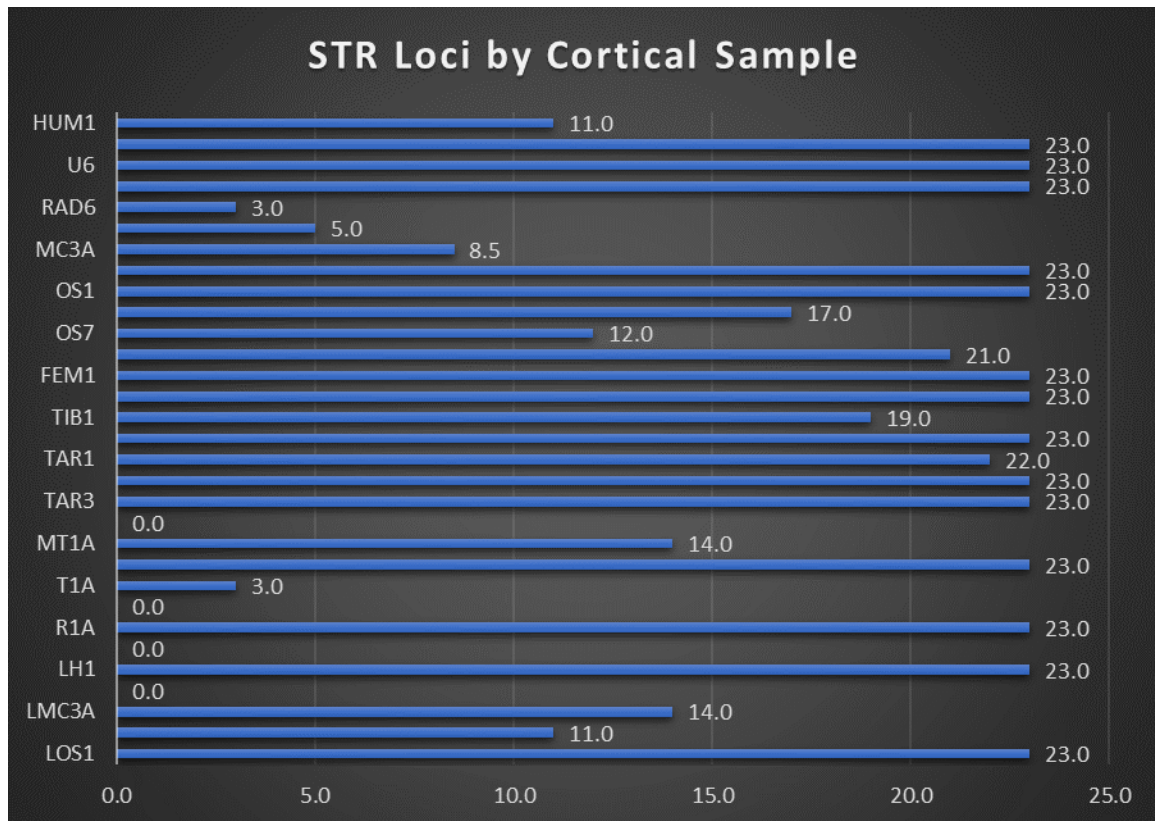


Figure 7- STR loci by cortical tissue. 23 loci is the maximum that can be amplified by the Qiagen Investigator kit and constitutes a 100% profile. The chart goes to 25 to aid in legibility.

Sample	# Loci
LP	23.0
LMC1B	16.0
R4B	23.0
R1B	7.0
L1B	0.0
T1B	5.0
C1B	10.5
MT1B	19.0
TIB2	19.0
FEM5	23.0
FEM2	14.0
STE2	6.5
MAN2	23.0
MC3B	9.0
MC1B	3.5
HUM2	22.0

Table 39- # Loci by trabecular tissue samples. # of loci is out of 23 total.

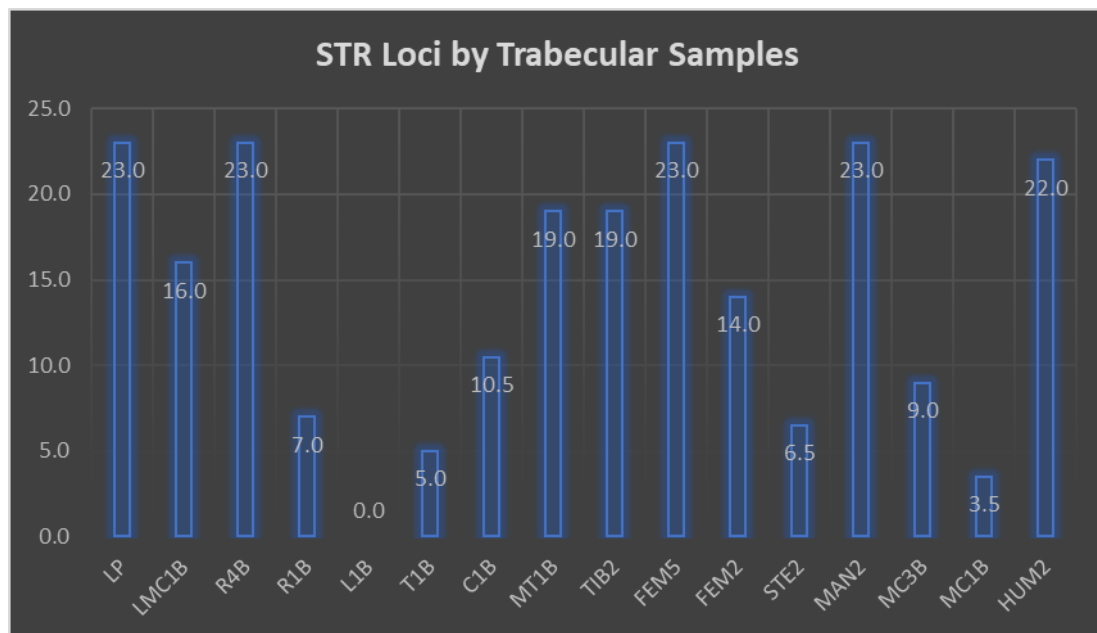


Figure 8- # STR Loci by trabecular tissue samples.

Sample	# Loci
LH4	0.0
FEM4	23.0
HUM4	11.5
TIB4	22.0

Table 40- # STR loci by osteonal tissue sample.

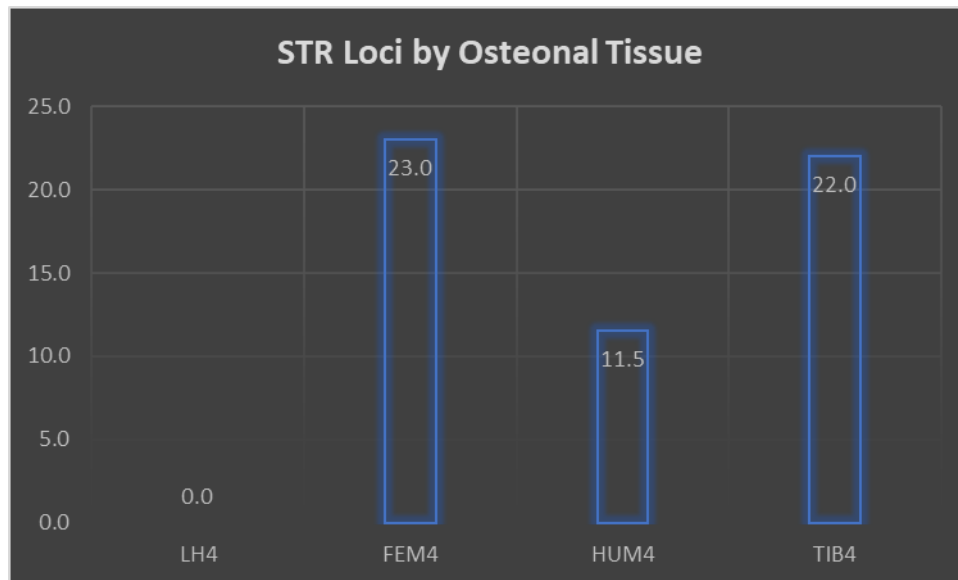


Figure 9- # STR loci by osteonal tissue sample.

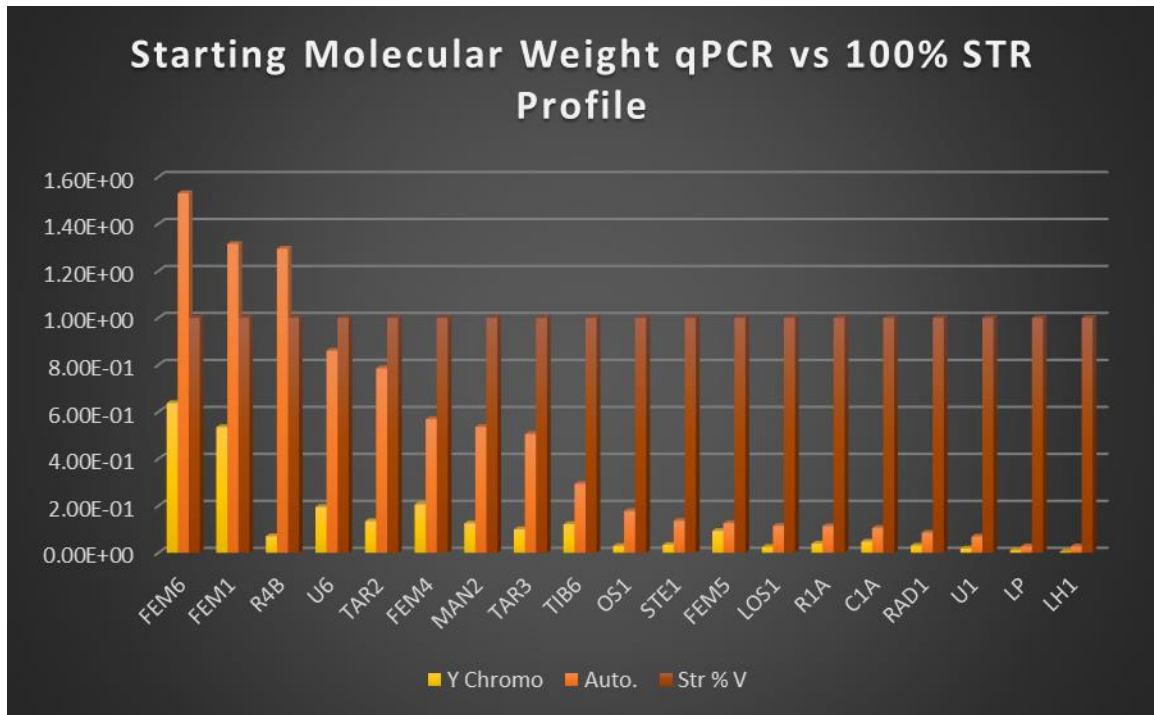


Figure 10- Graph showing how starting molecular weight from qPCR quantitation compares to samples that produced 100% STR profiles.

Nineteen of the 51 samples (37%) generated 23 STR loci which constitutes a full profile. Conversely, sixteen of the samples (31%) generated 0 STR loci. The breakdown for the remainder of the samples is as follows: three (3) samples generated 10% - 20% STR profile, nine (9) generated 21% - 49% profile, seven (7) generated from 50% - 75% profile, and eight (8) generated between 76% - 96% of a full profile. Because the STR kit used in the study indicates the presence of both/either the X and Y chromosomes, if only one appeared, it was counted as ½ of a locus.

In forensics, those samples which generate at least 21 loci (91% profile) are considered usable and in this study, 24 samples (47%) met that criterion. For bioarchaeologists and paleoanthropologists, however, even partial profiles may be instructive depending on the genetic locus or loci under study.

CONCLUSIONS & DISCUSSION

Examining the raw data, and especially cross-referencing said data to the actual skeletal material under investigation, can be instructive. Frequently, in forensic anthropology, investigators are forced to observe morphological features and make assessments that are difficult, if not impossible, to reliably quantify statistically. Some of the data from this project illustrates the underlying biology and biochemistry that directly pertains to those un-quantifiable features and indicates that statistical analyses are not absolutely essential for scientific understanding.

For example, the degree to which taphonomic factors may be influencing low starting DNA molecular weight are almost impossible to quantify, yet when comparing the left os coxa of the individual to the right os coxa, or some of the vertebral elements, it is easy to see that some elements are more heavily processed than others. And the raw data from qPCR analysis bears this out, even though statistical analysis does not. Statistical analytical methods are often times too large a brush for the detailed work that is needed. In this project specifically, where maceration of the body has rendered the skeletal tissue extremely pale and brittle, starting molecular weight DNA is not as good, yet moving from the iliac crest to the auricular surface yielded noticeably better DNA yield. Drawing this reasoning out, if DNA analysis is to be performed, obviously the first choice would be to obtain a sample from a fresh skeleton. However, since the underlying assumption of this study is that, in the real world, the nature and extent of taphonomic

influence is often unknown. Thus, relying on the traditional forensic anthropological features for sample procurement is wise.

The reason for this is that the features which forensic anthropologists examine are the results of lifelong cellular and biochemical activity on, or within, the bone tissue. Even if the individual is relatively young at the time of death, thorough understanding of the ontogeny, development, and decline of bone tissue allows a sound basis for sample selection. In some situations, for example when only fragments of bone are available, advanced knowledge of the processes of bone growth and remodeling may be necessary. Since not all who are engaged in the pursuit of DNA from human skeletal tissue may be so trained, attempting to address as many potential scenarios as possible, and thus provide a clear portrayal of the optimal sampling sites across the post-crania is the main objective of the project.

Furthermore, the project was successful in creating an effective sampling method that is far less destructive to human or hominin bone tissue than had been attempted in the past. By employing a deep understanding of skeletal cellular biology and biochemistry, this study shows that it is indeed possible to reduce the amount of tissue destruction to only that which is absolutely essential for scientific accuracy. In this case, that success comes in the form of a decrease of 30-50% of the requisite tissue from what has been used in past studies (3–5,134) and even from what was published in the protocols from the manufacturer of the DNA extraction kits (163). In fact, any deviation from the published protocols came in the form of *less*. Less bone tissue was used, and less time was spent incubating and agitating the samples. This speaks to effective

products used on samples that were strategically obtained from a human source that was ethically treated.

CORRELATING CELL TYPE POPULATIONS WITH DNA TYPE AND QUANTITY

In both hands, trabecular samples from the distal ends of the 3rd metacarpals were the highest scoring sites with 1.13E-05 from the left and 2.21E-05 from the right, respectively. Examining the skeletal material, there were five sesamoid bones present in the hands and seven in the feet. These small accessory ossicles develop over the course of an individual's life due primarily to heavy use of the appendages and function as support for them (164–167). Development of bone tissue like this is conclusive evidence of osteoblastic activity. And, if present for a long enough period of time, the metatarsal/metacarpals and phalanges adjacent to the sesamoids will often develop articular facets; a process which requires resorption of the existing bone tissue by osteoclast activity.

The pubic symphysis and the auricular surface of the os coxa are two regions that forensic anthropologists routinely examine during age-at-death estimations. These two regions undergo significant homeostatic alterations over the course of life. While the interpretations of these changes are debated in their accuracy of age-at-death estimations, the cellular populations involved with these changes are well-documented. In this study, raw qPCR data from cortical tissue of the pubic symphyses were some of the highest across the entire sample population and across all DNA types. Given that osteoclasts are multi-nucleated and highly active (requiring mitochondria for energy production), the high scores from both nuclear (autosomal and Y-chromosome) and mtDNA scores

indicate that there almost certainly was some *in vivo* osteoclast activity present at the time of death. The auricular surface, very similar in its utility to forensic anthropologists, differed in autosomal raw qPCR scores, but were still quite high. The auricular surface is where the os coxa articulates with the sacrum at the sacro-iliac joint. In this individual, the trabecular sample from sacro-iliac joint on the right side performed quite well in mtDNA quantification ($1.07E-03$), even though the surface cortical did not. While seemingly contradictory, remember that osteoclasts derive from hematopoietic stem cells that are found in trabeculae and bone marrow. Furthermore, bone creation cannot be carried out while bone destruction is occurring at the same place. From a functional morphological standpoint, if the bone on one side of the joint is being resorbed, the other side will most likely not also be undergoing resorption so as to limit the degree of destabilization.

Similarly, the sample taken from trabecular tissue at the distal end of the sternum was one of the highest overall performing sites for mtDNA at $3.17E-03$. Examination of the element shows a significant degree of remodeling occurring both on the sternal body itself, as well as at costal articulation sites. Trabecular tissue samples taken from C7 and T3 also performed well in mtDNA analysis, as did nearly all of the samples from the ribs and the mid-diaphyseal sites of the long bones from the right side.

It was not only trabecular tissue that performed well in mtDNA quantification. Cortical samples from the 1st proximal phalanx of the foot, the talus, calcaneus, and patella on the right side and the medial clavicle and the olecranon process of the ulna from the left side all scored well. Osteonal tissue samples, generally, did not perform well in mtDNA analysis, with the exception of the right femur.

Osteonal samples across the entirety of the right side performed better than did those of the left side. On the right femur, both the mid-diaphyseal cortical and trabecular samples failed to produce any mtDNA while the osteonal sample performed quite well. The opposite was true on the left side, with the osteonal sample failing to produce any mtDNA at all. Samples from the other long bones follow the pattern of being higher on the right side than the left. The left humerus performed well in nuclear DNA quantitation and poorly in mtDNA levels. If osteocyte populations predominate in this tissue, then this is the pattern that would be expected. Because this is the case with most sampling sites, it is difficult to say with any confidence whether osteonal tissue is a reliable source of mtDNA. Due to the very low starting molecular weight of mtDNA that was recovered, however, it can be suggested with some confidence, that there are more reliable sites throughout the post-cranial skeleton, if those elements are available for sampling. And if the femur is all that is available, this data does suggest that either proximal or distal sites are preferable.

Given that the mid-diaphyseal sites were located at the nutrient foramina, the major site of vascularization and innervation to and from the long bones, the low mtDNA scores may be easily explained in light of the processes of autolysis, decomposition, and/or maceration. These factors are important considerations in and of themselves in deciding where to sample for DNA. The enzymes involved with autolysis, the chemicals used in maceration, and bacterial agents in the case of natural decomposition, may have more access to the bone tissue through this point. The relative success of the right femur in mtDNA extraction from the osteonal tissue may be the result of increased osteoclastic activity in general on that side and may actually support the hypothesis of right-side

dominance in the individual. Whether this is the case or not is difficult to say, but mid-diaphyseal sampling on or around the nutrient foramina of long bones does not appear to be optimal if any other choices are available.

Another important consideration in attempting to correlate DNA levels with cellular populations is the activity of osteoblasts in proximity to the proposed sampling site. While not directly addressed in the hypotheses of this study, results of DNA analysis are consistent with the biochemical communication between, and activation/deactivation of, osteoclasts and osteoblasts (37,41,43,44). The lower thoracic and all of the lumbar vertebrae failed to produce any mtDNA whatsoever. Examination of these elements shows noticeable osteophytic development. Samples from the ribs bilaterally are consistent with this, as well. Where there is pronounced osteophytic growth, there is higher autosomal and Y-chromosome data, and lower mtDNA.

The data from this study also indicates that bone tissue quiescence may be an integral factor in DNA extractability. The seemingly poor performance of the petrous portions of the temporal bones ($5.85E-06$ from the left and 0.00 from the right), may indicate the predominance of terminally differentiated osteocytes or bone-lining cells over the more active osteoblasts or osteoclasts, at least on the right side. Post-developmentally, there may not be active cell populations sufficient to obtain adequate DNA in these tissues, barring injury or pathology. This may be the reason for poor mtDNA data in studies which have attempted extraction from other bones of the cranium, as well (85). While outside the scope of this project, the individual in this study did exhibit an anomaly attributed to a surgical procedure to the left frontal bone immediately inferior to the sagittal suture. It would be interesting to see how the bone tissue, both

cortical and diploic, surrounding the injury to the frontal bone would perform in DNA analysis. The complete lack of mtDNA data from samples of the dental tissue from the right 1st molar (the only one available for sampling in this individual) is most likely an artifact of extremely poor dental health overall in the individual. Data from other studies have routinely reported high mtDNA extraction and amplification from dental tissue. This individual, however, had several serious dental caries, an abscess, and exhibited a high degree of alveolar resorption from other missing teeth. As stated, the tooth selected for analysis was the only remaining molar. Usually, DNA extractions from teeth highly prioritize the molars due to their large size and robusticity in comparison to the other tooth types.

ATR/FTIR SPECTROSCOPIC ANALYSIS AND DNA EXTRACTION

Results of the correlation testing between amino acid, phosphate, and carbonate absorbance and the three DNA types in the different bone tissues was inconclusive. In the autosomal data, it appears that as phosphate and carbonate levels increase, DNA levels decrease. However, it is not clear from the data whether these mineral groups are actually excluding or entombing the DNA or if there are hidden variables influencing the data. More samples from a wider variety of taphonomic conditions and ages would need to be performed. The data certainly indicates that it is worth studying because if we can discern what the actual process is that drives the negative correlation between the minerals (especially phosphate) and DNA, then we can adapt DNA extraction protocols. For example, if the research indicates that the phosphate is really “entombing” the DNA, then we can increase the amount of EDTA and/or Proteinase K to account for their entrapment within the mineral matrix. Conversely, if the negatively charged carbonate increase is

shown to repel the also negatively charged DNA, then we can either alter the amplification protocols by adapting the primers and/or thermal cycling parameters accordingly.

The negative monotonic correlation between amino acid absorbance and DNA levels in the osteonal bone tissue was, at first, confusing. As analyses proceeded, however, it seems that this is most likely an artifact of taphonomy, especially in the case of Y-chromosome levels. The Y-chromosome is known to be smaller than the other chromosomes and more prone to molecular taphonomic damage (106,168,169). Regardless of the DNA type, the negative correlation can be easily explained in terms of the chemical bonds. DNA has a sugar phosphate “backbone” to which the nucleotides are attached. If the DNA strand is in small, un-amplifiable fragments, then ATR/FTIR spectroscopy will still “see” them, even if they are too small to be amplified either during qPCR or the amplification phase of fragment analysis. This is supported by much of the results of Qubit fluoroscopic analysis at the earliest stage of quantification immediately following the DNA extraction/purification phase.

The hypothesis that ATR/FTIR spectroscopy will aid in determining suitability for DNA extraction can neither be supported nor wholly rejected. It seems that ATR/FTIR analysis is valuable in identifying which samples are absolutely NOT suitable for extraction, and thus, maybe more useful in paleoanthropological studies than in forensic cases where there is the assumption of DNA survival. And it certainly aids with visualizing taphonomic and diagenetic processes that influence DNA extraction and amplification. With more research, this type of spectroscopy may prove useful in developing better extraction and purification methods and understanding the relationship

between phosphate/carbonate and DNA from bone tissue is certainly worth continued study. Utilizing ATR/FTIR spectroscopy on bone tissue from a wide range of taphonomic conditions-such as prolonged exposure to different soil pH levels and chemical types-may help elucidate the diagenetic process that seem to inhibit or prevent DNA extraction/amplification. It may also be useful in studies of grave soil to determine if there may be amplifiable DNA prior to attempting more expensive methods. Other studies of biochemical aspects of bone functional morphology in paleoanthropology, bioarchaeology, and zooarchaeology may also benefit from the use of ATR/FTIR spectroscopy.

OPTIMAL SAMPLING SITES

THE APPENDICULAR SKELETON

Overall results of DNA testing and comparisons between and within elements indicate that the optimal sampling sites are those associated with the heaviest life-long use and, thus, cellular remodeling. These regions almost ubiquitously involve proximity to articulation sites. While the specific bone tissues involved tend to indicate that the dense cortical bone is better, trabecular tissue did perform well at some sites, such as the left acromion process of the scapula, the ulnar notch of the radius, the olecranon process of the ulna, and others. Therefore, at least in the appendicular skeleton, tissue type seems to be less important than location.

Upper Body Elements

Results of DNA testing of the skeletal elements of the upper body (shoulder, arm, and hand) indicate that the indicate that the 5 most optimal sampling sites for autosomal DNA were:

1. The medial epicondyle of the distal humerus
2. The bicipital groove of the humerus
3. The ulnar notch or head of the radius
4. The extensor carpi of the distal ulna
5. The olecranon process of the proximal ulna

In the upper appendicular skeleton, the limbs of the right side of the upper body outperformed their left side counterparts. Forensic anthropological analysis also estimated the individual to most likely be right-handed. The DNA results are consistent with that assessment. Estimation of handedness in forensic anthropological analysis may inform sampling decisions for forensic DNA analysis as to which of the sides should be prioritized in cases where there is an option.

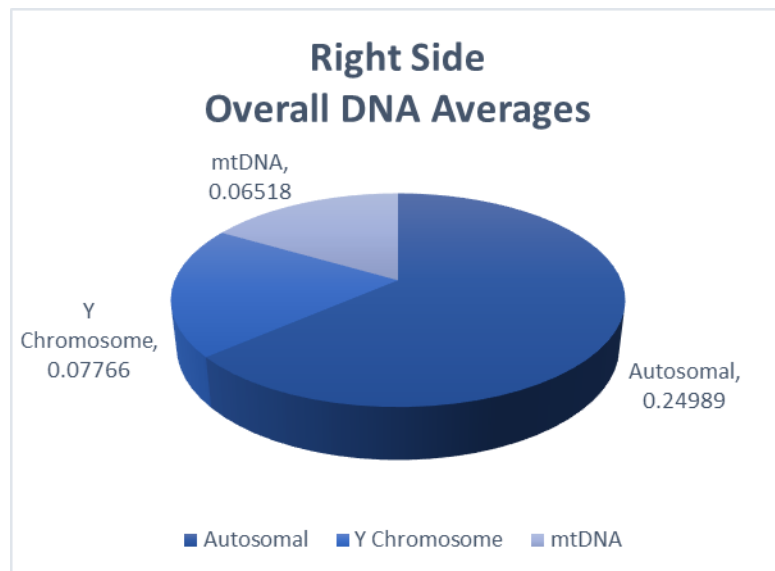


Figure 11- Averages of all qPCR results from the right side.

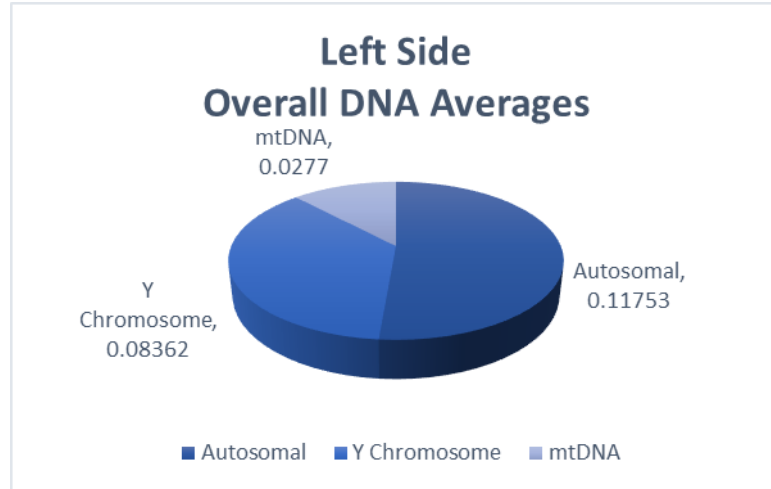


Figure 12- Averages of all qPCR results from the left side.

Lower Body Elements

As with the elements of the upper body, the right side performed better than the left side. Cortical tissue generally outperformed trabecular and osteonal tissue, but the top two sites from the lower body were the trabecular and cortical samples from the femoral head. The top five sampling sites for autosomal DNA from the lower limbs of the body were:

1. The fovea capitis of the femur (both trabecular and cortical performed well)
2. The intercondylar fossa of the distal femur
3. Cortical tissue from the tibial plateau
4. The nutrient foramen of the femur
5. The sustentaculum tali or calcaneal tuberosity of the calcaneus

While it is usually more difficult, if impossible, to empirically glean lower limb dominance than handedness, attention should still be paid to evidence of cellular activity. In this individual, due to the observation of increasing porosity in the femoral neck, that area was avoided for DNA sampling purposes. To some extent, the loss of bone mineral density (BMD) occurs as a natural process of age in humans. As age advances, osteocyte lacunae are no longer re-filled and new secondary osteons are not constructed once the cell has succumbed to apoptosis or programmed cell death. The transition from natural to pathological can be difficult to ascertain, but often takes the form of transition from microporosity to macroporosity as the minerals from bone tissue in the empty lacunae is “looted” to maintain homeostatic levels elsewhere. This is seen especially in or near the hips, knees, shoulders, and elbows. This process of homeostatic mineral reallocation and ensuing macroporosity can be accelerated and/or exacerbated by numerous factors (19,56,83,170–174). While the effect this may have on DNA extraction is not well characterized, since optimal DNA extractability was the main goal of the study, areas of visible macroporosity associated with BMD loss were avoided.

THE AXIAL SKELETON

Many of the elements of the axial skeleton in this individual were undergoing considerable remodeling. There was extensive visible evidence of cellular activity on the sternal rib ends, the manubrium, the sternum, and several vertebral elements. Additionally, the right 6th, 7th, and 8th ribs exhibited a bony callous consistent with a poorly healed fracture. The halves of the ribs had separated at the callous during maceration.



Image 7- Three ribs with photographic scale showing breakage at the site of ante- mortem callous growth.

This provided a perfect sampling site for this experiment. Additionally, upon attempting to obtain a trabecular tissue sample from the manubrium, it was discovered that the inside of the element was completely dominated by thick, brown, cartilaginous material. A sample of the material was taken for DNA analysis, but upon examination of the sample at extraction time, a significant bloom of mold had developed. The sample was retained, but no attempt was made at extraction due to the high probability of contamination. Full sequencing of the human and mold DNA would be an interesting project.

In the ribs, multiple elements from both sides performed well in DNA analysis. From the left side, the top sites for autosomal DNA were:

1. Cortical sample of the 4th rib

2. Cortical tissue from the 8th rib

Interestingly, the cortical tissue from the 4th rib yielded 0.00 mtDNA, despite a very high score in autosomal and Y-chromosome DNA. The 8th rib cortical sample, on the other hand, yielded high scores across all DNA types. On the right side, the top sampling sites for autosomal DNA were:

1. Cortical tissue of the 8th rib
2. Trabecular tissue of the 8th rib

In an interesting juxtaposition to its left-side counterparts, the right 8th rib yielded no mtDNA at all. The 4th rib, though it was third highest in autosomal and Y-chromosome DNA, was the top site for mtDNA. Again, sampling from the ribs was aimed directly at the visible areas of cellular activity. On the ribs that did not exhibit trauma, such as the first ribs, there was still visible evidence of cellular activity on the inferior surface near or on the sub-clavian groove and sampling was aimed there for the cortical tissue. Trabecular tissue was taken from the sternal ends, many of which exhibited the “crab claw” feature, which is known to be evidence of ossification of the costal cartilage (175–177), and thus, obvious sites of osteoblastic activity.

The sternum and the manubrium, despite having significant evidence of cellular activity, did not perform especially well in DNA extraction. The cortical sample taken from the clavicular notch of the manubrium was the highest performing site in both nuclear DNA, while the distal end of the sternal body yielded the highest amount of mtDNA. Because of these results, it recommended that these elements be avoided, if there are other options for sampling.

The vertebrae of this individual provided some very interesting results; although because of those results, it does not seem practical to attempt to effectively rank the best sampling sites. While the lumbar vertebrae failed to yield any mtDNA at all, they scored significantly higher than the other regions in nuclear DNA. Examination of the elements shows osteophytic activity on both the pedicles and at the anterior margins of the vertebral bodies. This development is not due to trauma, but more likely to osteoarthritis (OA), and thus, is not indicative of osteoclastic resorptive activity(19,56,174,178–180). All of the highest nuclear DNA scores came from cortical samples obtained from locations on the vertebral bodies or articular facets immediately adjacent to the areas of visible osteophytic growth. Trabecular samples taken from the 4th thoracic and the 7th cervical vertebrae scored highest in mtDNA. Both of these elements also show some signs of cellular activity and these results may indicate that the surfaces of the bones were undergoing osteoclastic resorption in preparation for osteoblastic matrix deposition. Or they be indicative of the early stages of osteoblastic activity when the cells are still actively depositing new tissue.

In either case, the results of this study indicate that vertebral elements may be useful targets of DNA extraction if there is visible evidence of cellular activity. In the spine, this usually presents as osteophytic development of some kind but will be highly dependent on the individual person. Since most spinal conditions associated with osteophytic development (OA, diffuse idiopathic skeletal hyperostosis, ankylosing spondylitis, etc.) begin in the lumbar region, if mtDNA is sought, it may be wise to target elements in the thoracic or even cervical spines at the earliest stages of whichever condition is diagnosed or suspected. Further investigation involving definite diagnosis of degenerative spinal

conditions such as those mentioned above, as well as cases of spinal stenosis, scoliosis and kyphosis, is definitely warranted and may provide valuable insight into the effects of interactions between osteoblasts and osteoclasts on a macroscopic scale.

The os coxa of the individual was the only group that yielded generally higher DNA results on the left side than on the right. Cortical tissue also generally outperformed trabecular, although the sample taken from the ischio-pubic ramus did quite well. This study received the highest nuclear DNA from:

1. Cortical tissue from the left auricular surface
2. Cortical tissue from the left posterior inferior spine
3. Cortical tissue from the right pubic symphysis
4. Trabecular tissue from the ischio-pubic ramus
5. Cortical tissue from the left pubic symphysis

Bilaterally, the iliac crest yielded the highest levels of mtDNA. Given that the iliac crest is a site of a major muscle attachment, it is not surprising that there might be higher levels of osteoclast activity than at other regions. Cortical tissue from the pubic symphysis on both sides was the second highest site of mtDNA.

Since the auricular surface scored highest in nuclear DNA and yielded 0.00 in mtDNA (bilaterally), it may be surmised that osteoblastic populations, very possibly in the form of bone-lining cells, are the predominant cell type, at least, in this individual at the time of death. Correlating this data with known *in vivo* remodeling that contributes to forensic age-at-death estimations, it may be assumed that the auricular surface is a reliable source of DNA, regardless of whether the predominant cell type is osteoblastic or

osteoclastic in nature. Bone tissue from the adjacent sacro-iliac joint of the sacrum yielded significantly lower nuclear DNA and higher mtDNA. In fact, the right sacro-iliac joint surface yielded the highest mtDNA across the entire sacrum. In this individual, the transverse line between S1 and S2 was clearly visible and so was targeted as another sampling site. Interestingly, that sample produced 0.00 mtDNA but performed adequately in nuclear DNA extraction. With the proximity to the auricular surface, and the data it provided, it is possible that the trabecular tissue which performed well was the site of osteoclastogenesis at the time of death.

Sesamoid Bones

The largest of the sesamoid bones-the patellas-were mirror images of each other in terms of DNA results, although in both cases, the trabecular samples outperformed the cortical tissue. The right patella yielded decent nuclear DNA and very little mtDNA. The left side was the opposite. While it is not uncommon to recover at least one patella in a forensic archaeological recovery, if there are other sampling options, they should be given priority.

The smaller sesamoids are classified as accessory ossicles of the hands and feet and are not found in all individuals. Additionally, for a variety of reasons, they are rarely recovered in archaeological contexts. While they actually performed reasonably well in DNA extraction, one of the three that was used failed to yield any mtDNA. Another yielded levels that was among the higher levels found the post-crania. The cell types involved with sesamoid bones are predominantly osteoblastic since the bones themselves derive from the ligamentous tissue of the hands and feet in order to increase stability. For

this reason, they are usually found in people of advancing age and those who engage in strenuous physical activity. Osteoclasts may be present if the bone has been present long enough to necessitate an articulation point with an adjoining element; and this is almost certainly the reason for the higher mtDNA results. However, whether osteoclasts will be present in sesamoids is difficult to determine. Therefore, if mtDNA is sought, it would be advisable to sample elsewhere. Another consideration for the exclusion of sesamoids as a source of DNA is that, due to their very small size, the entire bone usually has to be destroyed in order to procure enough sample for extraction. They are also too small to hold while attempting to drill the way the other elements were. Sampling for the present study required placing each sesamoid in a UV-sterilized plastic bag, placing a thick layer of paper towel around the bag and smashing the bone with a hammer. For these reasons, sesamoids should be a last resort.

DNA SURVIVABILITY

While it is difficult to conclusively say which tissue type preserves nuclear (autosomal and Y chromosomal) DNA or mtDNA more effectively, the results of this study do indicate concurrence with other studies which have suggested that cementum in teeth and denser cortical layer of bone protect DNA molecules more effectively than softer tissues (CITE Antinick & Foran, Higgins, Edson, et al). Additionally, the overall results of the study indicate strong support for the hypothesis that knowledge of cellular morphology and activity do inform choices of where to sample for the different types of DNA that may be needed or desired in forensic investigations.

In their 2015 study, Higgins, et al. state that higher mtDNA rates were found from softer dentine material in the roots of teeth. But they fail to adequately address the reason. Is it truly because of the tissue itself? Or is it because there were more mitochondria in the nerve-rich dentine, than in the cementum, to begin with? Similarly, in 2014, Antinick and Foran published a study of differential mtDNA and nuclear DNA from an inter- and intra-element study of bovine and porcine bone. The main issues with this are that 1-rates of skeletal maturation and degeneration in quadrupeds are known to vary from obligate bipeds due to differential rates of hormonal changes, overall lifetime homeostatic levels of hormones involved with various developmental and reproductive strategies, and 2-obvious differences in functional morphology. Indeed, the construction of lamellae, as well as primary and secondary osteons, are not the same between humans and non-human mammals. Furthermore, their methods of maceration and environmental exposure do not serve as adequate proxies for true forensic, or even archaeological, conditions that surely affect DNA of all types in human skeletal tissue.

A 2009 study by Edson, et al. compared mtDNA extraction success rates between the various commonly attempted elements of the cranium. Unsurprisingly, they found statistically significantly higher success rates from the petrous portion of the temporal bone than any other. This is consistent with the hypothesis that the hard cortical layers of, in that case, the tympanic region and internal auditory canal, will often protect the internal trabecular tissue and the endogenous DNA therein. In the current study, this can be seen most clearly in the results from the sampling site at the proximal end of the femur, for in the trabecular tissue of the femoral head (accessed via the fovea capitis), as well as in the petrous, vascularization occurs primarily through limited number of

canaliculi only. Whereas, in trabecular tissue taken from the mid-diaphyseal regions of the long bones, vascularization occurs through the much larger nutrient foramen, haversian canals, and canaliculi, the endogenous DNA is therefore more susceptible to autolytic destruction by nucleases or other enzymes or bacteria. Therefore, it is not merely a question of which tissue type is best for DNA sampling? Establishing the optimal sites for DNA extractive sampling requires a thorough understanding that DNA survivability depends on a myriad of intrinsic factors, such as starting cellular populations, functional morphology, and homeostatic processes.

Extrinsic, or taphonomic, factors certainly play a role in DNA survivability. While typical environmental factors (such as soil type and pH, exposure to sunlight, etc.) played a less prominent role in the current study, the effects of maceration techniques were prevalent. Maceration was carried out using mechanical removal of the flesh, followed by submersion in a sub-boiling solution of water and enzyme-based bleach. One benefit of using Y-chromosomal analysis in this study is its small size and relative fragility, and thus, it is somewhat illustrative of damage patterns, since the qPCR kit used in this project only amplifies one fragment size from the Y- chromosome. Unsurprisingly, where there was low autosomal data, there was also low Y-chromosome data and vice versa. Though it is not possible to assert with confidence that maceration was the true cause of low DNA scores in some elements (the lack of mtDNA in the lumbar vertebrae, for example), there is little doubt that it had some effect. Several elements of the vertebrae (C3-5, T1, 5, 7, 8, 10, and 12 and sacral vertebrae S2) all scored very low or 0.00 in Y-chromosomal data. Visual inspection of some of these elements, though not all, shows extreme bleaching and tissue damage.



Image 8- The thoracic vertebrae. Note the damage to T7, T9, and T10.

And some elements, like the os coxae, that were quite fragile to the touch and appeared to be heavily damaged, performed surprisingly well. The bottom line, from the results of this study, are that 1-the maceration techniques employed on the remains from the individual in this study most likely did have some effect 2-that DNA extraction sampling should either occur prior to maceration or 3-avoid sites that are obviously over-processed. Further study using the sampling method detailed in this study on remains with different taphonomic histories is needed.

Extraction Method as an Influence on Low Copy Number

The DNA extraction and purification kits that were used in this project were selected for their specificity in extracting DNA from bone. Bone is known as a very challenging substance from which to get DNA due to a number of factors. These include

the presence of PCR inhibitors such as fat, as well as factors that are difficult to identify, much less quantify, such as mineralization of the tissue itself. The latter can complicate extraction if the mineralization of the bone is too high, thus a main reason for ATR/FTIR testing in this study. But it can also complicate matters if the mineralization of the bone is abnormally low by allowing the demineralization chemicals, like EDTA or even water, too much direct access to the DNA molecule itself. Any of these factors can have a negative impact of the starting copy number of the DNA and can thus impact the starting molecular weight data in qPCR analyses and the ability of the primers used in fragment analysis to anneal to the DNA. Usually, damage patterns in DNA can be seen in which of the fragment sizes amplify preferentially. Lack of amplification of small fragments (i.e., those with small base pair length like the Y- chromosome fragment targeted in this study) in the data is typically a good indication of damage to the endogenous DNA. Additionally, there is significant debate regarding the exact process and extent of small fragment size loss during extraction (162,181). Researchers do agree, however, that some DNA will inevitably be lost during extraction regardless of the method used.

FRAGMENT ANALYSIS/ STR PROFILE DEVELOPMENT

Of the top performing samples (those that generated at least 21 out of 23 STR loci), 67% were cortical tissue samples, 25% were trabecular tissue samples, and the remaining were osteonal tissue samples. They represent articulation areas including the ankle (the sustentaculum tali and the calcaneal tuberosity of the calcaneus and the sulcus tali of the talus), the knee, the elbow, and the hip as well as sites of major muscle attachment (the bicipital groove and the iliac crest), known homeostatic processes such as

the pubic symphysis, and sites of direct vascularization (the nutrient foramen of the femur). Midline samples that performed well were the sternum which was undergoing visible changes and the ribs where ante- mortem trauma had occurred. It is interesting to note that the left petrous portion of the temporal bone produced a full STR profile while the right side produced 0 loci. Also of note, is that the cortical sample taken from the superior articular facets of the atlas (C1) produced a full STR profile. This element is often recovered and may prove useful in cases when the cranium is too fragmented to use for sampling from the petrous portion of the temporal bone(s). As the name implies, the samples were taken from the sites where the element articulates with the occipital bone of the cranium.

Analysis of the results shows that the three highest- scoring sites in starting molecular weight of autosomal DNA in qPCR quantitation were among those that failed to generate any STR loci. This is representative of the stochasticity of DNA analysis in general and can be especially confounding when attempting to generate a usable profile from bone tissue with an unknown degree of taphonomic damage. Equitable examination, however, will also reveal that some of the lower qPCR scores still yielded full or nearly full STR profiles. Despite this, the general trend remains that higher starting molecular weight will generally indicate better chances of full STR profile production. And most of the top performing samples in STR profile production were among the top performing sites in qPCR quantitation, as well and vice versa.

THE “HEAT MAP”

The concept of designing a “heat map” that can be used by anyone interested in building a genetic profile from bone tissue has changed somewhat over the course of the study. The data that has been produced has helped solidify how this may be done and how it might be best approached. This study has demonstrated that there are optimal and sub-optimal sampling sites on the human post-cranial skeleton and it has given some ideas on how to go about finding these sites. Developing a way to make it easier for DNA analysts to locate the sites and how best to source the bone tissue once the sites have been located is a very real possibility.

Using both the qPCR data for autosomal, Y chromosome, and mtDNA as well as the STR profile construction data, a website may be built that allows analysts to see what sampling and DNA analysis methods have been the most successful for the elements they have to work with. Color coding the sampling site names (using red for the highest data, and sliding through orange, yellow, green and blue for the lowest data) and then embedding specific information within each site that can be accessed with the click of a mouse will allow investigators to quickly and reliably determine where and how they should sample. This will lead to a marked increase in efficiency since analysts will no longer have to guess or do extensive research prior to sampling and it will also decrease costs associated with excessive sampling due to uncertainty or even failures arising from sub-optimal sampling site decisions.

This information will be useful from an ethical standpoint too, as it will help decrease the amount of destruction required for DNA analysis. Whether the remains are forensic, historic, or archaeological, no one wants to damage them any more than is absolutely essential. The sampling method used in this study, plus the results that indicate

the locations of cellular populations in bone tissue, will allow investigators from across biological anthropology and criminalistics to target and utilize minimal amounts of irreplaceable bone tissue to maximum effect.

Since science must maintain replicability, and since this study could only begin the process, the ‘heat map’ webpage can be open- source, or partially open- source. This will allow other investigators (with a subscription and login information) to add their methods, data, and even notes. This will also lend a real aspect of transparency to the endeavor. Certain security checks will have to be in place, but those issues will be addressed in their time. For now, this study has shown that a deep understanding and appreciation for the cellular contributions to bone growth and homeostatic maintenance can and does offer a much more precise and accurate way to begin sampling for DNA from the human post- cranial skeleton.

WORKS CITED

1. Antinick TC, Foran DR. Intra- and Inter-Element Variability in Mitochondrial and Nuclear DNA from Fresh and Environmentally Exposed Skeletal Remains,. *Journal of Forensic Sciences* 2019;64(1):88–97. <https://doi.org/10.1111/1556-4029.13843>.
2. Misner LM, Halvorson AC, Dreier JL, Ubelaker DH, Foran DR. The Correlation Between Skeletal Weathering and DNA Quality and Quantity*. *Journal of Forensic Sciences* 2009;54(4):822–8. <https://doi.org/10.1111/j.1556-4029.2009.01043.x>.
3. Emmons AL, Davoren J, DeBruyn JM, Mundorff AZ. Inter and intra-individual variation in skeletal DNA preservation in buried remains. *Forensic Science International: Genetics* 2019;:102193. <https://doi.org/10.1016/j.fsigen.2019.102193>.
4. Mundorff A, Davoren JM. Examination of DNA yield rates for different skeletal elements at increasing post mortem intervals. *Forensic Science International: Genetics* 2014;8(1):55–63. <https://doi.org/10.1016/j.fsigen.2013.08.001>.
5. Mundorff AZ, Bartelink EJ, Mar-Cash E. DNA Preservation in Skeletal Elements from the World Trade Center Disaster: Recommendations for Mass Fatality Management*, †. *Journal of Forensic Sciences* 2009;54(4):739–45. <https://doi.org/10.1111/j.1556-4029.2009.01045.x>.
6. Geršak ŽM, Zupanič Pajnič I, Črešnar M, Zupanc T. Determination of DNA yield rates in six different skeletal elements in ancient bones. *Forensic Science International: Genetics Supplement Series* 2019. <https://doi.org/10.1016/j.fsigss.2019.09.047>.
7. Goodwin WH. The use of forensic DNA analysis in humanitarian forensic action: The development of a set of international standards. *Forensic Science International* 2017;278:221–7. <https://doi.org/10.1016/j.forsciint.2017.07.002>.
8. Obal M, Zupanič Pajnič I, Gornjak Pogorelc B, Zupanc T. Different skeletal elements as a source of DNA for genetic identification of Second World War victims. *Forensic Science International: Genetics Supplement Series* 2019. <https://doi.org/10.1016/j.fsigss.2019.09.013>.
9. Higgins D, Rohrlach AB, Kaidonis J, Townsend G, Austin JJ. Differential Nuclear and Mitochondrial DNA Preservation in Post-Mortem Teeth with Implications for Forensic and Ancient DNA Studies. *PLOS ONE* 2015;10(5):e0126935. <https://doi.org/10.1371/journal.pone.0126935>.

10. Andronowski JM, Mundorff AZ, Pratt IV, Davoren JM, Cooper DML. Evaluating differential nuclear DNA yield rates and osteocyte numbers among human bone tissue types: A synchrotron radiation micro-CT approach. *Forensic Science International: Genetics* 2017;28:211–8. <https://doi.org/10.1016/j.fsigen.2017.03.002>.
11. Akchurin T, Aissiou T, Kemeny N, Prosk E, Nigam N, Komarova SV. Complex Dynamics of Osteoclast Formation and Death in Long-Term Cultures. *PLoS One* 2008;3(5). <https://doi.org/10.1371/journal.pone.0002104>.
12. Andronowski JM, Crowder CM, Martinez MS. Recent advancements in the analysis of bone microstructure: new dimensions in forensic anthropology. *Forensic Sciences Research* 2018;3(4):294–309. <https://doi.org/10.1080/20961790.2018.1483294>.
13. Baron R. Molecular mechanisms of bone resorption An update. *Acta Orthopaedica Scandinavica* 1995;66(sup266):66–70. <https://doi.org/10.3109/17453679509157650>.
14. Bilezikian JP, Raisz LG, Martin TJ. *Principles of Bone Biology*. Academic Press, 2008.
15. Buckwalter JA, Glimcher MJ, Cooper RR, Recker R. *Bone Biology*. *jbjs* 1995;77:1256–75.
16. Florencio-Silva R, Sasso GR da S, Sasso-Cerri E, Simões MJ, Cerri PS. *Biology of Bone Tissue: Structure, Function, and Factors That Influence Bone Cells*. *BioMed Research International*. 2015. <https://www.hindawi.com/journals/bmri/2015/421746/abs/> (accessed September 19, 2019).
17. Kalfas IH. Principles of bone healing. *Neurosurgical Focus* 2001;10(4):1–4. <https://doi.org/10.3171/foc.2001.10.4.2>.
18. Manolagas SC, Parfitt AM. For whom the bell tolls: Distress signals from long-lived osteocytes and the pathogenesis of metabolic bone diseases. *Bone* 2013;54(2):272–8. <https://doi.org/10.1016/j.bone.2012.09.017>.
19. Ortner DJ. *Identification of Pathological Conditions in Human Skeletal Remains*. Academic Press, 2003.
20. Rodan GA. Introduction to bone biology. *Bone* 1992;13:S3–6. [https://doi.org/10.1016/S8756-3282\(09\)80003-3](https://doi.org/10.1016/S8756-3282(09)80003-3).
21. Roodman GD. Advances in Bone Biology: The Osteoclast. *Endocr Rev* 1996;17(4):308–32. <https://doi.org/10.1210/edrv-17-4-308>.

22. Skerry TM. The response of bone to mechanical loading and disuse: Fundamental principles and influences on osteoblast/osteocyte homeostasis. *Archives of Biochemistry and Biophysics* 2008;473(2):117–23. <https://doi.org/10.1016/j.abb.2008.02.028>.
23. Vaananen HK, Zhao H, Mulari M, Halleen JM. The cell biology of osteoclast function. *J Cell Sci* 2000;113(3):377–81.
24. Leskovar T, Zupanič Pajnič I, Geršak ŽM, Jerman I, Črešnar M. ATR-FTIR spectroscopy combined with data manipulation as a pre-screening method to assess DNA preservation in skeletal remains. *Forensic Science International: Genetics* 2020;44:102196. <https://doi.org/10.1016/j.fsigen.2019.102196>.
25. Leskovar T, Zupanič Pajnič I, Jerman I, Črešnar M. Separating forensic, WWII, and archaeological human skeletal remains using ATR-FTIR spectra. *Int J Legal Med* 2020;134(2):811–21. <https://doi.org/10.1007/s00414-019-02079-0>.
26. Leskovar T, Pajnič IZ, Jerman I, Črešnar M. Preservation state assessment and post-mortem interval estimation of human skeletal remains using ATR-FTIR spectra. *Australian Journal of Forensic Sciences* 2020;0(0):1–22. <https://doi.org/10.1080/00450618.2020.1836254>.
27. Amadasi A, Cappella A, Cattaneo C, Cofrancesco P, Cucca L, Merli D, et al. Determination of the post mortem interval in skeletal remains by the comparative use of different physico-chemical methods: Are they reliable as an alternative to ¹⁴C? *HOMO* 2017;68(3):213–21. <https://doi.org/10.1016/j.jchb.2017.03.006>.
28. Boskey AL, Mendelsohn R. Infrared analysis of bone in health and disease. *JBO* 2005;10(3):031102. <https://doi.org/10.1117/1.1922927>.
29. Chan KLA, Kazarian SG. Attenuated total reflection Fourier-transform infrared (ATR-FTIR) imaging of tissues and live cells. *Chem Soc Rev* 2016;45(7):1850–64. <https://doi.org/10.1039/C5CS00515A>.
30. Fredericks JD, Bennett P, Williams A, Rogers KD. FTIR spectroscopy: A new diagnostic tool to aid DNA analysis from heated bone. *Forensic Science International: Genetics* 2012;6(3):375–80. <https://doi.org/10.1016/j.fsigen.2011.07.014>.
31. The National Missing and Unidentified Persons System (NamUs). [NamUs.gov](https://www.namus.gov/). <https://www.namus.gov/> (accessed October 10, 2019).
32. 2018 NCIC Missing Person and Unidentified Person Statistics. Federal Bureau of Investigation. <https://www.fbi.gov/file-repository/2018-ncic-missing-person-and-unidentified-person-statistics.pdf/view> (accessed October 10, 2019).

33. Pearson OM, Lieberman DE. The aging of Wolff's "law": Ontogeny and responses to mechanical loading in cortical bone. *American Journal of Physical Anthropology* 2004;125(S39):63–99. <https://doi.org/10.1002/ajpa.20155>.
34. Gegenbaur C. About the formation of bone tissue. *Jena Journal of Natural Sciences* 1864;1:343–60.
35. Kölliker A. Die normale Resorption des Knochengewebes und ihre Bedeutung für die Entstehung der typischen Knochenformen. F.C.W. Vogel, 1873.
36. Foote JS. *A Contribution to the Comparative Histology of the Femur*. Smithsonian institution, 1916.
37. Martin TJ. Historically significant events in the discovery of RANK/RANKL/OPG. *World J Orthop* 2013;4(4):186–97. <https://doi.org/10.5312/wjo.v4.i4.186>.
38. Bonewald LF. The amazing osteocyte. *Journal of Bone and Mineral Research* 2011;26(2):229–38. <https://doi.org/10.1002/jbmr.320>.
39. Arnold JS, Jee WSS. Bone growth and osteoclastic activity as indicated by radioautographic distribution of plutonium. *American Journal of Anatomy* 1957;101(3):367–417. <https://doi.org/10.1002/aja.1001010303>.
40. Cartier P. Biochemistry of ossification. Role of adenosine triphosphoric acid in the mineralisation of ossifiable cartilage. *Journal de Physiologie* 1951;43:677–8.
41. Takahashi N, Akatsu T, Udagawa N, Sasaki T, Yamaguchi A, Moseley JM, et al. OSTEOBLASTIC CELLS ARE INVOLVED IN OSTEOCLAST FORMATION. *Endocrinology* 1988;123(5):2600–2. <https://doi.org/10.1210/endo-123-5-2600>.
42. Chambers TJ. The pathobiology of the osteoclast. *Journal of Clinical Pathology* 1985;38(3):241–52. <https://doi.org/10.1136/jcp.38.3.241>.
43. Martin TJ, Sims NA. Osteoclast-derived activity in the coupling of bone formation to resorption. *Trends in Molecular Medicine* 2005;11(2):76–81. <https://doi.org/10.1016/j.molmed.2004.12.004>.
44. Sims NA, Gooi JH. Bone remodeling: Multiple cellular interactions required for coupling of bone formation and resorption. *Seminars in Cell & Developmental Biology* 2008;19(5):444–51. <https://doi.org/10.1016/j.semcdb.2008.07.016>.
45. Gould SJ, Gold SJ, Gould TAAP of ZSJ. *The Mismeasure of Man*. W. W. Norton & Company, 1996.
46. Butler J. *Fundamentals of Forensic DNA Typing*. USA: Academic Press, 2010.

47. Aubin J, Triffitt J. Mesenchymal Stem Cells and Osteoblast Differentiation. *Principles of Bone Biology*. Academic Press, 2002;59–81.
48. Christensen AM, Smith MA, Thomas RM. Validation of X-Ray Fluorescence Spectrometry for Determining Osseous or Dental Origin of Unknown Material*. *Journal of Forensic Sciences* 2012;57(1):47–51. <https://doi.org/10.1111/j.1556-4029.2011.01941.x>.
49. Zimmerman HA, Meizel-Lambert CJ, Schultz JJ, Sigman ME. Chemical Differentiation of Osseous, Dental, and Non-skeletal Materials in Forensic Anthropology using Elemental Analysis. *Science & Justice* 2015;55(2):131–8. <https://doi.org/10.1016/j.scijus.2014.11.003>.
50. Ubelaker DH. The forensic evaluation of burned skeletal remains: A synthesis. *Forensic Science International* 2009;183(1):1–5. <https://doi.org/10.1016/j.forsciint.2008.09.019>.
51. Tersigni-Tarrant MT, Shirley N. *Forensic Anthropology*. 1st ed. Boca Raton, FL, USA: CRC Press, 2013.
52. Byers S. *Introduction to Forensic Anthropology - Steven N. Byers - Google Books*. 5th ed. 2017.
53. Burns KR. *Forensic Anthropology Training Manual*. Routledge, 2015.
54. Komar DA, Buikstra J. *Forensic Anthropology: Contemporary Theory and Practice*. 1st ed. Oxford University Press, 2008.
55. Dirkmaat DC, Cabo LL, Ousley SD, Symes SA. New perspectives in forensic anthropology. *American Journal of Physical Anthropology* 2008;137(S47):33–52. <https://doi.org/10.1002/ajpa.20948>.
56. Brickley M, Ives R. *The Bioarchaeology of Metabolic Bone Disease*. 1st ed. Academic Press, 2008.
57. Blau S. How traumatic: a review of the role of the forensic anthropologist in the examination and interpretation of skeletal trauma. *Australian Journal of Forensic Sciences* 2017;49(3):261–80. <https://doi.org/10.1080/00450618.2016.1153715>.
58. Passalacqua NV, Fenton TW. *Developments in Skeletal Trauma: Blunt-Force Trauma. A Companion to Forensic Anthropology*. John Wiley & Sons, Ltd, 2012;400–11.
59. Love JC. Sharp force trauma analysis in bone and cartilage: A literature review. *Forensic Science International* 2019;299:119–27. <https://doi.org/10.1016/j.forsciint.2019.03.035>.

60. Sims NA, Vrahnas C. Regulation of cortical and trabecular bone mass by communication between osteoblasts, osteocytes and osteoclasts. *Archives of Biochemistry and Biophysics* 2014;561:22–8. <https://doi.org/10.1016/j.abb.2014.05.015>.
61. Galloway A, Zephro L. Skeletal Trauma Analysis of the Lower Extremity. In: Rich J, Dean DE, Powers RH, editors. *Forensic Medicine of the Lower Extremity: Human Identification and Trauma Analysis of the Thigh, Leg, and Foot*. Totowa, NJ: Humana Press, 2005;253–77.
62. Wedel VL, Galloway A. *BROKEN BONES: Anthropological Analysis of Blunt Force Trauma* (2nd Ed.). Charles C Thomas Publisher, 2013.
63. Christensen AM, Rickman JM, Berryman HE. Forensic fractography of bone: fracture origins from impacts, and an improved understanding of the failure mechanism involved in beveling. 2021. <https://doi.org/10.5744/fa.2020.0041>.
64. Lowe JS, Anderson PG. Chapter 13 - Musculoskeletal System. In: Lowe JS, Anderson PG, editors. *Stevens & Lowe's Human Histology (Fourth Edition)* (Fourth Edition). Philadelphia: Mosby, 2015;239–62.
65. Carter DR, Fyhrie DP, Whalen RT. Trabecular bone density and loading history: Regulation of connective tissue biology by mechanical energy. *Journal of Biomechanics* 1987;20(8):785–94. [https://doi.org/10.1016/0021-9290\(87\)90058-3](https://doi.org/10.1016/0021-9290(87)90058-3).
66. Cunningham C, Scheuer L, Black S. *Developmental Juvenile Osteology*. Academic Press, 2016.
67. Franz-Odenaal TA, Hall BK, Witten PE. Buried alive: How osteoblasts become osteocytes. *Developmental Dynamics* 2006;235(1):176–90. <https://doi.org/10.1002/dvdy.20603>.
68. Burr DB. Repair Mechanisms for Microdamage in Bone. *Journal of Bone and Mineral Research* 2014;29(12):2534–6. <https://doi.org/10.1002/jbmr.2366>.
69. Parfitt AM. Bone-forming cells in clinical conditions. *Bone: A Treatise*. Caldwell, NJ: Telford, 1990;351–429.
70. Bourne G. *The Biochemistry and Physiology of Bone*. 2nd ed. Elsevier, 2012.
71. Martin RB. Does osteocyte formation cause the nonlinear refilling of osteons? *Bone* 2000;26(1):71–8. [https://doi.org/10.1016/S8756-3282\(99\)00242-2](https://doi.org/10.1016/S8756-3282(99)00242-2).
72. Marotti G, Ferretti M, Remaggi F, Palumbo C. Quantitative evaluation on osteocyte canalicular density in human secondary osteons. *Bone* 1995;16(1):125–8. [https://doi.org/10.1016/8756-3282\(95\)80022-I](https://doi.org/10.1016/8756-3282(95)80022-I).

73. Dallas SL, Bonewald LF. Dynamics of the Transition from Osteoblast to Osteocyte. *Ann N Y Acad Sci* 2010;1192:437–43. <https://doi.org/10.1111/j.1749-6632.2009.05246.x>.
74. Palumbo C, Palazzini S, Mariotti G. Morphological Study of Intercellular Junctions during Osteocyte Differentiation. *Bone* 1990;(11):401–6.
75. Candaliere GA, Liu F, Aubin JE. Individual osteoblasts in the developing calvaria express different gene repertoires. *Bone* 2001;28:351–61.
76. Liu K-Z, Jackson M, Sowa MG, Ju H, Dixon IMC, Mantsch HH. Modification of the extracellular matrix following myocardial infarction monitored by FTIR spectroscopy. *Biochimica et Biophysica Acta (BBA) - Molecular Basis of Disease* 1996;1315(2):73–7. [https://doi.org/10.1016/0925-4439\(95\)00118-2](https://doi.org/10.1016/0925-4439(95)00118-2).
77. Frost HM. Bone Remodeling Dynamics. 1963;(CR Lam ed):65–75.
78. Pinhasi R, Fernandes D, Sirak K, Novak M, Connell S, Alpaslan-Roodenberg S, et al. Optimal Ancient DNA Yields from the Inner Ear Part of the Human Petrous Bone. *PLOS ONE* 2015;10(6):e0129102. <https://doi.org/10.1371/journal.pone.0129102>.
79. Pinhasi R, Fernandes DM, Sirak K, Cheronet O. Isolating the human cochlea to generate bone powder for ancient DNA analysis. *Nature Protocols* 2019;14(4):1194–205. <https://doi.org/10.1038/s41596-019-0137-7>.
80. de Souza Faloni AP, Schoenmaker T, Azari A, Katchburian E, Cerri PS, de Vries TJ, et al. Jaw and Long Bone Marrows Have a Different Osteoclastogenic Potential. *Calcif Tissue Int* 2011;88(1):63–74. <https://doi.org/10.1007/s00223-010-9418-4>.
81. Davenport CB. Responsive Bone. *Proceedings of the American Philosophical Society* 1941;84(1):65–70.
82. Hancox NM. The Osteoclast. *The Biochemistry and Physiology of Bone*. Elsevier, 2012.
83. Katsimbri P. The biology of normal bone remodelling. *European Journal of Cancer Care* 2017;26(6):e12740. <https://doi.org/10.1111/ecc.12740>.
84. Miloš A, Selmanović A, Smajlović L, Huel RLM, Katzmarzyk C, Rizvić A, et al. Success Rates of Nuclear Short Tandem Repeat Typing from Different Skeletal Elements. *Croat Med J* 2007;48(4):486–93.
85. Edson SM, Christensen AF, Barritt SM, Meehan A, Leney MD, Finelli LN. Sampling of the cranium for mitochondrial DNA analysis of human skeletal remains. *Forensic Science International: Genetics Supplement Series* 2009;2(1):269–70. <https://doi.org/10.1016/j.fsigss.2009.09.029>.

86. Marks SC, Odgren PR. Chapter 1 - Structure and Development of the Skeleton. In: Bilezikian JP, Raisz LG, Rodan GA, editors. *Principles of Bone Biology* (Second Edition). San Diego: Academic Press, 2002;3–15.
87. White T, Folkens P. *The Human Bone Manual*. 4th ed. Elsevier Academic Press, 2005.
88. Brundin M, Figdor D, Sundqvist G, Sjögren U. DNA Binding to Hydroxyapatite: A Potential Mechanism for Preservation of Microbial DNA. *Journal of Endodontics* 2013;39(2):211–6. <https://doi.org/10.1016/j.joen.2012.09.013>.
89. Ambrose SH, Krigbaum J. Bone chemistry and bioarchaeology. *Journal of Anthropological Archaeology* 2003;22(3):193–9. [https://doi.org/10.1016/S0278-4165\(03\)00033-3](https://doi.org/10.1016/S0278-4165(03)00033-3).
90. Olszta MJ, Cheng X, Jee SS, Kumar R, Kim Y-Y, Kaufman MJ, et al. Bone structure and formation: A new perspective. *Materials Science and Engineering: R: Reports* 2007;58(3):77–116. <https://doi.org/10.1016/j.mser.2007.05.001>.
91. Jeffreys AJ, Wilson V, Thein SL. Individual specific “fingerprints” of human DNA. *Nature* 1985;316.
92. Coble MD, Butler JM. Characterization of New MiniSTR Loci to Aid Analysis of Degraded DNA. *Journal of Forensic Sciences* 2005;50(1):1–11. <https://doi.org/10.1520/JFS2004216>.
93. Shewale J, Liu R, editors. *Forensic DNA Analysis: Current Practices and Emerging Technologies*. 1st ed. USA: Taylor & Francis, 2014.
94. Pilli E, Berti A, editors. *Forensic DNA Analysis: Technological Developments and Innovative Applications*. 1st ed. CRC Press, 2021.
95. Steffen CR, Kiesler KM, Borsuk LA, Vallone PM. Beyond the STRs: A comprehensive view of current forensic DNA markers characterized in the PCR-based DNA profiling standard SRM 2391D. *Forensic Science International: Genetics Supplement Series* 2017;6:e426–7. <https://doi.org/10.1016/j.fsigss.2017.09.152>.
96. Lee H-J, Lee JW, Jeong SJ, Park M. How many single nucleotide polymorphisms (SNPs) are needed to replace short tandem repeats (STRs) in forensic applications? *Int J Legal Med* 2017;131(5):1203–10. <https://doi.org/10.1007/s00414-017-1564-z>.
97. Hwa H-L, Lin C-P, Huang T-Y, Kuo P-H, Hsieh W-H, Lin C-Y, et al. A panel of 130 autosomal single-nucleotide polymorphisms for ancestry assignment in five Asian populations and in Caucasians. *Forensic Sci Med Pathol* 2017;13(2):177–87. <https://doi.org/10.1007/s12024-017-9863-8>.

98. Romanini C, Catelli ML, Borosky A, Pereira R, Romero M, Salado Puerto M, et al. Typing short amplicon binary polymorphisms: Supplementary SNP and Indel genetic information in the analysis of highly degraded skeletal remains. *Forensic Science International: Genetics* 2012;6(4):469–76. <https://doi.org/10.1016/j.fsigen.2011.10.006>.
99. Phillips C, Manzo L, de la Puente M, Fondevila M, Lareu MV. The MASTiFF panel—a versatile multiple-allele SNP test for forensics. *Int J Legal Med* 2020;134(2):441–50. <https://doi.org/10.1007/s00414-019-02233-8>.
100. Alonso A, Barrio PA, Müller P, Köcher S, Berger B, Martin P, et al. Current state-of-art of STR sequencing in forensic genetics. *ELECTROPHORESIS* 2018;39(21):2655–68. <https://doi.org/10.1002/elps.201800030>.
101. Moretti TR, Moreno LI, Smerick JB, Pignone ML, Hizon R, Buckleton JS, et al. Population data on the expanded CODIS core STR loci for eleven populations of significance for forensic DNA analyses in the United States. *Forensic Science International: Genetics* 2016;25:175–81. <https://doi.org/10.1016/j.fsigen.2016.07.022>.
102. Mulero JJ, Hennessy LK. Next generation STR Genotyping Kits for Forensic Applications. *Forensic DNA Analysis: Current Practices and Emerging Technologies*. CRC Press, 2014;163–80.
103. Parsons TJ, Huel RML, Bajunović Z, Rizvić A. Large scale DNA identification: The ICMP experience. *Forensic Science International: Genetics* 2019;38:236–44. <https://doi.org/10.1016/j.fsigen.2018.11.008>.
104. Barbisin M, Shewale J. Assessment of DNA Extracted from Forensic Samples Prior to Genotyping. *Forensic DNA Analysis: Current Practices and Emerging Technologies*. CRC Press, 2014;101–28.
105. Stray J, Shewale J. Extraction of DNA from Human Remains. *Forensic DNA Analysis: current practices and emerging technologies*. CRC Press, 2014.
106. Ballantyne KN, Keerl V, Wollstein A, Choi Y, Zuniga SB, Ralf A, et al. A new future of forensic Y-chromosome analysis: Rapidly mutating Y-STRs for differentiating male relatives and paternal lineages. *Forensic Science International: Genetics* 2012;6(2):208–18. <https://doi.org/10.1016/j.fsigen.2011.04.017>.
107. Kayser M. Forensic use of Y-chromosome DNA: a general overview. *Human Genetics* 2017;136(5):621–35. <https://doi.org/10.1007/s00439-017-1776-9>.
108. Yang X, Zhang X, Zhu J, Chen L, Liu C, Feng X, et al. Genetic analysis of 19 X chromosome STR loci for forensic purposes in four Chinese ethnic groups. *Scientific Reports* 2017;7(1):42782. <https://doi.org/10.1038/srep42782>.

109. Susana J-M, Celia G, Ester L, Miriam B, Eladio B, de Pancorbo Marian M. Genetic analysis of 12 X-chromosomal STRs an autochthonous population of Southeast Spain. *Forensic Science International: Genetics Supplement Series* 2019;7(1):482–4. <https://doi.org/10.1016/j.fsigss.2019.10.060>.
110. Cann R, Stoneking M, Wilson AC. Mitochondrial DNA and human evolution. *Nature* 1987;325(January):31–6.
111. Lewin R. The Unmasking of Mitochondrial Eve. *Science* 1987;238(4823):24–6.
112. Lassen C, Hummel S, Herrmann B. Comparison of DNA extraction and amplification from ancient human bone and mummified soft tissue. *International Journal of Legal Medicine* 1994;107(3):152–5. <https://doi.org/10.1007/BF01225603>.
113. Latham KE, Madonna ME. DNA Survivability in Skeletal Remains. *Manual of Forensic Taphonomy*. CRC Press, 2013;403–25.
114. Furtwängler A, Reiter E, Neumann GU, Siebke I, Steuri N, Hafner A, et al. Ratio of mitochondrial to nuclear DNA affects contamination estimates in ancient DNA analysis. *Scientific Reports* 2018;8(1):1–8. <https://doi.org/10.1038/s41598-018-32083-0>.
115. Dabney J, Knapp M, Glocke I, Gansauge M-T, Weihmann A, Nickel B, et al. Complete mitochondrial genome sequence of a Middle Pleistocene cave bear reconstructed from ultrashort DNA fragments. *Proceedings of the National Academy of Sciences* 2013;110(39):15758–63. <https://doi.org/10.1073/pnas.1314445110>.
116. Knapp M. From a molecules' perspective – contributions of ancient DNA research to understanding cave bear biology. *Historical Biology* 2019;31(4):442–7. <https://doi.org/10.1080/08912963.2018.1434168>.
117. Gibbons A. Who Were the Denisovans? *Science* 2011;333(6046):1084–7. <https://doi.org/10.1126/science.333.6046.1084>.
118. Slon V, Hopfe C, Weiß CL, Mafessoni F, Rasilla M de la, Lalueza-Fox C, et al. Neandertal and Denisovan DNA from Pleistocene sediments. *Science* 2017;356(6338):605–8. <https://doi.org/10.1126/science.aam9695>.
119. Rohland N, Hofreiter M. Ancient DNA extraction from bones and teeth. *Nature Protocols* 2007;2(7):1756–62. <https://doi.org/10.1038/nprot.2007.247>.
120. Leney MD. Sampling Skeletal remains for ancient DNA: A measure of success. *Historical Archaeology* 2006;40(3):31–49.

121. Götherström A, Collins MJ, Angerbjörn A, Lidén K. Bone preservation and DNA amplification. *Archaeometry* 2002;44(3):395–404. <https://doi.org/10.1111/1475-4754.00072>.
122. Gaytmenn R, Sweet D. Quantification of forensic DNA from various regions of human teeth. *J Forensic Sci* 2003;48(3):622–5.
123. Pinchi V, Torricelli F, Nutini AL, Conti M, Iozzi S, Norelli G-A. Techniques of dental DNA extraction: Some operative experiences. *Forensic Science International* 2011;204(1):111–4. <https://doi.org/10.1016/j.forsciint.2010.05.010>.
124. Kostyukevich Y, Bugrova A, Chagovets V, Brzhozovskiy A, Indeykina M, Vanyushkina A, et al. Proteomic and lipidomic analysis of mammoth bone by high-resolution tandem mass spectrometry coupled with liquid chromatography. *European Journal of Mass Spectrometry* 2018;24(6):411–9. <https://doi.org/10.1177/1469066718813728>.
125. Cleland TP, Schroeter ER. A Comparison of Common Mass Spectrometry Approaches for Paleoproteomics. *J Proteome Res* 2018;17(3):936–45. <https://doi.org/10.1021/acs.jproteome.7b00703>.
126. Latham KE, Miller JJ. DNA recovery and analysis from skeletal material in modern forensic contexts. *Forensic Sciences Research* 2019;4(1):51–9. <https://doi.org/10.1080/20961790.2018.1515594>.
127. Steadman DW, DiAntonio LL, Wilson JJ, Sheridan KE, Tammariello SP. The Effects of Chemical and Heat Maceration Techniques on the Recovery of Nuclear and Mitochondrial DNA from Bone*. *Journal of Forensic Sciences* 2006;51(1):11–7. <https://doi.org/10.1111/j.1556-4029.2005.00001.x>.
128. Lee EJ, Luedtke JG, Allison JL, Arber CE, Merriwether DA, Steadman DW. The Effects of Different Maceration Techniques on Nuclear DNA Amplification Using Human Bone. *Journal of Forensic Sciences* 2010;55(4):1032–8. <https://doi.org/10.1111/j.1556-4029.2010.01387.x>.
129. Blain H, Chavassieux P, Portero-Muzy N, Bonnel F, Canovas F, Chammas M, et al. Cortical and trabecular bone distribution in the femoral neck in osteoporosis and osteoarthritis. *Bone* 2008;43(5):862–8. <https://doi.org/10.1016/j.bone.2008.07.236>.
130. Gilbert MTP, Willerslev E, Hansen AJ, Barnes I, Rudbeck L, Lynnerup N, et al. Distribution Patterns of Postmortem Damage in Human Mitochondrial DNA. *The American Journal of Human Genetics* 2003;72(1):32–47. <https://doi.org/10.1086/345378>.
131. Gates KS. An Overview of Chemical Processes That Damage Cellular DNA: Spontaneous Hydrolysis, Alkylation, and Reactions with Radicals. *Chem Res Toxicol* 2009;22(11):1747–60. <https://doi.org/10.1021/tx900242k>.

132. M. Fleming A, J. Burrows C. On the irrelevancy of hydroxyl radical to DNA damage from oxidative stress and implications for epigenetics. *Chemical Society Reviews* 2020;49(18):6524–8. <https://doi.org/10.1039/D0CS00579G>.
133. Junod CA, Pokines JT. Subaerial Weathering. *Manual of Forensic Taphonomy*. CRC Press, 2013;287–314.
134. Edson SM, Root K, Kahline I, Dunn C, Trotter B, O'Rourke J. Flexibility in Testing Skeletonized Remains for DNA Analysis Can Lead to increased Success: Suggestions and Case Studies. In: Latham KE, Bartelink EJ, Finnegan M, editors. *New Perspectives in Forensic Human Skeletal Identification*. United States: Academic Press, 2018;141–56.
135. Allentoft ME, Collins M, Harker D, Haile J, Oskam CL, Hale ML, et al. The half-life of DNA in bone: measuring decay kinetics in 158 dated fossils. *Proceedings of the Royal Society B: Biological Sciences* 2012;279(1748):4724–33. <https://doi.org/10.1098/rspb.2012.1745>.
136. Thomas M, Gilbert P. Postmortem Damage of Mitochondrial DNA. In: Bandelt H-J, Macaulay V, Richards M, editors. *Human Mitochondrial DNA and the Evolution of Homo sapiens*. Berlin, Heidelberg: Springer, 2006;91–115.
137. Vass AA. Beyond the grave – understanding human decomposition. *Microbiology Today* 2001;28:190–3.
138. Briggs AW, Stenzel U, Johnson PLF, Green RE, Kelso J, Prufer K, et al. Patterns of damage in genomic DNA sequences from a Neandertal. *Proceedings of the National Academy of Sciences* 2007;104(37):14616–21. <https://doi.org/10.1073/pnas.0704665104>.
139. Collins MJ, Nielsen–Marsh CM, Hiller J, Smith CI, Roberts JP, Prigodich RV, et al. The survival of organic matter in bone: a review. *Archaeometry* 2002;44(3):383–94. <https://doi.org/10.1111/1475-4754.t01-1-00071>.
140. Darzynkiewicz Z, Juan G, Li X, Gorczyca W, Murakami T, Traganos F. Cytometry in cell necrobiology: Analysis of apoptosis and accidental cell death (necrosis). *Cytometry* 1997;27(1):1–20. [https://doi.org/10.1002/\(SICI\)1097-0320\(19970101\)27:1<1::AID-CYTO2>3.0.CO;2-L](https://doi.org/10.1002/(SICI)1097-0320(19970101)27:1<1::AID-CYTO2>3.0.CO;2-L).
141. Ginolhac A, Rasmussen M, Gilbert MTP, Willerslev E, Orlando L. mapDamage: testing for damage patterns in ancient DNA sequences. *Bioinformatics* 2011;27(15):2153–5. <https://doi.org/10.1093/bioinformatics/btr347>.
142. Fulton T. Setting Up an Ancient DNA Laboratory. In: Shapiro B, Hofreiter M, editors. *Ancient DNA*. Totowa, NJ: Humana Press, 2012.

143. Paabo S. Ancient DNA: extraction, characterization, molecular cloning, and enzymatic amplification. *Proceedings of the National Academy of Sciences* 1989;86(6):1939–43. <https://doi.org/10.1073/pnas.86.6.1939>.
144. Arismendi JL, Baker MALE, D P, Matteson KJ, D P. Effects of processing techniques on the forensic DNA analysis of human skeletal remains. 5. Armed Forces DNA Identification Laboratory. Armed Forces Institute of Pathology. 2004.
145. Duijs FE, Sijen T. A rapid and efficient method for DNA extraction from bone powder. *Forensic Science International: Reports* 2020;2:100099. <https://doi.org/10.1016/j.fsr.2020.100099>.
146. Kim TK. Understanding one-way ANOVA using conceptual figures. *Korean J Anesthesiol* 2017;70(1):22–6. <https://doi.org/10.4097/kjae.2017.70.1.22>.
147. Miller RG. *Beyond ANOVA: Basics of Applied Statistics*. CRC Press, 1997.
148. Delacre M, Leys C, Mora YL, Lakens D. Taking Parametric Assumptions Seriously: Arguments for the Use of Welch’s *F*-test instead of the Classical *F*-test in One-Way ANOVA. *International Review of Social Psychology* 2019;32(1):13. <https://doi.org/10.5334/irsp.198>.
149. Obertová Z, Stewart A, Cattaneo C, editors. *Statistics and Probability in Forensic Anthropology*. 1st ed. Elsevier Academic Press, 2020.
150. Stahle L, Wold S. Analysis of variance (ANOVA). *Chemometrics and Intelligent Laboratory Systems* 1989;6(4):259–72. [https://doi.org/10.1016/0169-7439\(89\)80095-4](https://doi.org/10.1016/0169-7439(89)80095-4).
151. Shaw RG, Mitchell-Olds T. Anova for Unbalanced Data: An Overview. *Ecology* 1993;74(6):1638–45. <https://doi.org/10.2307/1939922>.
152. Jan S-L, Shieh G. Sample size determinations for Welch’s test in one-way heteroscedastic ANOVA. *British Journal of Mathematical and Statistical Psychology* 2014;67(1):72–93. <https://doi.org/10.1111/bmsp.12006>.
153. Levy KJ. Some empirical power results associated with welch’s robust analysis of variance technique. *Journal of Statistical Computation and Simulation* 1978;8(1):43–8. <https://doi.org/10.1080/00949657808810246>.
154. Liu H. *Comparing Welch’s ANOVA, a Kruskal-Wallis test and traditional ANOVA in case of Heterogeneity of Variance*. 2015.
155. Ruxton GD, Beauchamp G. Time for some a priori thinking about post hoc testing. *Behavioral Ecology* 2008;19(3):690–3. <https://doi.org/10.1093/beheco/arn020>.

156. Akoglu H. User's guide to correlation coefficients. *Turkish Journal of Emergency Medicine* 2018;18(3):91–3. <https://doi.org/10.1016/j.tjem.2018.08.001>.
157. Armstrong RA. Should Pearson's correlation coefficient be avoided? *Ophthalmic and Physiological Optics* 2019;39(5):316–27. <https://doi.org/10.1111/opo.12636>.
158. Lee Rodgers J, Nicewander WA. Thirteen Ways to Look at the Correlation Coefficient. *The American Statistician* 1988;42(1):59–66. <https://doi.org/10.1080/00031305.1988.10475524>.
159. Fredricks GA, Nelsen RB. On the relationship between Spearman's rho and Kendall's tau for pairs of continuous random variables. *Journal of Statistical Planning and Inference* 2007;137(7):2143–50. <https://doi.org/10.1016/j.jspi.2006.06.045>.
160. Caruso JC, Cliff N. Empirical Size, Coverage, and Power of Confidence Intervals for Spearman's Rho. *Educational and Psychological Measurement* 1997;57(4):637–54. <https://doi.org/10.1177/0013164497057004009>.
161. Davoren J, Vanek D, Konjhodzić R, Crews J, Huffine E, Parsons TJ. Highly Effective DNA Extraction Method for Nuclear Short Tandem Repeat Testing of Skeletal Remains from Mass Graves. *Croat Med J* 2007;48(4):478–85.
162. Barta JL, Monroe C, Teisberg JE, Winters M, Flanigan K, Kemp BM. One of the key characteristics of ancient DNA, low copy number, may be a product of its extraction. *Journal of Archaeological Science* 2014;46:281–9. <https://doi.org/10.1016/j.jas.2014.03.030>.
163. Purification of DNA from Bone Samples Using Bone DNA Extraction Kit, Custom and DNA IQ™ Chemistry. <https://www.promega.com/resources/pubhub/applications-notes/an343-purification-of-dnafrom-bone-samples-using-bone-dnaextraction-kit-custom/> (accessed December 2, 2022).
164. Sarin VK, Erickson GM, Giori NJ, Bergman AG, Carter DR. Coincident development of sesamoid bones and clues to their evolution. *The Anatomical Record* 1999;257(5):174–80. [https://doi.org/10.1002/\(SICI\)1097-0185\(19991015\)257:5<174::AID-AR6>3.0.CO;2-O](https://doi.org/10.1002/(SICI)1097-0185(19991015)257:5<174::AID-AR6>3.0.CO;2-O).
165. Goldberg I, Nathan H. Anatomy and pathology of the sesamoid bones. *International Orthopaedics* 1987;11(2):141–7. <https://doi.org/10.1007/BF00266700>.
166. WOOD VE. The Sesamoid Bones of the Hand and their Pathology. *Journal of Hand Surgery* 1984;9(3):261–4. [https://doi.org/10.1016/0266-7681\(84\)90038-X](https://doi.org/10.1016/0266-7681(84)90038-X).

167. Yammine K. The prevalence of the sesamoid bones of the hand: A systematic review and meta-analysis. *Clinical Anatomy* 2014;27(8):1291–303. <https://doi.org/10.1002/ca.22378>.
168. Jobling M, Pandya A, Tyler-Smith C. The Y chromosome in forensic analysis and paternity testing. *International Journal of Legal Medicine* 1997;110(3):118–24.
169. Roewer L. Y chromosome STR typing in crime casework. *Forensic Science, Medicine, and Pathology* 2009;5(2):77–84.
170. Abate M, Vanni D, Pantalone A, Salini V. Cigarette smoking and musculoskeletal disorders. *Muscles Ligaments Tendons J* 2013;3(2):63–9. <https://doi.org/10.11138/mltj/2013.3.2.063>.
171. Bethard JD, Berger JM, Maiers J, Ross AH. Bone Mineral Density Adult Age Estimation in Forensic Anthropology: A Test of the DXAGE Application. *Journal of Forensic Sciences* 2019;64(4):1125–8. <https://doi.org/10.1111/1556-4029.13987>.
172. Crowder CM, Andronowski JM, Dominguez VM. Chapter 18 - Bone Histology as an Integrated Tool in the Process of Human Identification. In: Latham KE, Bartelink EJ, Finnegan M, editors. *New Perspectives in Forensic Human Skeletal Identification*. Academic Press, 2018;201–13.
173. Maurel DB, Boisseau N, Benhamou CL, Jaffre C. Alcohol and bone: review of dose effects and mechanisms. *Osteoporos Int* 2012;23(1):1–16. <https://doi.org/10.1007/s00198-011-1787-7>.
174. Waldron T. Chapter 20 - Joint Disease. In: Buikstra JE, editor. *Ortner's Identification of Pathological Conditions in Human Skeletal Remains (Third Edition)*. San Diego: Academic Press, 2019;719–48.
175. Bayaroğulları H, Yengil E, Davran R, Ağlagül E, Karazincir S, Balcı A. Evaluation of the postnatal development of the sternum and sternal variations using multidetector CT. *Diagn Interv Radiol* 2014;20(1):82–9. <https://doi.org/10.5152/dir.2013.13121>.
176. Hartnett KM. Analysis of Age-at-Death Estimation Using Data from a New, Modern Autopsy Sample—Part II: Sternal End of the Fourth Rib*,†. *Journal of Forensic Sciences* 2010;55(5):1152–6. <https://doi.org/10.1111/j.1556-4029.2010.01415.x>.
177. İşcan MY, Loth SR, Wright RK. Age Estimation from the Rib by Phase Analysis: White Males. *JFS* 1984;29(4):1094–104. <https://doi.org/10.1520/JFS11776J>.
178. Barnes E. *Atlas of Developmental Field Anomalies of the Human Skeleton: A Paleopathology Perspective*. John Wiley & Sons, 2012.

179. Glyn-Jones S, Palmer AJR, Agricola R, Price AJ, Vincent TL, Weinans H, et al. Osteoarthritis. *The Lancet* 2015;386(9991):376–87. [https://doi.org/10.1016/S0140-6736\(14\)60802-3](https://doi.org/10.1016/S0140-6736(14)60802-3).
180. Klaassen Z, Tubbs RS, Apaydin N, Hage R, Jordan R, Loukas M. Vertebral spinal osteophytes. *Anat Sci Int* 2011;86(1):1–9. <https://doi.org/10.1007/s12565-010-0080-8>.
181. Iyavoo S, Hadi S, Goodwin W. Evaluation of five DNA extraction systems for recovery of DNA from bone. *Forensic Science International: Genetics Supplement Series* 2013;4(1):e174–5. <https://doi.org/10.1016/j.fsigss.2013.10.090>.

APPENDIX A



Image 9- Overview of the skeletal remains used in the study.



Image 10- The Left clavicle.



Image 11- The right scapula.



Image 12- The right humerus.



Image 13- The right ulna.



Image 14- The right radius.



Image 15- The right hand.



Image 16- The manubrium.



Image 17- The corpus sterni.



Image 18- Right ribs.



Image 19- Closeup of the right 12th rib.



Image 20- Cervical vertebrae 3-7 (from right to left).



Image 21- Thoracic vertebrae. T1 is on the far right.



Image 22- Lumbar vertebrae. L1 is at the far left.



Image 23- The sacrum.



Image 24- The right os coxa.



Image 25- The proximal right femur (posterior aspect is up).



Image 26- The right femoral head (posterior aspect is up).



Image 27- The right tibia.



Image 28- The superior aspect of the proximal tibia (tibial plateau).



Image 29- The right fibula.



Image30- The right foot plus sesamoid bones.

APPENDIX B

ATR/FTIR Stats

Ammino Acid Absorbance by tissue type

ANOVA

	Sum of sqrs	df	Mean square	F	p (same)
Between groups:	0.0138306	2	0.00691532	0.5097	0.6037
Within groups: (n=99999)	0.705555	52	0.0135684		Permutation p
Total:	0.719386	54			0.6991

Components of variance (only for random effects):

Var(group): -0.000401666

Var(error): 0.0135684

ICC: -0.0305062

omega2: 0

Levene's test for homogeneity of variance, from means p (same): 0.1516

Levene's test, from medians p (same): 0.4258

Welch F test in the case of unequal variances: F=0.3978, df=15.61, p=0.6784

No significance detected at p < 0.05

Phosphate Absorbance by tissue type

	Sum of sqrs	df	Mean square	F	p (same)
Between groups:	0.0716473	2	0.0358237	4.676	0.01357
Within groups: (n=99999)	0.398369	52	0.00766094		Permutation p
Total:	0.470016	54			0.01307

Components of variance (only for random effects):

Var(group): 0.00170027 Var(error): 0.00766094 ICC: 0.18163
 omega2: 0.1179

Levene's test for homogeneity of variance, from means p (same): 0.1731
 Levene's test, from medians p (same): 0.252

Welch F test in the case of unequal variances: F=4.343, df=15.1, p=0.03237

Significance detected at p < 0.05

Carbonate Absorbance by tissue type

	Sum of sqrs	df	Mean square	F	p (same)
Between groups:	0.0787873	2	0.0393936	6.413	0.003239
Within groups: (n=99999)	0.319402	52	0.00614234		Permutation p
Total:	0.398189	54			0.00318

Components of variance (only for random effects):

Var(group): 0.00200749
 Var(error): 0.00614234
 ICC: 0.246323
 omega2: 0.1645

Levene's test for homogeneity of variance, from means p (same): 0.2217
 Levene's test, from medians p (same): 0.284

Welch F test in the case of unequal variances: F=6.353, df=15.13, p=0.009933

Significance detected, despite homogeneity of variance, at p < 0.05

Amino Acid Absorbance by Tissue Type

	Sum of sqrs	df	Mean square	F	p (same)
--	-------------	----	-------------	---	----------

Between groups:	0.0138306	2	0.00691532	0.5097	0.6037
Within groups: (n=99999)	0.705555	52	0.0135684		Permutation p
Total:	0.719386	54			0.7012

Components of variance (only for random effects):

Var(group): -0.000401666

Var(error): 0.0135684

ICC: -0.0305062

omega2: 0

Levene's test for homogeneity of variance, from means p (same): 0.1516

Levene's test, from medians p (same): 0.4258

Welch F test in the case of unequal variances: F=0.3978, df=15.61, p=0.6784

No significant difference detected.

Cortical Samples Only

Correlation (Pearson's R)

	AA Abs	Auto
AA Abs		0.13701
Auto	0.13701	
	AA Abs	Y Chromo
AA Abs		0.69626
Y Chromo	0.69626	
	AA Abs	Mito
AA Abs		0.24743
Mito	0.24743	
<hr/>		
	Ph Abs	Auto
Ph Abs		0.15592

Auto	0.15592		
		Ph Abs	Y Chromo
Ph Abs			0.51472
Y Chromo	0.51472		
		Ph Abs	Mito
Ph Abs			0.47651
Mito	0.47651		
		Ca Abs	Auto
Ca Abs			0.14663
Auto	0.14663		
		Ca Abs	Y Chromo
Ca Abs			0.49512
Y Chromo	0.49512		
		Ca Abs	Mito
Ca Abs			0.58146
Mito	0.58146		

ANOVA

Test for equal means

	Sum of sqrs	df	Mean square	F	p (same)
Between groups:	0.683614	3	0.227871	4.402	0.005045
Within groups: (n=99999)	10.3539	200	0.0517695		Permutation p
Total:	11.0375	203			0.00185

Components of variance (only for random effects):

Var(group): 0.00345298

Var(error): 0.0517695

ICC: 0.0625284

omega2: 0.04764

Levene's test for homogeneity of variance, from means p (same): 1.476E-08

Levene's test, from medians p (same): 0.001629

Welch F test in the case of unequal variances: F=18.48, df=105.8, p=1.025E-09

No homogeneity of variance, Welch's F is significant at p < 0.05

Am Acid Ab vs Ph Ab vs C Ab vs Y- Chromo

	Sum of sqrs	df	Mean square	F	p (same)
Between groups:	1.13529	3	0.378429	41.53	6.616E-21
Within groups: (n=99999)	1.82261	200	0.00911303		Permutation p
Total:	2.95789	203			1E-05

Components of variance (only for random effects):

Var(group): 0.00724149

Var(error): 0.00911303

ICC: 0.442782

omega2: 0.3734

Levene's test for homogeneity of variance, from means p (same): 0.2614

Levene's test, from medians p (same): 0.1628

Welch F test in the case of unequal variances: F=42.76, df=109.8, p=2.209E-18

ANOVA- Am Acid Abs vs Phos Abs vs Carb Abs vs Mito

	Sum of sqrs	df	Mean square	F	p (same)
Between groups:	1.83189	3	0.610631	91.97	1.935E-37
Within groups: (n=99999)	1.32784	200	0.00663919		Permutation p
Total:	3.15973	203			1E-05

Components of variance (only for random effects):

Var(group): 0.011843

Var(error): 0.00663919

ICC: 0.640779

omega2: 0.5723

Levene's test for homogeneity of variance, from means p (same): 1.084E-07

Levene's test, from medians p (same): 2.16E-07

Welch F test in the case of unequal variances: F=276.2, df=83.34, p=3.507E-43

Significance detected at p < 0.05

Trabecular Samples Only

Pearson's R

	AA Abs	Auto
AA Abs		0.79112
Auto	-0.058437	

WEAK negative monotonic correlation

	AA Abs	Y Chromo
AA Abs		0.77478
Y Chromo	-0.063123	

Weak negative monotonic correlation

	AA Abs	Mito
AA Abs		0.93026
Mito	-0.019325	

WEAK monotonic correlation

	Ph Abs	Auto
Ph Abs		0.34747
Auto	-0.20525	

Moderate negative monotonic correlation

	Ph Abs	Y Chromo
Ph Abs		0.31151
Y Chromo	0.22072	

Weak positive

	Ph Abs	Mito
Ph Abs		0.88409
Mito	-0.032186	

Weak, monotonic negative correlation

	Car Abs	Auto
Car Abs		0.29079
Auto	-0.23013	

Weak, negative, monotonic correlation

	Car Abs	Y Chromo
Car Abs		0.30894
Y Chromo	0.22186	

Very Weak positive correlation

	Car Abs	Mito
Car Abs		0.77917
Mito	-0.06186	

Weak negative correlation

Amino Acid vs Phosphate vs Carbonate Absorbance

Osteonal Tissue

	AA Abs	Auto
AA Abs		0.2423
Auto	0.50996	

Weak positive

	AA Abs	Y Chromo
AA Abs		0.94658
Y Chromo	-0.03148	

Weak negative

	AA Abs	Mito
AA Abs		0.68898
Mito	0.18643	

Weak, monotonic, correlation.

	Ph Abs	Auto
Ph Abs		0.73005
Auto	0.16109	

Weak positive

	Ph Abs	Y Chromo
Ph Abs		0.82899
Y Chromo	-0.10125	

Weak negative correlation.

	Ph Abs	Mito
Ph Abs		0.42004
Mito	0.35714	

Weak positive correlation.

	Car Abs	Auto
Car Abs		0.476188
Auto	0.14168	

Weak positive correlation.

	Car Abs	Y Chromo
Car Abs		0.88054
Y Chromo	-0.07054	

Weak negative correlation

	Car Abs	Mito
Car Abs		0.51452
Mito	0.29918	

Weak positive correlation.

ANOVA

	Sum of sqrs	df	Mean square	F	p (same)
Between groups:	0.110029	2	0.0550144	3.927	0.02447
Within groups: (n=99999)	0.924623	66	0.0140094		Permutation p
Total:	1.03465	68			0.01258

Components of variance (only for random effects):

Var(group): 0.00178282

Var(error): 0.0140094

ICC: 0.112892

omega2: 0.0782

Levene's test for homogeneity of variance, from means p (same): 0.7308

Levene's test, from medians p (same): 0.9636

Welch F test in the case of unequal variances: F=2.565, df=40.65, p=0.08932

With homogeneity of variance, significance is detected at p < 0.05

ANOVA- AA vs Ph vs Car vs Y Chromosome

	Sum of sqrs	df	Mean square	F	p (same)
Between groups:	0.392769	3	0.130923	11.9	1.289E-06
Within groups: (n=99999)	0.967781	88	0.0109975		Permutation p
Total:	1.36055	91			1E-05

Components of variance (only for random effects):

Var(group): 0.00521415

Var(error): 0.0109975

ICC: 0.32163

omega2: 0.2623

Levene's test for homogeneity of variance, from means p (same): 0.3316

Levene's test, from medians p (same): 0.5754

Welch F test in the case of unequal variances: F=38.45, df=45.89, p=1.405E-12

Significance is indicated at p < 0.05

ANOVA- AAA vs Ph Abs vs Car Abs vs Mito

	Sum of sqrs	df	Mean square	F	p (same)
Between groups:	0.541404	3	0.180468	17.18	7.275E-09
Within groups: (n=99999)	0.924633	88	0.0105072		Permutation p
Total:	1.46604	91			1E-05

Components of variance (only for random effects):

Var(group): 0.0073896

Var(error): 0.0105072

ICC: 0.412901

omega2: 0.3453

Levene's test for homogeneity of variance, from means p (same): **0.01691**
 Levene's test, from medians p (same): 0.08333

Welch F test in the case of unequal variances: F=96.71, df=36.67, **p=1.778E-17**
No homogeneity of variance, Welch's F detected significance at p < 0.05

Osteonal Samples Only

ANOVA- AA vs Ph vs Car

	Sum of sqrs	df	Mean square	F	p (same)
Between groups:	0.203382	2	0.101691	8.354	0.002714
Within groups: (n=99999)	0.219111	18	0.0121728		Permutation p
Total:	0.422493	20			0.00357

Components of variance (only for random effects):

Var(group): 0.0127883

Var(error): 0.0121728

ICC: 0.512329

omega2: 0.4119

Levene's test for homogeneity of variance, from means p (same): **0.1207**
 Levene's test, from medians p (same): 0.1473

Welch F test in the case of unequal variances: F=14.09, df=9.025, **p=0.001674**
Significant difference detected, despite homogeneity of variance, at p < 0.05

ANOVA- AAA vs Ph Abs vs Car Abs vs Auto DNA

	Sum of sqrs	df	Mean square	F	p (same)
Between groups:	0.318876	3	0.106292	9.905	0.0001954

Within groups: (n=99999)	0.257544	24	0.010731	Permutation p
Total:	0.57642	27		0.00046

Components of variance (only for random effects):

Var(group): 0.0136516

Var(error): 0.010731

ICC: 0.55989

omega2: 0.4883

Levene's test for homogeneity of variance, from means p (same): 0.1585

Levene's test, from medians p (same): 0.2022

Welch F test in the case of unequal variances: F=9.402, df=11.6, p=0.00196

Significance detected at p < 0.05

ANOVA – AA Abs vs Ph Abs vs Car Abs vs Y chromo

	Sum of sqrs	df	Mean square	F	p (same)
Between groups:	0.392138	3	0.130713	13.89	1.863E-05
Within groups: (n=99999)	0.225865	24	0.00941106		Permutation p
Total:	0.618004	27			8E-05

Components of variance (only for random effects):

Var(group): 0.0173288

Var(error): 0.00941106

ICC: 0.648052

omega2: 0.58

Levene's test for homogeneity of variance, from means p (same): 0.04098

Levene's test, from medians p (same): 0.05805

Welch F test in the case of unequal variances: $F=14.69$, $df=12.29$, $p=0.0002303$

No homogeneity of variance, Welch's F detects significance at $p < 0.05$.

ANOVA- AA Abs vs Ph Abs vs Car Abs vs Mito

	Sum of sqrs	df	Mean square	F	p (same)
Between groups:	0.440159	3	0.14672	16.07	6.093E-06
Within groups: (n=99999)	0.219111	24	0.00912963		Permutation p
Total:	0.65927	27			4E-05

Components of variance (only for random effects):

Var(group): 0.0196557

Var(error): 0.00912963

ICC: 0.682837

omega2: 0.6175

Levene's test for homogeneity of variance, from means p (same): 0.01065

Levene's test, from medians p (same): 0.01938

Welch F test in the case of unequal variances: $F=27.56$, $df=10$, $p=3.776E-05$

No homogeneity of variance, Welch's F detects significance at $p < 0.05$

Left side Inter- element

Left Arm vs L Leg

ANOVA

Test for equal means

	Sum of sqrs	df	Mean square	F	p (same)
Between groups:	0.274381	1	0.274381	1.681	0.2022

Within groups:	6.52918	40	0.163229	Permutation p
(n=99999)				
Total:	6.80356	41	0.206	

Components of variance (only for random effects):

Var(group):	0.00529292	Var(error):	0.163229	ICC:	0.0314078
-------------	------------	-------------	----------	------	-----------

omega2:	0.01595
---------	---------

Levene's test for homogeneity of variance, from means	p (same):	0.1001
Levene's test, from medians	p (same):	0.2249

Welch F test in the case of unequal variances: F=1.681, df=25.27, p=0.2065

No significant difference at p<0.05

Left Hand vs Left Foot

Test for equal means

	Sum of sqrs	df	Mean square	F	p (same)
Between groups:	0.246507	1	0.246507	6.398	0.01873
Within groups:	0.8861 23	0.0385261			Permutation p
(n=99999)					
Total:	1.13261	24			0.01514

Components of variance (only for random effects):

Var(group):	0.0168816	Var(error):	0.0385261	ICC:	0.304679
-------------	-----------	-------------	-----------	------	----------

omega2:	0.1776
---------	--------

Levene's test for homogeneity of variance, from means	p (same):	0.106
Levene's test, from medians	p (same):	0.1208

Welch F test in the case of unequal variances: F=7.315, df=20.91, p=0.0133

Left Hip vs Left Shoulder

Test for equal means

	Sum of sqrs	df	Mean square	F	p (same)
Between groups:	0.000807313	1	0.000807313	0.003227	0.9552
Within groups:	6.00486	24	0.250203	Permutation p	(n=99999)
Total:	6.00567	25	0.9602		

Components of variance (only for random effects):

Var(group): -0.0202634 Var(error): 0.250203 ICC: -0.0881249

omega2: 0

Levene's test for homogeneity of variance, from means p (same): 0.1109

Levene's test, from medians p (same): 0.6192

Welch F test in the case of unequal variances: F=0.00472, df=20.03, p=0.9459

Kruskal-Wallis test for equal medians

H (chi2): 2.336

Hc (tie corrected): 2.338

p (same): 0.1263

There is no significant difference between sample medians

Y CHROMOSOME

L Arm vs L leg

Test for equal means

	Sum of sqrs	df	Mean square	F	p (same)
Between groups:	0.000301875	1	0.000301875	0.1052	0.7474
Within groups:	0.114784	40	0.00286961	Permutation p (n=99999)	
Total:	0.115086	41	0.7476		

Components of variance (only for random effects):

Var(group): -0.000122273 Var(error): 0.00286961 ICC: -0.044506

omega2: 0

Levene's test for homogeneity of variance, from means p (same): 0.5754

Levene's test, from medians p (same): 0.7011

Welch F test in the case of unequal variances: F=0.1052, df=39.93, p=0.7474

No signif Diff at p<0.05

L Hand vs L foot

Test for equal means

	Sum of sqrs	df	Mean square	F	p (same)
Between groups:	0.0224674	1	0.0224674	7.418	0.01211

Within groups:	0.0696592	23	0.00302866	Permutation p (n=99999)
Total:	0.0921265	24	0.00255	

Components of variance (only for random effects):

Var(group):	0.00157782	Var(error):	0.00302866	ICC:	0.342521
-------------	------------	-------------	------------	------	----------

omega2: 0.2043

Levene's test for homogeneity of variance, from means p (same): 0.006095

Levene's test, from medians p (same): 0.02025

Welch F test in the case of unequal variances: F=9.483, df=13.32, p=0.008572

Kruskal-Wallis test for equal medians

H (chi2): 10.43

Hc (tie corrected): 10.44

p (same): 0.001235

There **is** a significant difference between sample medians

There IS signif diff at p<0.05

L Hip vs L Shoulder

Test for equal means

	Sum of sqrs	df	Mean square	F	p (same)
Between groups:	0.0285161	1	0.0285161	11.69	0.002246
Within groups:	0.0585213	24	0.00243839		Permutation p (n=99999)
Total:	0.0870374	25	0.00045		

Components of variance (only for random effects):

Var(group):	0.00211881	Var(error):	0.00243839	ICC:	0.464937
-------------	------------	-------------	------------	------	----------

omega2: 0.2914

Levene's test for homogeneity of variance, from means p (same): 0.0001663

Levene's test, from medians p (same): 0.001108

Welch F test in the case of unequal variances: F=7.417, df=9.453, p=0.02249

Kruskal-Wallis test for equal medians

H (chi2): 8.711

Hc (tie corrected): 8.777

p (same): 0.00305

There **is** a significant difference between sample medians

There is signif diff at $p < 0.05$

Inter- element Tissue type Comparisons

Autosomal Only

Test for equal means

	Sum of sqrs	df	Mean square	F	p (same)
Between groups:	0.382579	2	0.19129	1.175	0.3282
Within groups: (n=99999)	3.418	21	0.162762		Permutation p
Total:	3.80058	23			0.2703

Components of variance (only for random effects):

Var(group): 0.00395763

Var(error): 0.162762

ICC: 0.0237383

omega2: 0.0144

Levene's test for homogeneity of variance, from means p (same): 0.2258

Levene's test, from medians p (same): 0.5222

Welch F test in the case of unequal variances: $F=1.411$, $df=4.623$, $p=0.3325$

There is no significant difference at $p < 0.05$

Cortical Y vs Trab Y vs Osteo Y

Test for equal means

	Sum of sqrs	df	Mean square	F	p (same)
Between groups:	0.0208796	2	0.0104398	1.45	0.2545
Within groups: (n=99999)	0.172848	24	0.00720202		Permutation p
Total:	0.193728	26			0.2422

Components of variance (only for random effects):

Var(group): 0.000378441 Var(error): 0.00720202 ICC: 0.0499233

omega2: 0.03223

Levene's test for homogeneity of variance, from means p (same): 0.6139

Levene's test, from medians p (same): 0.6647

Welch F test in the case of unequal variances: F=1.831, df=15.77, p=0.1927

There is no significant difference at $p < 0.05$

mtDNA Only

Test for equal means

	Sum of sqrs	df	Mean square	F	p (same)
Between groups:	5.1692E-07	2	2.5846E-07	0.3356	0.7182
Within groups: (n=99999)	1.84817E-05	24	7.70069E-07		Permutation p
Total:	1.89986E-05	26			0.6924

Components of variance (only for random effects):

Var(group): -5.97985E-08

Var(error): 7.70069E-07

ICC: -0.0841911

omega2: 0

Levene's test for homogeneity of variance, from means p (same): 0.3972

Levene's test, from medians p (same): 0.7523

Welch F test in the case of unequal variances: F=1.362, df=13.55, p=0.2891

No significant difference at $p < 0.05$

Kruskal-Wallis test for equal medians

H (chi2): 6.335

Hc (tie corrected): 6.337

p (same): 0.04207

There is a significant difference between sample medians

Dunn's post- hoc:

	<u>Cort Mito</u>	<u>Trab Mito</u>	<u>Osteo Mito</u>
Cort Mito		0.116	0.0152
Trab Mito	0.116		0.236
Osteo Mito	0.0152	0.236	

With Bonferroni corrected p values:

	Cort Mito	Trab Mito	Osteo Mito
Cort Mito		0.3481	0.0456
Trab Mito	0.3481		0.7079
Osteo Mito	0.0456	0.7079	

DNA Types

Cortical A/Y/M

Test for equal means

	Sum of sqrs	df	Mean square	F	p (same)
Between groups:	1.1279	2	0.56395	5.417	0.009805
Within groups: (n=99999)	3.12315	30	0.104105		Permutation p
Total:	4.25105	32			1E-05

Components of variance (only for random effects):

Var(group):	0.0418041
Var(error):	0.104105
ICC:	0.286507
omega2:	0.2112

Levene's test for homogeneity of variance, from means	p (same):	0.01556
Levene's test, from medians	p (same):	0.1201

Welch F test in the case of unequal variances: F=8.445, df=13.33, p=0.004271

There IS a significant difference at $p < 0.05$

Kruskal-Wallis test for equal medians

H (chi2):	25.83
Hc (tie corrected):	25.84
p (same):	2.452E-06

There is a significant difference between sample medians

Dunn's post- hoc

Raw p values

	Cortical A	Cort Y	Cort Mito
Cortical A		0.03427	4.179E-07
Cort Y	0.03427		0.003243
Cort Mito	4.179E-07	0.003243	

Bonferroni corrected p values

	Cortical A	Cort Y	Cort Mito
Cortical A		0.1028	1.254E-06
Cort Y	0.1028		0.009728
Cort Mito	1.254E-06	0.009728	

Trabecular A/Y/M

Test for equal means

	Sum of sqrs	df	Mean square	F	p (same)
Between groups:	0.150962	2	0.0754811	14.23	4.948E-05
Within groups: (n=99999)	0.15385	29	0.00530516		Permutation p
Total:	0.304812	31			0.00018

Components of variance (only for random effects):

Var(group):	0.00658543
Var(error):	0.00530516
ICC:	0.553835
omega2:	0.4526

Levene's test for homogeneity of variance, from means	p (same):	0.000337
Levene's test, from medians	p (same):	0.004344

Welch F test in the case of unequal variances: F=15.74, df=12.63, p=0.0003716

There IS a significant difference at $p < 0.05$

Kruskal-Wallis test for equal medians

H (chi2):	24.74
Hc (tie corrected):	24.74
p (same):	4.242E-06

There is a significant difference between sample medians

Dunn's post- hoc

Raw p values

	Trabec A	Trab Y	Trab Mito
Trabec A		0.05322	8.808E-07
Trab Y	0.05322		0.002235
Trab Mito	8.808E-07	0.002235	

Bonferroni corrected p values

Trabec A	Trab Y	Trab Mito
----------	--------	-----------

Trabec A		0.1597	2.643E-06
Trab Y	0.1597		0.006705
Trab Mito	2.643E-06	0.006705	

Osteonal A/Y/M

Test for equal means

	Sum of sqrs	df	Mean square	F	p (same)
Between groups:	0.244599	2	0.1223	3.844	0.05126
Within groups: (n=99999)	0.381764	12	0.0318136		Permutation p
Total:	0.626363	14			0.00527

Components of variance (only for random effects):

Var(group):	0.0180972
Var(error):	0.0318136
ICC:	0.362591
omega2:	0.275

Levene's test for homogeneity of variance, from means	p (same):	0.03314
Levene's test, from medians	p (same):	0.06082

Welch F test in the case of unequal variances: F=3.707, df=5.333, p=0.09794

There IS a significant difference at $p < 0.05$

Kruskal-Wallis test for equal medians

H (chi2):	11.18
Hc (tie corrected):	11.18
p (same):	0.003735

There is a significant difference between sample medians

Dunn's post- hoc

Raw p values

	Osteo A	Osteo Y	Osteo Mito
Osteo A		0.1791	0.0008893
Osteo Y	0.1791		0.04771
Osteo Mito	0.0008893	0.04771	

Bonferroni corrected- p values

Osteo A	Osteo Y	Osteo Mito
---------	---------	------------

Osteo A		0.5373	0.002668
Osteo Y	0.5373		0.1431
Osteo Mito	0.002668	0.1431	

Trabecular A/Y/M

Test for equal means

	Sum of sqrs	df	Mean square	F	p (same)
Between groups:	0.188283	2	0.0941417	16.95	8.608E-06
Within groups: (n=99999)	0.183231	33	0.00555246		Permutation p
Total:	0.371515	35			7E-05

Components of variance (only for random effects):

Var(group):	0.00738244
Var(error):	0.00555246
ICC:	0.570738
omega2:	0.4699

Levene's test for homogeneity of variance, from means	p (same):	4.096E-05
Levene's test, from medians	p (same):	0.0005655

Welch F test in the case of unequal variances: F=18.27, df=14.67, p=0.0001041

Turkey's Pairwise

	Trabec A	Trab Y	Trab Mito
Trabec A		0.0006741	8.628E-06
Trab Y	5.833		0.305
Trab Mito	7.951	2.118	

Kruskal-Wallis test for equal medians

H (chi2):	28.14
Hc (tie corrected):	28.16
p (same):	7.694E-07

There is a significant difference between sample medians

Dunn's Post- hoc

	Trabec A	Trab Y	Trab Mito
Trabec A		0.02854	1.288E-07
Trab Y 0	.02854		0.001996
Trab Mito	1.288E-07	0.001996	

LEFT Side Proximal vs Mid vs Distal by Tissue and DNA Type

Proximal Cortical vs Mid Cortical vs Distal Cortical (Autosomal)

	Sum of sqrs	df	Mean square	F	p (same)
Between groups:	0.807295	2	0.403648	9.303	0.002358
Within groups: (n=99999)	0.650847	15	0.0433898		Permutation p
Total:	1.45814	17			0.00225

Components of variance (only for random effects):

Var(group):	0.060043	Var(error):	0.0433898	ICC:	0.580502
omega2:	0.4799				

Levene's test for homogeneity of variance, from means	p (same):	0.3866
Levene's test, from medians	p (same):	0.5371

Welch F test in the case of unequal variances: F=6.726, df=8.167, p=0.01877

Significance detected with equal variance at p < 0.05

Dunn's Post- hoc

	L Prox Cort Auto	L Mid Cort Au	L Dist Cort Auto
L Prox Cort Auto		0.6653	0.004926
L Mid Cort Au	0.6653		0.01735
L Dist Cort Auto	0.004926	0.01735	

Significance between Prox & distal and mid & distal samples

Y- CHROMO

	Sum of sqrs	df	Mean square	F	p (same)
Between groups:	0.018561	2	0.00928051	4.105	0.03786
Within groups: (n=99999)	0.0339141	15	0.00226094		Permutation p
Total:	0.0524751	17			0.04192

Components of variance (only for random effects):

Var(group):	0.00116993	Var(error):	0.00226094	ICC:	0.341001
omega2:	0.2565				

Levene's test for homogeneity of variance, from means p (same): 0.9732
 Levene's test, from medians p (same): 0.9463

Welch F test in the case of unequal variances: F=3.979, df=9.994, p=0.05356

With equal variance, signif diff at p < 0.05

Dunn's post- hoc

	L Prox Cort Y	L Mid Cort Y	L Dist Cort Y
L Prox Cort Y		0.3042	0.01735
L Mid Cort Y	0.3042		0.1764
L Dist Cort Y	0.01735	0.1764	

Variance between proximal Y and Distal Y

MITO

	Sum of sqrs	df	Mean square	F	p (same)
Between groups:	8.96033E-08	2	4.48017E-08	0.5545	0.5857
Within groups: (n=99999)	1.21192E-06	15	8.07947E-08		Permutation p
Total:	1.30152E-06	17			0.7829

Components of variance (only for random effects):

Var(group): -5.99883E-09 Var(error): 8.07947E-08 ICC: -0.0802028
 omega2: 0

Levene's test for homogeneity of variance, from means p (same): 0.1055
 Levene's test, from medians p (same): 0.6155

Welch F test in the case of unequal variances: F=0.3431, df=8.696, p=0.7187

With equal variance, NO signif diff detected.

LEFT side proximal vs mid vs distal TRABECULAR tissue by DNA type

AUTOSOMAL

	Sum of sqrs	df	Mean square	F	p (same)
Between groups:	0.0723324	2	0.0361662	0.9424	0.4116
Within groups: (n=99999)	0.575678	15	0.0383785		Permutation p
Total:	0.64801	17			0.4501

Components of variance (only for random effects):

Var(group): -0.000368721 Var(error): 0.0383785 ICC: -0.00970068
omega2: 0

Levene's test for homogeneity of variance, from means p (same): 0.2886
Levene's test, from medians p (same): 0.7295

Welch F test in the case of unequal variances: F=1.271, df=8.309, p=0.3298

NO signif diff detected

Y- CHROMO

Test for equal means

	Sum of sqrs	df	Mean square	F	p (same)
Between groups:	0.000901807	2	0.000450903	0.1519	0.8604
Within groups:	0.0445213	15	0.00296808		Permutation p
(n=99999)					
Total:	0.0454231	17			0.9052

Components of variance (only for random effects):

Var(group): -0.00041953 Var(error): 0.00296808 ICC: -0.164615
omega2: 0

Levene's test for homogeneity of variance, from means p (same): 0.4673
Levene's test, from medians p (same): 0.8991

Welch F test in the case of unequal variances: F=0.232, df=8.574, p=0.7978

No signif diff detected

MITO

Test for equal means

	Sum of sqrs	df	Mean square	F	p (same)
Between groups:	6.01421E-09	2	3.00711E-09	0.8549	0.445
Within groups:	5.27596E-08	15	3.51731E-09		Permutation p
(n=99999)					
Total:	5.87738E-08	17			0.4804

Components of variance (only for random effects):

Var(group): -8.50334E-11 Var(error): 3.51731E-09 ICC: -0.0247747
omega2: 0

Levene's test for homogeneity of variance, from means p (same): 0.1401
Levene's test, from medians p (same): 0.4247

Welch F test in the case of unequal variances: F=1.055, df=7.647, p=0.394
No signif diff detected

Right Side

Arm (Hum, Rad, Ulna) versus Leg (Fem, Tib, Fib) AUTOSOMAL ONLY

ANOVA

	Sum of sqrs	df	Mean square	F	p (same)
Between groups:	2.61885	5	0.523771	0.7634	0.582
Within groups: (n=99999)	25.3869	37	0.686133		Permutation p
Total:	28.0058	42			0.633

Components of variance (only for random effects):

Var(group): -0.0226674

Var(error): 0.686133

ICC: -0.0341652

omega2: 0

Levene's test for homogeneity of variance, from means p (same): 0.0223

Levene's test, from medians p (same): 0.7051

Welch F test in the case of unequal variances: F=2.177, df=15.63, p=0.1094

No signif Diff at p < 0.05

Arm vs Leg Y CHROMO ONLY

	Sum of sqrs	df	Mean square	F	p (same)
Between groups:	0.479243	5	0.0958485	5.489	0.0007072
Within groups: (n=99999)	0.646117	37	0.0174626		Permutation p
Total:	1.12536	42			0.00133

Components of variance (only for random effects):

Var(group): 0.0109435

Var(error): 0.0174626

ICC: 0.385251

omega2: 0.3429

Levene's test for homogeneity of variance, from means p (same): 6.568E-06

Levene's test, from medians p (same): 0.004102

Welch F test in the case of unequal variances: F=3.049, df=15.64, p=0.04115

Arm vs Leg MITO ONLY

ANOVA

	Sum of sqrs	df	Mean square	F	p (same)
Between groups:	1.47042E-06	5	2.94083E-07	1.066	0.3949
Within groups: (n=99999)	1.02089E-05	37	2.75917E-07		Permutation p
Total:	1.16793E-05	42			0.3929

Components of variance (only for random effects):

Var(group): 2.53628E-09

Var(error): 2.75917E-07

ICC: 0.00910849

omega2: 0.007598

Levene's test for homogeneity of variance, from means p (same): 6.744E-05

Levene's test, from medians p (same): 0.3672

Welch F test in the case of unequal variances: F=4.016, df=14.59, p=0.01702

Because of unequal variance, Welch's F show signif diff at p < 0.05

Clav versus Scap AUTOSOMAL ONLY

	Sum of sqrs	df	Mean square	F	p (same)
Between groups:	0.0584119	1	0.0584119	0.1745	0.6907
Within groups: (n=99999)	2.00842	6	0.334736		Permutation p
Total:	2.06683	7			0.8577

Components of variance (only for random effects):

Var(group): -0.0690811

Var(error): 0.334736

ICC: -0.26004

omega2: 0

Levene's test for homogeneity of variance, from means p (same): 0.2883

Levene's test, from medians p (same): 0.3726

Welch F test in the case of unequal variances: F=0.1745, df=4.36, p=0.6959

No signif diff detected.

Scap vs Clav Y CHROMO ONLY

	Sum of sqrs	df	Mean square	F	p (same)
Between groups:	0.0157123	1	0.0157123	0.424	0.5391
Within groups: (n=99999)	0.222331	6	0.0370551		Permutation p
Total:	0.238043	7			0.655

Components of variance (only for random effects):

Var(group): -0.00533571

Var(error): 0.0370551

ICC: -0.168216

omega2: 0

Levene's test for homogeneity of variance, from means p (same): 0.08187

Levene's test, from medians p (same): 0.1379

Welch F test in the case of unequal variances: F=0.424, df=3.478, p=0.5554

No signif diff detected.

Clav vs Scap MITO ONLY

	Sum of sqrs	df	Mean square	F	p (same)
Between groups:	7.72259E-09	1	7.72259E-09	1.766	0.2322
Within groups: (n=99999)	2.62439E-08	6	4.37399E-09		Permutation p
Total:	3.39665E-08	7			0.1977

Components of variance (only for random effects):

Var(group): 8.37151E-10

Var(error): 4.37399E-09

ICC: 0.160646

omega2: 0.08734

Levene's test for homogeneity of variance, from means p (same): 0.05628

Levene's test, from medians p (same): 0.257

Welch F test in the case of unequal variances: F=1.766, df=3.123, p=0.2727

No signif diff detected.

Scap vs Clav vs Hum vs Rad vs Ulna AUTOSOMAL

	Sum of sqrs	df	Mean square	F	p (same)
Between groups:	0.710921	4	0.17773	0.2001	0.9359
Within groups: (n=99999)	22.2003	25	0.888014		Permutation p
Total:	22.9113	29			0.9891

Components of variance (only for random effects):

Var(group): -0.120728

Var(error): 0.888014

ICC: -0.157344

omega2: 0

Levene's test for homogeneity of variance, from means p (same): 0.1334

Levene's test, from medians p (same): 0.8973

Welch F test in the case of unequal variances: F=0.1552, df=10.19, p=0.9563

No signif diff detected.

Scap vs Clav vs Hum vs Rad vs Ulna Y CHROMO

	Sum of sqrs	df	Mean square	F	p (same)
Between groups:	0.0767496	4	0.0191874	1.551	0.2182
Within groups: (n=99999)	0.309278	25	0.0123711		Permutation p
Total:	0.386028	29			0.1916

Components of variance (only for random effects):

Var(group): 0.00115857

Var(error): 0.0123711

ICC: 0.0856317

omega2: 0.06844

Levene's test for homogeneity of variance, from means p (same): 0.001391

Levene's test, from medians p (same): 0.02475

Welch F test in the case of unequal variances: F=0.7446, df=9.698, p=0.5838

Despite Leven's, NO signif diff detected.

Scap vs Clav vs Hum vs Rad vs Ulna MITO

	Sum of sqrs	df	Mean square	F	p (same)
Between groups:	8.58505E-08	3	2.86168E-08	1.646	0.2076
Within groups: (n=99999)	3.82444E-07	22	1.73838E-08		Permutation p
Total:	4.68294E-07	25			0.1871

Components of variance (only for random effects):

Var(group): 1.75939E-09

Var(error): 1.73838E-08

ICC: 0.0919067

omega2: 0.06939

Levene's test for homogeneity of variance, from means p (same): 0.003948

Levene's test, from medians p (same): 0.2103

Welch F test in the case of unequal variances: F=2.866, df=10.27, p=0.08873

Despite Levene's, NO signif diff detected.

R Hand vs R Foot AUTO

	Sum of sqrs	df	Mean square	F	p (same)
--	-------------	----	-------------	---	----------

Between groups:	1.3412	1	1.3412	4.183	0.05244
Within groups: (n=99999)	7.37478	23	0.320643		Permutation p
Total:	8.71598	24			0.05165

Components of variance (only for random effects):

Var(group):	0.0828375	Var(error):	0.320643	ICC:	0.205308
omega2:	0.1129				

Levene's test for homogeneity of variance, from means	p (same):	0.003408
Levene's test, from medians	p (same):	0.03213

Welch F test in the case of unequal variances: F=5.2, df=15.25, p=0.03736

Welch's F indicates significance at p < 0.05.

Carpals vs MC vs Fingers vs Tarsals vs MT vs Toes AUTOSOMAL

Test for equal means

	Sum of sqrs	df	Mean square	F	p (same)
Between groups:	4.87984	5	0.975968	4.834	0.005093
Within groups: (n=99999)	3.83614	19	0.201902		Permutation p
Total:	8.71598	24			0.01504

Components of variance (only for random effects):

Var(group):	0.188245	Var(error):	0.201902	ICC:	0.482498
omega2:	0.434				

Levene's test for homogeneity of variance, from means	p (same):	2.321E-06
Levene's test, from medians	p (same):	0.07036

Welch F test in the case of unequal variances: F=4.106, df=8.065, p=0.03772

Signif Diff at p < 0.05

Y- CHROMOSOME

Test for equal means

	Sum of sqrs	df	Mean square	F	p (same)
Between groups:	0.0440494	5	0.00880988	0.9729	0.4592
Within groups: (n=99999)	0.172043	19	0.00905489		Permutation p
Total:	0.216092	24			0.3945

Components of variance (only for random effects):

Var(group): -5.95855E-05 Var(error): 0.00905489 ICC: -0.00662407
omega2: 0

Levene's test for homogeneity of variance, from means p (same): 0.009799

Levene's test, from medians p (same): 0.4138

Welch F test in the case of unequal variances: F=1.165, df=7.811, p=0.404

Despite lack of homogeneity in variance, no signif diff detected at p < 0.05.

MITO

	Sum of sqrs	df	Mean square	F	p (same)
Between groups:	1.6582E-06	5	3.31641E-07	0.8744	0.5166
Within groups: (n=99999)	7.20627E-06	19	3.79277E-07		Permutation p
Total:	8.86448E-06	24			0.5247

Components of variance (only for random effects):

Var(group): -1.15848E-08 Var(error): 3.79277E-07 ICC: -0.0315066
omega2: 0

Levene's test for homogeneity of variance, from means p (same): 0.001029
 Levene's test, from medians p (same): 0.4972

Welch F test in the case of unequal variances: F=5.08, df=5.779, p=0.03877

Signif diff detected at p < 0.05

ALL Cortical Avg's vs ALL Trab Avg's vs ALL osteo avg's

Test for equal means

	Sum of sqrs	df	Mean square	F	p (same)
Between groups:	2.7546	2	1.3773	3.639	0.03637
Within groups: (n=99999)	13.6265	36	0.378514		Permutation p
Total:	16.3811	38			0.03523

Components of variance (only for random effects):

Var(group): 0.0848642 Var(error): 0.378514 ICC: 0.183142
 omega2: 0.1192

Levene's test for homogeneity of variance, from means p (same): 0.01501
 Levene's test, from medians p (same): 0.1094

Welch F test in the case of unequal variances: F=2.912, df=11.98, p=0.09318

Signif diff at p < 0.05

	Cortical Au.	Trabecular Au.	Osteonal Au.
Cortical Au.		0.009264	0.004876
Trabecular Au.	0.009264		0.2888
Osteonal Au.	0.004876	0.2888	

Variance is between cortical & trabecular and cortical & osteonal.

Y- CHROMOSOME BY TISSUE TYPE

	Sum of sqrs	df	Mean square	F	p (same)
Between groups:	0.152092	2	0.0760462	5.115	0.01109
Within groups: (n=99999)	0.535228	36	0.0148675		Permutation p
Total:	0.687321	38			0.01199

Components of variance (only for random effects):

Var(group): 0.0051982 Var(error): 0.0148675 ICC: 0.259059
 omega2: 0.1743

Levene's test for homogeneity of variance, from means p (same): 0.0002092
 Levene's test, from medians p (same): 0.02938

Welch F test in the case of unequal variances: F=4.152, df=9.899, p=0.04905

Welch's F shows signif diff at p < 0.05

Dunn's post- hoc

	Cortical Y	Trabecular Y	Osteonal Y
Cortical Y		0.002045	0.00375
Trabecular Y	0.002045		0.4125
Osteonal Y	0.00375	0.4125	

As with the cortical, the variance is between cortical & trabecular and cortical & osteonal

MITO BY TISSUE TYPE

Test for equal means

	Sum of sqrs	df	Mean square	F	p (same)
Between groups:	6.03961E-07	2	3.01981E-07	1.391	0.2645
Within groups: (n=99999)	6.51398E-06	30	2.17133E-07		Permutation p
Total:	7.11794E-06	32			0.2585

Components of variance (only for random effects):

Var(group): 8.33327E-09 Var(error): 2.17133E-07 ICC: 0.0369602
omega2: 0.02313

Levene's test for homogeneity of variance, from means p (same): 0.007249
Levene's test, from medians p (same): 0.2642

Welch F test in the case of unequal variances: F=1.235, df=8.55, p=0.3379

No signif diff detected

Tissue Type by LOCATION

Prox vs Mid vs Dist Cortical AUTOSOMAL

	Sum of sqrs	df	Mean square	F	p (same)
Between groups:	4.29019	2	2.1451	1.954	0.1761
Within groups: (n=99999)	16.4653	15	1.09769		Permutation p
Total:	20.7555	17			0.1167

Components of variance (only for random effects):

Var(group): 0.174568 Var(error): 1.09769 ICC: 0.137211
omega2: 0.09586

Levene's test for homogeneity of variance, from means p (same): 0.1404
Levene's test, from medians p (same): 0.4621

Welch F test in the case of unequal variances: F=1.264, df=8.461, p=0.3308

Prox vs Mid vs Distal Cortical Y CHROMO

	Sum of sqrs	df	Mean square	F	p (same)
Between groups:	0.016872	2	0.00843598	0.1934	0.8262

Within groups: (n=99999)	0.654248	15	0.0436165	Permutation p
Total:	0.67112	17		0.83

Components of variance (only for random effects):

Var(group):	-0.00586343	Var(error):	0.0436165	ICC:	-0.15531
omega2:	0				

Levene's test for homogeneity of variance, from means	p (same):	0.6629
Levene's test, from medians	p (same):	0.9593

Welch F test in the case of unequal variances: F=0.1893, df=9.936, p=0.8304

No signif diff Detected

Prox vs Mid vs Distal Cortical MITO

	Sum of sqrs	df	Mean square	F	p (same)
Between groups:	5.36593E-07	2	2.68296E-07	0.5674	0.5787
Within groups: (n=99999)	7.0934E-06	15	4.72893E-07		Permutation p
Total:	7.62999E-06	17			0.5846

Components of variance (only for random effects):

Var(group):	-3.40995E-08	Var(error):	4.72893E-07	ICC:	-0.0777118
omega2:	0				

Levene's test for homogeneity of variance, from means	p (same):	0.07921
Levene's test, from medians	p (same):	0.5833

Welch F test in the case of unequal variances: F=0.8881, df=6.685, p=0.4549

No signif diff detected.

Prox vs mid vs Distal Trabecular AUTOSOMAL

	Sum of sqrs	df	Mean square	F	p (same)
Between groups:	0.815469	2	0.407735	1.8	0.1992
Within groups: (n=99999)	3.39751	15	0.226501		Permutation p
Total:	4.21298	17			0.1563

Components of variance (only for random effects):

Var(group): 0.0302056 Var(error): 0.226501 ICC: 0.117666
 omega2: 0.08165

Levene's test for homogeneity of variance, from means p (same): 0.01593
 Levene's test, from medians p (same): 0.2319

Welch F test in the case of unequal variances: F=2.753, df=6.771, p=0.1333

Despite some heterogeneity of variance, no signif diff detected.

Prox vs Mid vs Distal Trabecular Y- CHROMOSOME

	Sum of sqrs	df	Mean square	F	p (same)
Between groups:	0.0425192	2	0.0212596	1.544	0.2456
Within groups: (n=99999)	0.206541	15	0.0137694		Permutation p
Total:	0.24906	17			0.1358

Components of variance (only for random effects):

Var(group): 0.00124836 Var(error): 0.0137694 ICC: 0.0831256
 omega2: 0.057

Levene's test for homogeneity of variance, from means p (same): 0.05803
 Levene's test, from medians p (same): 0.3562

Welch F test in the case of unequal variances: F=0.8894, df=8.914, p=0.4445

No signif diff detected.

Prox vs Mid vs Distal Trabecular MITO

	Sum of sqrs	df	Mean square	F	p (same)
Between groups:	9.13247E-09	2	4.56623E-09	0.5191	0.6053
Within groups: (n=99999)	1.31935E-07	15	8.79569E-09		Permutation p
Total:	1.41068E-07	17			0.6453

Components of variance (only for random effects):

Var(group): -7.04909E-10 Var(error): 8.79569E-09 ICC: -0.087125
omega2: 0

Levene's test for homogeneity of variance, from means p (same): 0.1364

Levene's test, from medians p (same): 0.5869

Welch F test in the case of unequal variances: F=0.9206, df=6.872, p=0.4423

No signif diff detected.

Right Ribs vs Sternum vs Manub AUTOSOMAL

	Sum of sqrs	df	Mean square	F	p (same)
Between groups:	10.1035	2	5.05174	0.3206	0.7323
Within groups: (n=99999)	173.328	11	15.7571		Permutation p
Total:	183.432	13			0.7657

Components of variance (only for random effects):

Var(group): -2.67634

Var(error): 15.7571

ICC: -0.204601

omega2: 0

Levene's test for homogeneity of variance, from means p (same): 0.2391

Levene's test, from medians p (same): 0.7005

Welch F test in the case of unequal variances: F=4.002, df=4.121, p=0.1082

No signif diff detected.

R ribs vs stern vs manub Y CHROMO

	Sum of sqrs	df	Mean square	F	p (same)
Between groups:	0.160581	2	0.0802907	0.2883	0.755
Within groups: (n=99999)	3.06369	11	0.278518		Permutation p
Total:	3.22428	13			0.8189

Components of variance (only for random effects):

Var(group): -0.0495567

Var(error): 0.278518

ICC: -0.216442

omega2: 0

Levene's test for homogeneity of variance, from means p (same): 0.2518

Levene's test, from medians p (same): 0.7236

Welch F test in the case of unequal variances: F=3.928, df=2.596, p=0.164

No signif diff detected.

R ribs vs Stern vs Manub MITO

	Sum of sqrs	df	Mean square	F	p (same)
--	-------------	----	-------------	---	----------

Between groups:	1.82179E-06	2	9.10893E-07	1.324	0.3054
Within groups: (n=99999)	7.56927E-06	11	6.88116E-07		Permutation p
Total:	9.39106E-06	13			0.2148

Components of variance (only for random effects):

Var(group): 5.56943E-08

Var(error): 6.88116E-07

ICC: 0.074877

omega2: 0.04421

Levene's test for homogeneity of variance, from means p (same): 0.002507

Levene's test, from medians p (same): 0.2795

Welch F test in the case of unequal variances: F=0.7849, df=2, p=0.5602

Despite Levene's, no signif diff detected.

Autosomal qPCR Data

Tests for equal means

Cortical

Trabecular

N: 17

N: 17

Mean: 0.73417

Mean: 0.21514

95% conf.: (0.27735 1.191)

95% conf.: (0.10207 0.32821)

Variance: 0.78941

Variance: 0.048364

Difference between means: 0.51903

95% conf. interval (parametric): (0.066849 0.97122)

95% conf. interval (bootstrap): (0.047858 0.88007)

t: 2.3381 p (same mean): 0.025797 Critical t value (p=0.05): 2.0369

Uneq. var. t: 2.3381 p (same mean): 0.031161

Monte Carlo permutation: p (same mean): 0.007

Tests for equal variances

Cortical	Trabecular
N: 17	N: 17
Variance: 0.78941	Variance: 0.048364
F: 16.322	p (same var.): 1.0988E-06
Critical F value (p=0.05): 2.7614	
Monte Carlo permutation:	p (same var.): 0.0171

SocSciStatistics.com

(<https://www.socscistatistics.com/tests/ttestdependent/default2.aspx>)

Significance Level:

0.01

0.05

0.10

One-tailed or two-tailed hypothesis?:

One-tailed

Two-tailed

Difference Scores Calculations

Mean: -0.52

$\mu = 0$

$S^2 = SS/df = 12.45/(17-1) = 0.78$

$S^2_M = S^2/N = 0.78/17 = 0.05$

$S_M = \sqrt{S^2_M} = \sqrt{0.05} = 0.21$

T-value Calculation

$t = (M - \mu)/S_M = (-0.52 - 0)/0.21 = -2.43$

The value of t is -2.426354. The value of p is .02744. The result is significant at $p < .05$.

Y- Chromo qPCR Data

Tests for equal means

Cortical Y	Trabecular Y
N: 17	N: 17
Mean: 0.16487	Mean: 0.03679
95% conf.: (0.077161 0.25258)	95% conf.: (0.011789 0.061791)
Variance: 0.0291	Variance: 0.0023644

Difference between means: 0.12808
 95% conf. interval (parametric): (0.040447 0.21571)
 95% conf. interval (bootstrap): (0.041912 0.20469)

t : 2.9771 p (same mean): 0.0055071 Critical t value (p=0.05): 2.0369
 Uneq. var. t : 2.9771 p (same mean): 0.0078784
 Monte Carlo permutation: p (same mean): 0.0025

F- Test

Tests for equal variances

Cortical Y	Trabecular Y
N: 17	N: 17
Variance: 0.0291	Variance: 0.0023644
F: 12.307	p (same var.): 8.0772E-06
Critical F value (p=0.05): 2.7614	
Monte Carlo permutation:	p (same var.): 0.0217

Coeff of Var
Fligner-Kileen test for equal coefficients of variation

Cortical Y	Trabecular Y
N: 17	N: 17
CV: 103.47	CV: 132.17
95% conf.: (74.197 132.85)	95% conf.: (96.734 201.71)

T: 15.035
Expected T: 14.512
z: 0.1627
p (one-tailed): 0.43538
p (two-tailed): 0.87075

ANOVA All 3 Tissue Types Comparison

Test for equal means

	Sum of sqrs	df	Mean square	F	p
(same)					
Between groups:	2.7546	2	1.3773	3.639	
	0.03637				
Within groups:	13.6265	36	0.378514	Permutation p	
(n=99999)					
Total:	16.3811	38		0.03541	

Components of variance (only for random effects):

Var(group): 0.0848642 Var(error): 0.378514 ICC: 0.183142

omega2: 0.1192

Levene's test for homogeneity of variance, from means p (same): **0.01501**
Levene's test, from medians p (same): 0.1094

Welch F test in the case of unequal variances: F=2.912, df=11.98, **p=0.09318**

Despite ANOVA and Levene's, Welch's F detected no signif diff. This may be an example of Type I error common to ANVOA when variance is unequal.

ANOVA – Midline

VERTS- Cervical vs Thoracic vs Lumbar Autosomal DNA

	Sum of sqrs	df	Mean square	F	p (same)
Between groups:	1.44012	2	0.720059	5.133	0.009819
Within groups: (n=99999)	6.31288	45	0.140286		Permutation p
Total:	7.753	47			0.00741

Components of variance (only for random effects):

Var(group): 0.0388674

Var(error): 0.140286

ICC: 0.21695

omega2: 0.1469

Levene's test for homogeneity of variance, from means p (same): 6.599E-06

Levene's test, from medians p (same): 0.002156

Welch F test in the case of unequal variances: F=1.676, df=18, p=0.2151

Variance in means may indicate Type I error in ANOVA. Welch's F indicates no signif diff at p < 0.05.

Cervical vs Thoracic vs Lumbar Y- Chromo

Test for equal means

	Sum of sqrs	df	Mean square	F	p (same)
Between groups:	0.0657863	2	0.0328932	0.748	0.4791

Within groups: (n=99999)	1.97898	45	0.0439772	Permutation p
Total:	2.04476	47		0.5434

Components of variance (only for random effects):

Var(group): -0.000743066
 Var(error): 0.0439772
 ICC: -0.017187
 omega2: 0

Levene's test for homogeneity of variance, from means p (same): 0.3555
 Levene's test, from medians p (same): 0.5042

Welch F test in the case of unequal variances: F=1.67, df=19.46, p=0.2141

There is NO significant difference at p < 0.05

Cerv vs Thoracic vs Lumbar MITO

FAILED due to NO variance in lumbar vert mtDNA.

Cervical vs Thoracic vs R Os Coxa vs Sacrum

	Sum of sqrs	df	Mean square	F	p (same)
Between groups:	1.0996E-07	3	3.66535E-08	0.4843	0.6946
Within groups: (n=99999)	4.08723E-06	54	7.56894E-08		Permutation p
Total:	4.19719E-06	57			0.8264

Components of variance (only for random effects):

Var(group): -2.8491E-09
 Var(error): 7.56894E-08
 ICC: -0.0391144
 omega2: 0

Levene's test for homogeneity of variance, from means p (same): 0.1855
 Levene's test, from medians p (same): 0.6981

Welch F test in the case of unequal variances: F=0.9061, df=19.04, p=0.4565

No signif diff detected.

Cerv vs Thoracic vs LEFT Os Coxa vs Sacrum

	Sum of sqrs	df	Mean square	F	p (same)
Between groups:	6.35229E-08	3	2.11743E-08	0.2762	0.8423

Within groups: (n=99999)	4.29323E-06	56	7.66649E-08	Permutation p
Total:	4.35676E-06	59		0.9158

Components of variance (only for random effects):

Var(group): -3.88953E-09
 Var(error): 7.66649E-08
 ICC: -0.0534457
 omega2: 0

Levene's test for homogeneity of variance, from means p (same): 0.4194
 Levene's test, from medians p (same): 0.8422

Welch F test in the case of unequal variances: F=0.1982, df=21.69, p=0.8965

No signif diff detected.

R Os vs L Os vs Sacrum

	Sum of sqrs	df	Mean square	F	p (same)
Between groups:	0.67222	2	0.33611	1.796	0.1829
Within groups: (n=99999)	5.80248	31	0.187177		Permutation p
Total:	6.4747	33			0.1651

Components of variance (only for random effects):

Var(group): 0.0134673
 Var(error): 0.187177
 ICC: 0.0671206
 omega2: 0.04471

Levene's test for homogeneity of variance, from means p (same): 0.02319
 Levene's test, from medians p (same): 0.1934

Welch F test in the case of unequal variances: F=1.318, df=19.98, p=0.29

Despite Levene's, no signif diff detected.

Sternum vs Manubrium vs Ribs

LEFT Ribs Autosomal

Test for equal means

	Sum of sqrs	df	Mean square	F	p (same)
--	-------------	----	-------------	---	----------

Between groups:	2.15496	2	1.07748	0.3789	0.6932
Within groups: (n=99999)	31.2825	11	2.84386		Permutation p
Total:	33.4374	13			0.7103

Components of variance (only for random effects):

Var(group): -0.441595
 Var(error): 2.84386
 ICC: -0.183824
 omega2: 0

Levene's test for homogeneity of variance, from means p (same): 0.1741
 Levene's test, from medians p (same): 0.6221

Welch F test in the case of unequal variances: F=4.007, df=4.101, p=0.1085

No Stat differences

LEFT Ribs Y

Test for equal means

	Sum of sqrs	df	Mean square	F	p (same)
Between groups:	0.0791287	2	0.0395643	0.6245	0.5535
Within groups: (n=99999)	0.696847	11	0.0633497		Permutation p
Total:	0.775976	13			0.5716

Components of variance (only for random effects):

Var(group): -0.00594635
 Var(error): 0.0633497
 ICC: -0.103589
 omega2: 0

Levene's test for homogeneity of variance, from means p (same): 0.02971
 Levene's test, from medians p (same): 0.5186

Welch F test in the case of unequal variances: F=4.344, df=2.599, p=0.1483

No stat signif diff

LEFT Ribs Mito

RIGHT Ribs vs Sternum vs Manub Auto

Test for equal means

	Sum of sqrs	df	Mean square	F	p (same)
Between groups:	10.1035	2	5.05174	0.3206	0.7323
Within groups: (n=99999)	173.328	11	15.7571		Permutation p
Total:	183.432	13			0.7641

Components of variance (only for random effects):

Var(group): -2.67634

Var(error): 15.7571

ICC: -0.204601

omega2: 0

Levene's test for homogeneity of variance, from means p (same): 0.2391

Levene's test, from medians p (same): 0.7005

Welch F test in the case of unequal variances: F=4.002, df=4.121, p=0.1082

No Stat signif diff

RIGHT Ribs Y

Test for equal means

	Sum of sqrs	df	Mean square	F	p (same)
Between groups:	0.160581	2	0.0802907	0.2883	0.755
Within groups: (n=99999)	3.06369	11	0.278518		Permutation p
Total:	3.22428	13			0.818

Components of variance (only for random effects):

Var(group): -0.0495567

Var(error): 0.278518

ICC: -0.216442

omega2: 0

Levene's test for homogeneity of variance, from means p (same): 0.2518

Levene's test, from medians p (same): 0.7236

Welch F test in the case of unequal variances: F=3.928, df=2.596, p=0.164

No stat signif diff

RIGHT Ribs Mito

Right Os Cox vs Left Os coxa vs Sacrum

Test for equal means

	Sum of sqrs	df	Mean square	F	p (same)
Between groups:	0.67222	2	0.33611	1.796	0.1829
Within groups: (n=99999)	5.80248	31	0.187177		Permutation p
Total:	6.474733				0.1646

Components of variance (only for random effects):

Var(group): 0.0134673

Var(error): 0.187177

ICC: 0.0671206

omega2: 0.04471

Levene's test for homogeneity of variance, from means	p (same):	0.02319
Levene's test, from medians	p (same):	0.1934

Welch F test in the case of unequal variances: F=1.318, df=19.98, p=0.29

Despite Unequal variances*, there is no significant difference at $p < 0.05$

* Welch's F test is best in cases like this where the data is heterogenous, normal and unbalanced (Liu, 2015)

Right Os Coxa vs Left Os Coxa vs Sacrum Y- Chromosome

Test for equal means

	Sum of sqrs	df	Mean square	F	p (same)
Between groups:	0.000405919	2	0.00020296	0.2309	0.7951
Within groups: (n=99999)	0.0272431	31	0.000878811		Permutation p
Total:	0.0276491	33			0.8051

Components of variance (only for random effects):

Var(group): -6.11142E-05

Var(error): 0.000878811

ICC: -0.0747395

omega2: 0

Levene's test for homogeneity of variance, from means	p (same):	0.785
-------------------------------------------------------	-----------	-------

Levene's test, from medians p (same): 0.7905

Welch F test in the case of unequal variances: F=0.1897, df=16.65, p=0.829

There is NO significant difference at p < 0.05

Cervical vs Thoracic Vs Lumbar Autosomal
Test for equal means

	Sum of sqrs	df	Mean square	F	p (same)
Between groups:	1.44012	2	0.720059	5.133	0.009819
Within groups: (n=99999)	6.31288	45	0.140286		Permutation p
Total:	7.753	47			0.00736

Components of variance (only for random effects):

Var(group): 0.0388674

Var(error): 0.140286

ICC: 0.21695

omega2: 0.1469

Levene's test for homogeneity of variance, from means p (same): 6.599E-06

Levene's test, from medians p (same): 0.002156

Welch F test in the case of unequal variances: F=1.676, df=18, p=0.2151

Turkey's Pairwise

	Cervical Auto.	Thoracic Auto.	Lumbar Auto.
Cervical Auto.		0.983	0.02883
Thoracic Auto.	0.2492		0.009707
Lumbar Auto.	3.756	4.354	

Kruskal-Wallis test for equal medians

H (chi2): 2.744

Hc (tie corrected): 2.744

p (same): 0.2536

There is no significant difference between sample medians

Dunn's Post- hoc

Cervical Auto. Thoracic Auto. Lumbar Auto.

Cervical Auto.		0.7472	0.1188
Thoracic Auto.	0.7472		0.1533
Lumbar Auto.	0.1188	0.1533	

Cervical vs Thoracic vs Lumbar Y- Chromo

Test for equal means

	Sum of sqrs	df	Mean square	F	p (same)
Between groups:	0.0657863	2	0.0328932	0.748	0.4791
Within groups: (n=99999)	1.97898	45	0.0439772		Permutation p
Total:	2.04476	47			0.5441

Components of variance (only for random effects):

Var(group): -0.000743066
 Var(error): 0.0439772
 ICC: -0.017187
 omega2: 0

Levene's test for homogeneity of variance, from means p (same): 0.3555
 Levene's test, from medians p (same): 0.5042

Welch F test in the case of unequal variances: F=1.67, df=19.46, p=0.2141

No stats signif diff

Cervical vs Thoracic vs Lumbar vs Sacrum Autosomal

Test for equal means

	Sum of sqrs	df	Mean square	F	p (same)
Between groups:	1.50062	3	0.500207	3.989	0.01244
Within groups: (n=99999)	6.5207 52	0.125398			Permutation p
Total:	8.02132	55			0.01174

Components of variance (only for random effects):

Var(group): 0.0286217
 Var(error): 0.125398
 ICC: 0.185831
 omega2: 0.138

Levene's test for homogeneity of variance, from means p (same): 3.278E-06

Levene's test, from medians p (same): 0.002285

Welch F test in the case of unequal variances: F=1.098, df=20.21, p=0.3729

Turkey's Pairwise

	Cervical Auto.	Thoracic Auto.	Lumbar Auto.	Sacrum Auto
Cervical Auto.		0.9977	0.03419	0.9993
Thoracic Auto.	0.2636		0.0104	1
Lumbar Auto.	3.972	4.605		0.06153
Sacrum Auto	0.1733	0.02903	3.629	

Cervical vs Thoracic vs Lumbar vs Sacrum Y- Chromo

Test for equal means

	Sum of sqrs	df	Mean square	F	p (same)
Between groups:	0.0823002	3	0.0274334	0.7175	0.546
Within groups: (n=99999)	1.98827	52	0.0382359		Permutation p
Total:	2.07057	55			0.5874

Components of variance (only for random effects):

Var(group): -0.000824917

Var(error): 0.0382359

ICC: -0.0220501

omega2: 0

Levene's test for homogeneity of variance, from means p (same): 0.3187

Levene's test, from medians p (same): 0.5632

Welch F test in the case of unequal variances: F=1.225, df=24.62, p=0.3219

Intra- Group Variability

Lumbar Vertebrae versus Sacrum Autosomal DNA (T- test)

Tests for equal means

Lumbar Auto.	Sacrum Auto
N: 10	N: 8
Mean: 0.58176	Mean: 0.15069
95% conf.: (0.061896 1.1016)	95% conf.: (0.0066386 0.29473)
Variance: 0.52813	Variance: 0.029689

Difference between means: 0.43107
 95% conf. interval (parametric): (-0.12885 0.991)
 95% conf. interval (bootstrap): (-0.04819 0.83324)

t: 1.6321 p (same mean): 0.12219 Critical t value (p=0.05):
 2.1199
 Uneq. var. t: 1.8132 p (same mean): 0.099171
 Monte Carlo permutation: p (same mean): 0.1248
 Exact permutation: p (same mean): 0.12702

Tests for equal variances

Lumbar Auto.	Sacrum Auto
N: 10	N: 8
Variance: 0.52813	Variance: 0.029689

F: 17.789 p (same var.): 0.00099856
 Critical F value (p=0.05): 4.8232
 Monte Carlo permutation: p (same var.): 0.0726
 Exact permutation: p (same var.): 0.07281

Fligner-Kileen test for equal coefficients of variation

Lumbar Auto.	Sacrum Auto
N: 10	N: 8
CV: 124.92	CV: 114.35
95% conf.: (56.068 177.47)	95% conf.: (54.878 167.08)

T: 5.3916
 Expected T: 5.9585
 z: -0.28135
 p (one-tailed): 0.38922
 p (two-tailed): 0.77844

Despite UNEqual variances, there is NO significant difference at $p < 0.05$

Lumbar versus Sacrum Y- Chromosome

Tests for equal means

Lumbar Y	Sacrum Y
N: 10	N: 8
Mean: 0.13493	Mean: 0.026123
95% conf.: (-0.0012786 0.27114)	95% conf.: (-0.0043337 0.056579)
Variance: 0.036256	Variance: 0.0013272

Difference between means: 0.10881
 95% conf. interval (parametric): (-0.036822 0.25444)
 95% conf. interval (bootstrap): (-0.019402 0.20728)

t: 1.5839 p (same mean): 0.13278 Critical t value (p=0.05):
2.1199
 Uneq. var. t: 1.7671 p (same mean): 0.10822
 Monte Carlo permutation: p (same mean): 0.0957
 Exact permutation: p (same mean): 0.098839

Tests for equal variances

Lumbar Y	Sacrum Y
N: 10	N: 8
Variance: 0.036256	Variance: 0.0013272

F: 27.318 p (same var.): 0.00024372
 Critical F value (p=0.05): **4.8232**
 Monte Carlo permutation: p (same var.): 0.0501
 Exact permutation: p (same var.): 0.049225

Fligner-Kileen test for equal coefficients of variation

Lumbar Y	Sacrum Y
N: 10	N: 8
CV: 141.12	CV: 139.46
95% conf.: (76.041 211.53)	95% conf.: (82.832 219.24)

T: 8.0592
 Expected T: 5.9585
 z: 1.0425
 p (one-tailed): 0.14859
 p (two-tailed): 0.29718

There is NO significant difference at $p < 0.05$

Carpals and Hand vs Tarsals and Foot

Test for equal means

	Sum of sqrs	df	Mean square	F	p (same)
Between groups:	1.64762	3	0.549206	1.632	0.2122
Within groups:	7.06836	21	0.336589	Permutation p (n=99999)	
Total:	8.71598	24	0.1921		

Components of variance (only for random effects):

Var(group): 0.0367426 Var(error): 0.336589 ICC: 0.0984182

omega2: 0.07046

Levene's test for homogeneity of variance, from means p (same): 2.44E-05

Levene's test, from medians p (same): 0.156

Welch F test in the case of unequal variances: F=5.582, df=10.17, p=0.01598

R Os Coxa vs L Os Coxa

Autosomal

Test for equal means

	Sum of sqrs	df	Mean square	F	p (same)
Between groups:	0.741433	1	0.741433	3.092	0.0926
Within groups: (n=99999)	5.27591	22	0.239814		Permutation p
Total:	6.01734	23			0.08398

Components of variance (only for random effects):

Var(group): 0.0418016 Var(error): 0.239814 ICC: 0.148435

omega2: 0.08017

Levene's test for homogeneity of variance, from means p (same): 0.0226

Levene's test, from medians p (same): 0.06866

Welch F test in the case of unequal variances: F=3.092, df=13.25, p=0.1018

No significant difference at p < 0.05

Y- Chromosome

Test for equal means

	Sum of sqrs	df	Mean square	F	p (same)
Between groups:	1.02704E-05	1	1.02704E-05	0.013	0.9102
Within groups: (n=99999)	0.0173763	22	0.000789833		Permutation p
Total:	0.0173866	23			0.9212

Components of variance (only for random effects):

Var(group): -6.49635E-05 Var(error): 0.000789833 ICC: -0.089621
omega2: 0

Levene's test for homogeneity of variance, from means p (same): 0.7249
Levene's test, from medians p (same): 0.8732

Welch F test in the case of unequal variances: F=0.013, df=21.99, p=0.9102

No significant difference at $p < 0.05$

mtDNA

Test for equal means

	Sum of sqrs	df	Mean square	F	p (same)
Between groups:	1.77862E-08	1	1.77862E-08	1.922	0.1795
Within groups: (n=99999)	2.03587E-07	22	9.25396E-09		Permutation p
Total:	2.21373E-07	23			0.05903

Components of variance (only for random effects):

Var(group): 7.11016E-10 Var(error): 9.25396E-09 ICC: 0.0713515
omega2: 0.037

Levene's test for homogeneity of variance, from means p (same): 0.04176
Levene's test, from medians p (same): 0.1718

Welch F test in the case of unequal variances: F=1.922, df=11.14, p=0.1928

No significant difference at $p < 0.05$